UNIVERSITY OF CALIFORNIA
RIVERSIDE

Photooxidation Yields of Organic Nitrates and the Influence of the Nitrate Moiety on Aerosol Formation

A Dissertation submitted in partial satisfaction
of the requirements for the degree of

Doctor of Philosophy

in

Chemistry

by

Geoffrey Keith Yeh

August 2013

Dissertation Committee:
Dr. Paul J. Ziemann, Chairperson
Dr. Ryan R. Julian
Dr. Yinsheng Wang

The Dissertation of Geoffrey Keith Yeh is approved:

_____

_____

_____

Committee Chairperson

University of California, Riverside

ACKNOWLEDGEMENTS

This material is based on work supported by the National Science Foundation under Grant AGS-1219508. Any opinions, findings, and conclusions or recommendations expressed in this material are my own, and do not necessarily reflect the views of the National Science Foundation (NSF).

I would like to thank Janet Arey and Roger Atkinson for helpful discussions and for the loan of equipment, and Jose Luis Jimenez for his guidance in the use of IGOR Pro technical graphing and data analysis software.

DEDICATION

This work is dedicated to the memories of my grandmother, Ouyang Mei-Teh (Bertha), and my brother, Curtis Ayag.

ABSTRACT OF THE DISSERTATION

Photooxidation Yields of Organic Nitrates and the
Influence of the Nitrate Moiety on Aerosol Formation

by

Geoffrey Keith Yeh

Doctor of Philosophy, Graduate Program in Chemistry
University of California, Riverside, August 2013
Dr. Paul J. Ziemann, Chairperson

Organic nitrates occur throughout the atmosphere, routinely detected in rural, marine, and urban environments as gases and as components of particles. They can be formed in substantial quantities from the reactions of volatile organic compounds (VOCs) with OH radicals in the presence of nitrogen oxides (NO_x), and from the reactions of alkenes with NO_3 radicals. Formation of organic nitrates affects ozone concentrations by sequestering NO_x, the catalyst required for ozone formation. Organic nitrates of sufficiently low volatility condense to form secondary organic aerosol (SOA), a major component of atmospheric aerosol, which affects surface albedo and cloud formation, and therefore climate. Since organic nitrates contribute to particle mass and affect NO_x concentrations, quantitative understanding of the conditions governing their formation is needed for accurate atmospheric modeling of ozone and aerosol.

In these studies, yields of organic nitrates were measured in environmental chamber reactions of C_8–C_{16} *n*-alkanes with OH in the presence of NO_x, and in reactions of 1-alkenes with NO_3. Yield measurements of monofunctional organic nitrates, *i.e.* alkyl

nitrates, were made to observe a yield plateau with respect to carbon number, which was predicted by previous studies, but never confirmed experimentally due to the analytical challenge posed by partitioning of large alkyl nitrates into chamber walls. A strategy to correct gas chromatographic (GC) alkyl nitrate measurements for gas-wall partitioning was developed, and a yield plateau was measured at ~30%. Particle-phase 1,4-hydroxynitrate yields were measured by analyzing particle filter extracts by liquid chromatography with UV absorbance and mass spectrometric detection (LC/UV/MS), and a yield plateau of ~13% was observed. These yield measurements were combined with over 140 previously reported measurements to update the parameterization of an existing yield estimation model for organic nitrate formation. The effect of the nitrate moiety on the decomposition of alkoxy radicals was investigated by reacting 1-pentadecene with NO_3, and measuring aerosol yield and 1,2-hydroxynitrate, 1,2-carbonylnitrate, and organic peroxide product yields in particles. The branching ratio of decomposition/isomerization of the β-nitrooxyalkoxy radical was extrapolated, and indicated that the nitrate moiety substantially enhances the decomposition of the alkoxy radical, inhibiting the formation of aerosol.

Table of Contents

List of Schemes

List of Figures

List of Tables

Introduction

The preservation of air quality is essential to human health and quality of life. To better manage human activity and technology in the interests of air quality and the amelioration of detrimental effects of air pollutant exposure, scientists, engineers, and regulatory bodies have invested great effort in understanding pollutant emissions, climatology, atmospheric dynamics, atmospheric physics, and atmospheric chemistry. The six major hazardous air pollutants are ozone, particulate matter (aerosol), nitrogen oxides, carbon monoxide, sulfur dioxide, and lead. Of these, ozone and aerosol, with their ubiquity in developed and undeveloped regions, and their high potential for deleterious health effects, are currently under great scrutiny, and strategies to understand and reduce the formation and occurrence of these two pollutants are being developed worldwide. Atmospheric modeling is a critical component of these strategies, but the sophistication and accuracy of contemporary models are insufficient as reliably predictive tools, especially in the modeling of particulate matter (Zhang et al., 2007). In the last decade, the importance of atmospheric organic chemistry, especially the oxidation of volatile organic compounds (VOCs) and its relationship to aerosol and ozone formation, has been realized. In this study, the oxidations of two classes of VOCs, the alkanes and alkenes, are studied, and yields of the organic nitrates, a major class of oxidized VOC that is intimately related to both ozone and aerosol formation, produced from these reactions are measured. The yield measurements are intended for incorporation into atmospheric models that require detailed, quantitative characterization of chemical transformations to constrain and enhance the accuracy of the predictions of ozone and aerosol occurrence.

Organic nitrates are a product of the atmospheric oxidation of VOCs, and are ubiquitous gas- and particle-phase components of tropospheric air, being routinely detected in urban, rural, and marine atmospheres (Russo et al., 2010; Schneider et al., 1999; Ballschmiter 2002; Cleary et al., 2011). They can arise from the daytime oxidation of VOCs by reaction with the hydroxyl radical (OH) in the presence of nitrogen oxides (NO_x), a condition typical of polluted atmospheres. They also form by the nighttime reactions of alkenes with nitrate radical (NO_3), a condition independent of the degree of pollution. Unsubstituted organic nitrates, the alkyl nitrates, are produced by the daytime reaction of alkanes with OH in the presence of NO_x ($NO_x \equiv NO + NO_2$). Substituted organic nitrates, such as hydroxynitrates and carbonylnitrates, are formed by a variety of mechanisms in daylight and darkness. The chemical structures of the substituted and unsubstituted organic nitrates addressed in this study are shown in Figure I.1.

Figure I.1: Chemical structures of the organic nitrates studied. (a) alkyl nitrate (b) 1,4-hydroxynitrate (c) 1,2-hydroxynitrate (d) 1,2-carbonylnitrate.

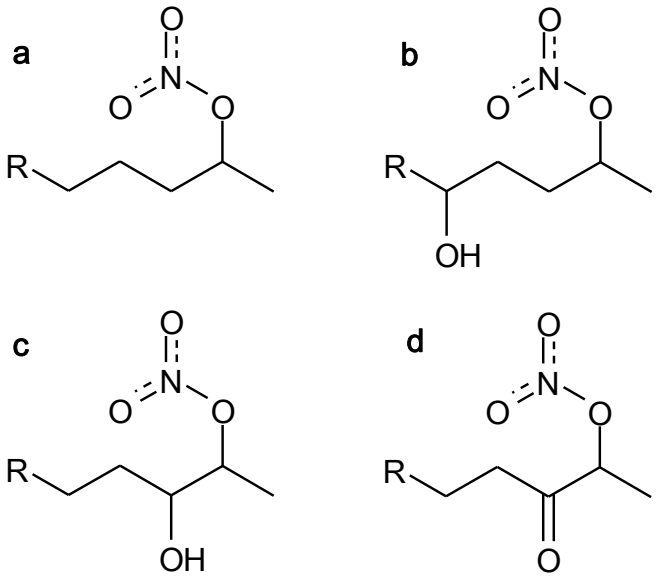

Organic nitrates are so widespread that they have been defined as "the missing NO_y," routinely composing 10-20% of total NO_y ($NO_y \equiv NO_x$ + all other oxidized nitrogen species), making them a major sink of nitrogen oxides (Day et al., 2003), and, through the sequestration of NO_x that occurs as a result of their formation, they can affect ozone the catalytic production of ozone by NO_x (Atkinson, 2000; Day et al., 2003).

Multifunctional organic nitrates and alkyl nitrates of high carbon number, and therefore low volatility, can partition into particles to form secondary organic aerosol (SOA) (Ziemann, 2011), a major component of fine particles (Zhang et al., 2007). Fine particles are currently a topic of great interest because they influence global climate by absorbing and scattering radiation (Dickerson et al., 1997; Lohmann and Feichter, 2005), and by affecting the formation and properties of clouds (Forster et al., 2007; Andreae and Rosenfeld, 2008). Fine particulate matter is also a human health hazard as heart and lung disease, asthma, and mortality have been linked to particle exposure in a dose-dependent manner (Alfaro-Moreno et al., 2007; Etzel, 2003; Pope et al., 2007). The formation of SOA depends on the degree of chemical processing that diminishes the vapor pressures of gaseous compounds. While functionalization of a VOC reduces that compound's vapor pressure via the incorporation of functional groups such as hydroxyl, carbonyl, or nitrooxy groups, fragmentation reactions lead to cleavage of carbon-carbon bonds with the potential to reduce the vapor pressure of reaction products relative to that of the parent VOC. Fragmentation generally results from the decomposition of an alkoxy radical, a reaction intermediate common to the oxidation of many volatile compounds by hydroxyl radical and nitrate radical (Atkinson and Arey, 2003), and if the parent

molecule loses more than two carbons, the vapor pressure of product is generally diminished relative to that of the parent (Pankow and Asher, 2008; Chacon-Madrid et al., 2010; Chacon-Madrid and Donahue, 2011). Accurate prediction of the fraction of VOC transformed into SOA mass via functionalization, and the fraction that is fragmented into volatile molecules that do not contribute to SOA is critical to the translation of emissions inventories and chemical reaction mechanisms into comprehensive and predictive models of SOA formation. Therefore, a quantitative understanding of the tendency of the alkoxy radical to decompose, and of the conditions affecting its rate of decomposition is vital to SOA modeling. To more accurately model the formation and occurrence of SOA, ozone, and NO_x, quantitative studies of the yields of organic nitrate products formed by atmospheric processes are necessary (Atkinson and Arey, 2003; Atkinson, 2007; Ziemann and Atkinson, 2012).

To estimate the product yields of organic nitrates formed from the reactions of VOCs with hydroxyl radical in the presence of NO_x, results of studies quantifying the dependence of temperature, pressure, and carbon number on nitrate formation were compiled to develop an expression to estimate the yields of alkyl nitrates from the secondary alkyl peroxy radical, the reaction intermediate following the abstraction of a hydrogen atom from a VOC by the OH radical under tropospheric (high oxygen) conditions (Atkinson et al., 1983). The expression is adapted from the generalized falloff equation for simple addition reactions (Troe 1974; Luther and Troe, 1979). The falloff expression describes the reduction in rate constant relative to the reduction in the concentration of a third body, [M], and the line it describes is termed the "falloff curve,"

a yield calculated as a function of carbon number, temperature, and pressure. In each of its evolutions, the yield estimation expression predicts a near-linear increase in the formation of secondary alkyl nitrates with increasing carbon number up to ~C_8, consistent with values measured for OH/NO_x reactions of *n*-alkanes, followed by a rapid approach to a plateau such that the yield only increases from ~0.24 at C_8 to ~0.29 between C_{13}–C_{17}. The increase in alkyl nitrate yield with increasing carbon number is due to a corresponding increase in the number of vibrational degrees of freedom, which are sinks of vibrational energy, and therefore allow more time for collisional stabilization leading to nitrate products (Atkinson et al.,1983; Robinson and Holbrook, 1972). Although the near-linear dependence of alkyl nitrate yields on carbon number has been demonstrated experimentally for unsubstituted secondary alkyl peroxy radicals up to C_{10} (Atkinson et al., 1982, Atkinson et al., 1987, Arey et al., 2001; Aschmann et al.,2001), alkyl nitrate yields have not been reported for carbon numbers high enough to observe the occurrence of a plateau.

In the first chapter of the present work, the results of reactions of C_8–C_{14} *n*-alkanes with OH radicals in the presence of NO_x, and the isomer-specific yields of alkyl nitrates measurements are described. The major difficulty with measuring alkyl nitrate yields from reactions of *n*-alkanes larger than C_8 in order to explore the predicted plateau region is that the marginal volatility of these compounds enhances their tendency to partition to the chamber walls, and by this mechanism, alkyl nitrates of high carbon number escape sampling and analysis. This phenomenon was apparently observed in a study of the yields of alkyl nitrates formed from reactions of a suite of C_{10} alkanes, in

which partitioning to the walls was cited as a possible explanation for why the yield measured for the reaction of *n*-decane was not significantly higher than the yield measured previously for the reaction of *n*-octane (Aschmann et al., 2001). This explanation is consistent with recent studies of gas-wall partitioning of C_8–C_{13} ketones and alcohols in a Teflon chamber, in which the onset of partitioning to the walls occurred at ~C_{10}, and the fraction of compound absorbed into the walls at equilibrium increased with increasing carbon number (Matsunaga and Ziemann, 2010a). To account for reaction products lost to the chamber walls, a series of separate experiments were conducted in which synthesized *n*-alkyl nitrate standards with a range of carbon numbers and a variety of isomer structures were added to the chamber, and their concentrations measured over time. With these data, a structure-activity model was developed to estimate gas-wall partitioning of alkyl nitrates, and the model was used to correct all measured isomer-specific alkyl nitrate yields for losses to chamber walls.

Although the yields of alkyl nitrates formed from reactions of *n*-alkanes have been investigated over the range of carbon numbers, the yields of 1,4-hydroxynitrates are much less well known. Arey et al. (Arey et al., 2001) measured yields of ~0.05 for gas-phase 1,4-hydroxynitrates resulting from the OH/NO_x photooxidations of C_5–C_8 *n*-alkanes. In studies of the oxidation of alkenes by OH radical in the presence of NO_x, yields approximately 50% less than those of modeled alkyl nitrate yields at equivalent carbon number were observed (O'Brien et al., 1998; Matsunaga and Ziemann, 2010b). In the second chapter of this work, the results of reactions of C_8-C_{16} *n*-alkanes with OH radicals in the presence of NO_x and the measured yields of 1,4-hydroxynitrates in particle

filter samples were measured by high-performance liquid chromatography with UV detection (HPLC/UV). Authentic analytical standards of 1,4-hydroxynitrates were purified from filter extracts and used for the preparation of standard curves for accurate quantitation. Structural confirmation of 1,4-hydroxynitrate products was obtained using thermal desorption particle beam mass spectrometry (TDPBMS) coupled to HPLC/UV, and an electron ionization fragmentation mechanism was developed that can be used to explain the observed mass spectra and identify each of the 1,4-hydroxynitrate isomers.

Recent studies determining nitrate formation as a function of carbon number, temperature, pressure, and functionalization have supplemented the database of organic nitrate yield data, but have not yet been incorporated into the parameterization of the yield estimation method (Atkinson et al., 1983). In the third chapter of this work, organic nitrate yield data was compiled from eighteen studies to update the parameterization of the yield estimation method, and to determine scaling factors for organic nitrate formation from primary, secondary , and tertiary organic peroxy radicals, and peroxy radicals substituted with β-hydroxyl, δ-hydroxyl, and bromo groups.

Multifunctional alkoxy radicals have varied tendencies to decompose based on the identities of functional groups present on the carbon backbone, as well as where they are located relative to the alkoxy group. Studies have demonstrated that some functional groups proximal to the alkoxy group can affect the rate of alkoxy decomposition. β-hydroxy alkoxy radicals have been shown to decompose more quickly than their alkoxy analogs in theoretical and experimental studies. In RKKM analysis of 1-butoxy and β-hydroxy butoxy radicals, the calculated rate constants for decomposition of the hydroxy

alkoxy radicals were roughly 10^6 times greater than those for the unsubstituted alkoxy radical (Méreau et al., 2000). In environmental chamber studies of the hydroxyl radical-mediated oxidation of 1-octene and 7-tetradecene in the presence of NO_x, C_8 and C_{14} β-hydroxy alkoxy radicals exhibited decomposition branching ratios of ~42% and ~65%, respectively (Aschmann et al., 2010). A study of the OH/NO_x oxidation of 2-methyl-1-alkenes showed that the presence of a β-methyl group did not affect the rate of alkoxy decomposition when compared to a similar study of 1-alkene oxidation (Matsunaga and Ziemann, 2009; Matsunaga and Ziemann, 2010b).

To date, there are no measurements of the relative fragmentation and isomerization yields of β-nitrooxyalkoxy radicals. The β-nitrooxyalkoxy radical is an important multifunctional intermediate in the reaction mechanism of alkene oxidation by nitrate radical, as well as a second generation oxidation product of alkane oxidation by hydroxyl radical in a high-NO_x atmosphere. It is possible that the nitrooxy group, similar to the hydroxyl group in its electron withdrawing properties, may accelerate decomposition like the hydroxyl group, but the technical barrier to an experimental investigation of this condition is the introduction or production of known amounts of gas-phase β-nitrooxyalkoxy radicals in an environmental chamber or flow reactor. In the final chapter of this work, the NO_3-mediated oxidation of a 1-alkene is used to produce β-nitrooxyalkoxy radicals in estimable amounts, and their isomerization:decomposition branching is indirectly determined by quantitation of major aerosol products and aerosol yield in conjunction with mass balance calculations.

References

1. Alfaro-Moreno, E., Nawrot, T. S., Nemmar, A., & Nemery, B. (**2007**). Particulate matter in the environment: pulmonary and cardiovascular effects. *Current Opinion in Pulmonary Medicine*, 13(2), 98-106.

2. Andreae, M. O., & Rosenfeld, D. (**2008**). Aerosol–cloud–precipitation interactions. Part 1. The nature and sources of cloud-active aerosols. *Earth-Science Reviews*, 89(1), 13-41.

3. Arey, J., Aschmann, S. M., Kwok, E. S., & Atkinson, R. (**2001**). Alkyl nitrate, hydroxyalkyl nitrate, and hydroxycarbonyl formation from the NO_x-air photooxidations of C_5-C_8 *n*-alkanes. *The Journal of Physical Chemistry A*, 105(6), 1020-1027.

4. Aschmann, S. M., Arey, J., & Atkinson, R. (**2001**). Atmospheric chemistry of three C_{10} alkanes. *The Journal of Physical Chemistry A*, 105(32), 7598-7606.

5. Aschmann, S. M., Tuazon, E. C., Arey, J., & Atkinson, R. (**2010**). Products and Mechanisms of the Gas-Phase Reactions of OH Radicals with 1-Octene and 7-Tetradecene in the Presence of NO. *Environmental Science & Technology*, 44(10), 3825-3831.

6. Atkinson, R., Aschmann, S. M., Carter, W. P., Winer, A. M., & Pitts Jr, J. N. (**1982**). Alkyl nitrate formation from the nitrogen oxide (NO_x)-air photooxidations of C_2-C *n*-alkanes. *The Journal of Physical Chemistry*, 86(23), 4563-4569.

7. Atkinson, R., Carter, W. P., & Winer, A. M. (**1983**). Effects of temperature and pressure on alkyl nitrate yields in the nitrogen oxide (NO_x) photooxidations of *n*-pentane and *n*-heptane. *The Journal of Physical Chemistry*, 87(11), 2012-2018.

8. Atkinson, R., Aschmann, S. M., & Winer, A. M. (**1987**). Alkyl nitrate formation from the reaction of a series of branched RO_2 radicals with NO as a function of temperature and pressure. *Journal of Atmospheric Chemistry*, 5(1), 91-102.

9. Atkinson, R. "*Atmospheric oxidation*" pp.335-354 in *Handbook of Property Estimation Methods for Chemicals: Environmental and Health Services*; Boethling, R.S.; Mackay, D., Eds. CRC Press: Boca Raton, FL, 2000.

10. Atkinson, R., & Arey, J. (**2003**). Atmospheric degradation of volatile organic compounds. *Chemical Reviews*, 103(12), 4605-4638.

11. Atkinson, R. (**2007**). Gas-phase tropospheric chemistry of organic compounds: a review. *Atmospheric Environment*, 41, 200-240.

12. Ballschmiter, K. (**2002**). A marine source for alkyl nitrates. *Science*, 297(5584), 1127-1128.

13. Chacon-Madrid, H. J., Presto, A. A., & Donahue, N. M. (**2010**). Functionalization vs. fragmentation: *n*-aldehyde oxidation mechanisms and secondary organic aerosol formation. *Physical Chemistry Chemical Physics*, 12(42), 13975-13982.

14. Chacon-Madrid, H. J., & Donahue, N. M. (**2011**). Fragmentation vs. functionalization: chemical aging and organic aerosol formation. *Atmospheric Chemistry and Physics*, 11(10), 553.

15. Cleary, P.A.; Murphy, J.G.; Wooldridge, P.J.; Day, D.A.; Millet, D.B.; McKay, M.; Goldstein, A.H.; Cohen R.C. (**2005**). Observations of total alkyl nitrates within the Sacramento Urban Plume. *Atmospheric Chemistry and Physics Discussions*, 5(4), 4801-4843.

16. Day, D. A., Dillon, M. B., Wooldridge, P. J., Thornton, J. A., Rosen, R. S., Wood, E. C., & Cohen, R. C. (**2003**). On alkyl nitrates, O_3, and the "missing NO_y". *Journal of Geophysical Research*, 108(D16), 4501.

17. Dickerson, R. R., Kondragunta, S., Stenchikov, G., Civerolo, K. L., Doddridge, B. G., & Holben, B. N. (**1997**). The impact of aerosols on solar ultraviolet radiation and photochemical smog. *Science*, 278(5339), 827-830.

18. Etzel, R. A. (**2003**). How environmental exposures influence the development and exacerbation of asthma. *Pediatrics*, 112(Supplement 1), 233-239.

19. Forster, P.; Ramaswamy, V.; Artaxo, P.; Berntsen, T.; Betts, R.; Fahey, D.W.; Haywood, J.; Lean, J.; Lowe, D.C.; Myhre, G.; Nganga, J.; Prinn, R.; Raga, G.; Schulz, M.; Van Dorland, R. *"Changes in Atmospheric Constituents and in Radiative Forcing"* in *Climate Change 2007: The Physical Science Basis. Contribution of Working Group I to the Fourth Assessment Report of the Intergovernmental Panel on Climate Change*; Solomon, S.; Qin, D.; Manning, M.; Chen, Z.; Marquis, M.; Averyt, K. B.; Tignor, M.; Miller, H. L., Eds. Cambridge University Press, New York, NY, 2007.

20. Lohmann, U., & Feichter, J. (**2005**). Global indirect aerosol effects: a review. *Atmospheric Chemistry and Physics*, 5(3), 715-737.

21. Luther, K., & Troe, J. (**1979**, December). Weak collision effects in dissociation reactions at high temperatures. In Symposium (International) on Combustion (Vol. 17, No. 1, pp. 535-542). Elsevier

22. Matsunaga, A., & Ziemann, P. J. (**2009**). Yields of β-hydroxynitrates and dihydroxynitrates in aerosol formed from OH radical-initiated reactions of linear alkenes in the presence of NO_x. *The Journal of Physical Chemistry A*, 113(3), 599-606.

23. Matsunaga, A., & Ziemann, P. J. (**2010a**). Gas-wall partitioning of organic compounds in a Teflon film chamber and potential effects on reaction product and aerosol yield measurements. *Aerosol Science and Technology*, 44(10), 881-892.

24. Matsunaga, A., & Ziemann, P. J. (**2010b**). Yields of β-hydroxynitrates, dihydroxynitrates, and trihydroxynitrates formed from OH radical-initiated reactions of 2-methyl-1-alkenes. *Proceedings of the National Academy of Sciences*, 107(15), 6664-6669

25. Méreau, R., Rayez, M. T., Caralp, F., & Rayez, J. C. (**2000**). Theoretical study on the comparative fate of the 1-butoxy and β-hydroxy-1-butoxy radicals. *Physical Chemistry Chemical Physics*, 2(9), 1919-1928.

26. O'Brien, J. M., Czuba, E., Hastie, D. R., Francisco, J. S., & Shepson, P. B. (**1998**). Determination of the hydroxy nitrate yields from the reaction of C_2-C_6 alkenes with OH in the presence of NO. *The Journal of Physical Chemistry A*, 102(45), 8903-8908.

27. Pankow, J. F., & Asher, W. E. (**2008**). SIMPOL. 1: a simple group contribution method for predicting vapor pressures and enthalpies of vaporization of multifunctional organic compounds. *Atmospheric Chemistry and Physics*, 8(10), 2773-2796.

28. Pope, C. A., Ezzati, M., & Dockery, D. W. (**2009**). Fine-particulate air pollution and life expectancy in the United States. *New England Journal of Medicine*, 360(4), 376-386.

29. Robinson, P.J.; Holbrook, K.A. *Unimolecular Reactions* Wiley, New York, NY, 1972.

30. Russo, R.S.; Zhou, Y.; Haase, K.B.; Wingenter, O.W.; Frinak, E.K.; Mao, H.; Talbot, R.W.; Sive, B.C. (**2010**). Temporal variability, sources, and sinks of C_1-C_5 alkyl nitrates in coastal New England. *Atmospheric Chemistry and Physics*, 10(4), 1865-1883.

31. Schneider, M., & Ballschmiter, K. (**1999**). C_3-C_{14} alkyl nitrates in remote south Atlantic air. *Chemosphere*, 38(1), 233-244.

32. Troe, J. (**1974**). Fall-off Curves of Unimolecular Reactions. *Berichte der Bunsengesellschaft für physikalische Chemie*, 78(5), 478-488.

33. Zhang, Q.; Jimenez, J.L.; Canagaratna, M.R.; Allan, J.D.; Cole, H.; Ulbrich, I.; Alfarra, M.R.; Takami, A.; Middlebrook, A.M.; Sun, Y.L.; Dzepina, K.; Dunlea, E.; Docherty, K.; DeCarlo, P.F.; Salcedo, D.; Onasch, T.; Jayne, J.T.; Miyoshi, T.; Shimono, A.; Hatakeyama, S.; Takegawa, N.; Kondo, Y.; Schneider, J.; Zrewnick, F.; Borrmann, S.; Weimer, S.; Demerjian, K.; Williams, P.; Bower, K.;

Zahreini, R.; Cottrell, L.; Griffin, R.J.; Rautiainen, J.; Sun, J.Y.; Zhang, Y.M.; Worsnop, D.R. (**2007**). Ubiquity and dominance of oxygenated species in organic aerosols in anthropogenically-influenced Northern Hemisphere midlatitudes. *Geophysical Research Letters*, 34(13), L13801.

34. Ziemann, P. J. (**2011**). Effects of molecular structure on the chemistry of aerosol formation from the OH-radical-initiated oxidation of alkanes and alkenes. *International Reviews in Physical Chemistry*, 30(2), 161-195.

35. Ziemann, P. J., & Atkinson, R. (**2012**). Kinetics, products, and mechanisms of secondary organic aerosol formation. *Chemical Society Reviews*, 41(19), 6582-6605.

Chapter 1: Alkyl nitrate formation from the reactions of C_8–C_{14} *n*-alkanes with OH radicals in the presence of NO_x: Measured yields with essential corrections for gas-wall partitioning

Abstract

In this study, C_8–C_{14} *n*-alkanes were reacted with OH radicals in the presence of NO_x in a Teflon film environmental chamber and isomer-specific yields of alkyl nitrates were determined using gas chromatography with flame ionization detection. Total molar yields of alkyl nitrates formed from reactions of *n*-octane, *n*-decane, *n*-dodecane, *n*-tridecane, and *n*-tetradecane after corrections for secondary reactions with OH radicals were 20.8, 18.9, 16.5, 12.5, and 8.5%, respectively. The observed decrease in yield with increasing carbon number was opposite to the trend expected and indicated the possible loss of alkyl nitrates to the chamber walls. Gas-wall partitioning was thus investigated by monitoring the concentrations of a suite of alkyl nitrates that had been synthesized and added to the chamber. Gas-to-wall partitioning increased with increasing carbon number and with proximity of the nitrooxy group to the terminal carbon, with losses as high as 86%. The results were used to develop a structure-activity model to predict the effects of carbon number and isomer structure on gas-wall partitioning, which was then used to correct the measured yields of 27 secondary alkyl nitrate isomers formed in chamber reactions. The resulting isomer-specific branching ratios for the formation of secondary alkyl nitrates were similar for each carbon number, as expected, and total molar yields of alkyl nitrates formed from reactions of *n*-octane, *n*-decane, *n*-dodecane, *n*-tridecane, and *n*-tetradecane were 20.9, 19.8, 24.7, 28.4, and 30.9, respectively. Yields obtained using

the isomer-specific structure-activity model to correct for gas-wall partitioning agreed well with values predicted by the model of Arey et al.(Arey et al., 2001) for the carbon number dependence of alkyl nitrate formation, and indicate that a plateau value of ~0.30 is reached at about C_{13}–C_{14}, also consistent with model predictions.

Introduction

Alkanes are released into the environment by human activities and by natural processes. A small fraction of atmospheric alkanes are attributed to oceanic sources (Kvenvolden et al.,1987; Saito et al., 2004), but most are emitted by fossil fuel and biomass combustion processes and constitute 40-50% of anthropogenic non-methane organic compound (NMOC) emissions (Lurmann and Main, 1992; Calvert et al.,2002; Williams and Koppmann 2007; Gentner et al.,2012). In the atmosphere, daytime reactions with OH radicals limit alkane lifetimes to days, and yield a variety of oxygenated products (Atkinson et al., 2008; Lim and Ziemann, 2009). When NO_x (NO + NO_2) concentrations are sufficiently high the products include organic nitrates, which have been detected in marine (Schneider and Ballschmiter, 1999; Russo et al., 2010; Ballschmiter 2002) and terrestrial environments encompassing urban, suburban, and rural atmospheres (Day et al., 2003; Cleary et al., 2005). Organic nitrates routinely compose 10-20% of total NO_y (NO_x + all other oxidized nitrogen species) (Day et al., 2009), and because they are a major sink for NO_x they affect ozone formation (Atkinson, 2000). Those with large carbon number or multiple functional groups can have sufficiently low volatility to partition into particles to form secondary organic aerosol (SOA), (Ziemann 2011) a major component of fine particles (Zhang et al., 2007). Fine particles are currently a topic of great interest because they influence global climate by absorbing and scattering radiation (Dickerson et al.,1997; Lohmann and Feichter, 2005) and by affecting the formation and properties of clouds (Forster et al., 2007; Andreae and Rosenfeld, 2008). They are also a human health hazard since heart and lung disease, asthma, and

mortality have been linked to fine particle exposure in a dose-dependent manner (Alfaro-Moreno et al., 2007; Etzel 2003; Pope, 2009). To more accurately model the formation and occurrence of SOA, ozone, and NO_x, comprehensive, quantitative studies of the yields of products from alkane-OH radical reactions are necessary (Atkinson, 2007).

The mechanism of formation of alkyl nitrates, which are the dominant organic nitrate formed from the OH radical-initiated reaction of alkanes in air in the presence of NO_x, is shown in scheme 1.1.

Scheme 1.1: Reaction mechanism for the formation of alkyl nitrates formed from oxidation of alkanes by OH radical in the presence of NO_x.

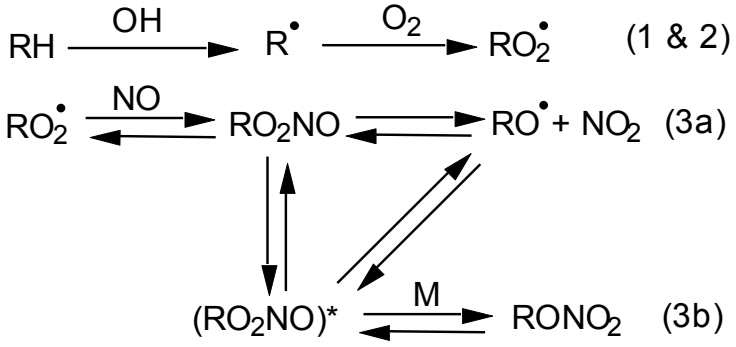

Note that each numbered reaction (x = 1, 2, 3a, and 3b) has a corresponding rate constant k_x (x = 1, 2, 3a, 3b). The OH radical first abstracts an H atom from the alkane (RH) to form H_2O and an alkyl radical (R•), which reacts exclusively with O_2 (Atkinson, 2003) to form an alkyl peroxy radical (RO_2•). The RO_2• radical then reacts with NO via the formation of a vibrationally excited intermediate (RO_2NO*) to produce either an alkoxy radical (RO•) and NO_2, or an alkyl nitrate ($RONO_2$) (Atkinson et al., 1983a). The RO_2• radical can also react with NO_2 to form an alkyl peroxynitrate ($ROONO_2$), but because this compound undergoes rapid reverse thermal decomposition and thus does not alter the overall reaction mechanism or products, it is not shown in the scheme. The mechanism of the reaction of RO_2• radicals with NO is not fully understood, but it has been proposed that the excited $RONO_2$* intermediate can exist as either of two non-interconverting conformers, of which only one has the potential to form alkyl nitrates (Zhao et al., 2004; Cassanelli et al., 2005; Lesar et al., 2006). Factors affecting the branching ratio $k_{3b}/(k_{3a} + k_{3b})$, and therefore the yields of alkyl nitrates, include temperature (Atkinson et al.,1983a; Atkinson et al., 1983b; Atkinson et al.,1987; Harris and Kerr, 1989; Orlando et al., 2000; Chow et al., 2003; Cassanelli et al., 2007) and pressure (Atkinson et al.,1983a; Atkinson et al.,1987; Aschmann et al., 2006), as well as structural features of the RO_2• radical such as carbon number (Atkinson et al.,1987; Atkinson et al.,1982; Arey et al., 2001; Aschmann et al., 2001), alkyl chain branching (Atkinson et al., 1987; Atkinson et al., 2003; Espada et al., 2005; Cassanelli et al., 2007), and the presence of functional groups (Matsunaga and Ziemann, 2009; Matsunaga and Ziemann, 2010a). Data on the effects of temperature, pressure, and carbon number were used by Atkinson and coworkers

(Atkinson et al., 1983a), to develop a model for predicting values of k_{3b}/k_{3a} (and therefore $k_{3b}/(k_{3a} + k_{3b})$) for secondary RO_2• radicals, the parameters for which have been revised a few times in light of a growing dataset (Atkinson et al., 1985; Carter and Atkinson., 1989; Arey et al., 2001). Data regarding the effect of carbon number on reactions of primary and tertiary RO_2• radicals are much more sparse. It is worth noting that for the C_8–C_{14} *n*-alkanes investigated here, the ratios of primary to secondary RO_2• radicals and alkyl nitrates are expected to be <5% (Kwok and Atkinson, 1995), so only secondary RO_2• radicals and alkyl nitrate products are important.

The version of the Atkinson et al. (Atkinson et al., 1983a) model presented by Arey and coworkers (Arey et al., 2001) predicts a near-linear increase in the yield of secondary alkyl nitrates with increasing carbon number up to ~C_8, consistent with values measured for reactions of *n*-alkanes, followed by a fairly rapid approach to a plateau such that the yield only increases from ~0.24 at C_8 to ~0.29 between C_{13}–C_{17}. The increase in alkyl nitrate yield with increasing carbon number is due to a corresponding increase in the number of vibrational degrees of freedom, which as sinks of vibrational energy decrease the rate of unimolecular decomposition of the excited RO_2NO* intermediate and therefore allow more time for collisional stabilization and rearrangement to form $RONO_2$ (Robinson and Holbrook, 1972; Atkinson et al., 1983a). The yields are predicted to reach a plateau at a value less than unity at high carbon numbers because the reaction proceeds through the formation of two non-interconverting intermediate isomers, both of which can be formed by the reaction of the alkyl peroxy radical with NO (Zhang et al., 2004). Only one of the two excited RO_2NO* intermediate conformers decomposes sufficiently

slowly for this process to compete with collisional cooling, while the other undergoes much faster decomposition as its only reaction pathway (Zhao et al., 2004; Cassanelli et al., 2005; Lesar et al., 2006). Although the near-linear dependence of alkyl nitrate yields on carbon number has been demonstrated experimentally for unsubstituted secondary alkyl peroxy radicals up to C_8 (Arey et al., 2001; Atkinson et al., 1987; Atkinson et al., 1982; Aschmann et al., 2001), alkyl nitrate yields have not been reported for carbon numbers large enough to observe the occurrence of a plateau. To date this has only been done for the reactions of NO with primary, secondary, and tertiary β-hydroxyperoxy radicals formed from reactions of OH radicals with 1-alkenes and 2-methyl-1-alkenes, in which a plateau region was observed between ~C_{14}–C_{17} (Matsunaga and Ziemann, 2009; Matsunaga and Ziemann, 2010a). It was also shown (Matsunaga and Ziemann, 2009) that if the values calculated using the Arey et al.(Arey et al., 2001) version of the yield estimation model were scaled by a factor of ~0.5 to account for the reduction in yields due to the presence of a β-hydroxy group, the model predictions agreed very well with branching ratios $k_{3b}/(k_{3a} + k_{3b})$ measured for reactions of 1-alkenes with carbon numbers in both the near-linear (C_3–C_6) (O'Brien et al. 1998) and plateau (C_{14}–C_{17}) (Matsunaga and Ziemann, 2009) regions.

The major difficulty with measuring alkyl nitrate yields from reactions of *n*-alkanes larger than C_8 in order to explore the predicted plateau region is that the lower volatility of these compounds enhances their tendency to partition to the chamber walls and thus be lost from the analysis. This was apparently observed in a study of the yields of alkyl nitrates formed from reactions of a suite of C_{10} alkanes, in which partitioning to

the walls was cited as a possible explanation for why the yield measured for the reaction of *n*-decane was not significantly higher than the yield measured previously for the reaction of *n*-octane (Aschmann et al., 2001). This explanation is consistent with results of our recent studies of gas-wall partitioning of C_8–C_{13} ketones and alcohols in a Teflon chamber, in which the onset of partitioning to the walls occurred at ~C_{10} and the fraction of compound absorbed into the walls at equilibrium increased with increasing carbon number (Matsunaga and Ziemann, 2010b).

In the present study, reactions of C_8–C_{14} *n*-alkanes with OH radicals in the presence of NO_x were conducted in a Teflon environmental chamber and the isomer-specific yields of alkyl nitrates were measured. To account for reaction products lost to the chamber walls, a series of separate experiments were conducted in which synthesized *n*-alkyl nitrate standards with a range of carbon numbers (chain lengths) and variety of isomer structures were added to the chamber and their concentrations measured over time. From the results of these experiments gas-wall partitioning was quantified for each compound and a structure-activity model was developed to estimate gas-wall partitioning of alkyl nitrates. This model was then used to correct all measured isomer-specific alkyl nitrate yields for losses to chamber walls.

Experimental Methods

Chemicals

Acetonitrile, dichloromethane, ethyl acetate, and water were HPLC grade and were purchased from Fisher Scientific. *n*-Octane (99+%), *n*-decane (99+%), *n*-dodecane (99+%), *n*-tridecane (99+%), 2-ethylhexyl nitrate (97%), 1-dodecanol (98%), and 2-dodecanol (99%) were purchased from Sigma Aldrich. *n*-Tetradecane (99%) was purchased from Alfa Aesar. 2-tetradecanol (98%), 7-tetradecanol (96+%), 3-dodecanol (97%), 4-dodecanol (98%), 5-dodecanol (97%), 6-dodecanol (97%), 2-decanol (96%), 5-decanol (99%), and 2-octanol (99%) were purchased from ChemSampCo.

N_2O_5 and methyl nitrite were synthesized according to the procedures of Atkinson et al. (Atkinson et al., 1984) and Taylor et al. (Taylor et al., 1980), respectively, and kept on a glass vacuum rack in liquid nitrogen until used. Eleven alkyl nitrates with carbon numbers C_8–C_{14} and a variety of isomeric structures were synthesized by reacting alcohols with N_2O_5 using a procedure similar to that of Kames et al. (Kames et al, 1993), which is described here in detail. Approximately 30 mg of liquid or solid alcohol was dissolved or suspended in 2 mL of ethyl acetate in a 250 mL glass vacuum bulb and in some cases suspensions were sonicated to create finer particles. A stream of N_2 was blown into the bulb to evaporate the solvent while the solution or suspension was swirled to coat the walls with alcohol as uniformly as possible. The bulb was transferred to a vacuum rack and evacuated to remove any residual ethyl acetate, leaving the walls coated with a thin layer of solid or liquid alcohol. N_2O_5 was added to the bulb at a 1.5:1 molar ratio of N_2O_5 to alcohol. The reaction between the alcohol and N_2O_5 proceeded

instantaneously (as indicated by the rapid conversion of solid alcohol to liquid), but even when left to react for up to 10 minutes with excess N_2O_5 consumed only 50% to 90% of the alcohol. Reaction product mixtures containing alcohols and alkyl nitrates were not purified, since gas chromatographic peaks of alcohols did not interfere with those of alkyl nitrates, and gas-wall partitioning experiments only required measurements of the fraction (not absolute amount) of alkyl nitrate lost to the chamber walls. Product mixtures were transferred into glass storage vials and stored at -20°C until used. At the time of use, the product mixtures were thawed at room temperature and subsequent material handling was performed in a fume hood.

Environmental chamber experiments

Experiments were conducted in an 8.2 m^3 Teflon FEP environmental chamber filled with clean, dry air (<5 ppbv hydrocarbons, <0.1% RH) at room temperature (23–30°C) and pressure (740 torr). Two opposite sides of the chamber frame are covered by blacklights that are used to initiate photolysis reactions.

For reactions of *n*-alkanes with OH radicals in the presence of NO_x, dioctyl sebacate (DOS) seed particles with ~100 nm diameter were generated in a flow of N_2 using an evaporation-condensation source and added to the chamber to achieve a mass concentration of ~100 μg m^{-3} as measured using a TSI 3081 scanning mobility particle sizer (SMPS) with a Model 3772 condensation particle counter, and then 1 ppmv of *n*-alkane and 10 ppmv each of methyl nitrite and NO were added from a glass bulb using a flow of N_2. The added NO prevents the formation of O_3 and NO_3 radicals. A Teflon-coated fan was run for 1 min after adding chemicals to enhance mixing, and then

reactions were initiated by turning on the blacklights (irradiation equivalent to $J_{NO2} \sim 0.37$ min^{-1}) to generate OH radicals via methyl nitrite photolysis (Atkinson et al. 1981) for 3 minutes.

For measurements of gas-wall partitioning of alkyl nitrates, solutions containing 3–5 synthesized alkyl nitrates (chosen on the basis of chromatographic resolution) dissolved in 1 mL of dichloromethane (CH_2Cl_2) were added to the environmental chamber by evaporation from a glass bulb into a stream of N_2 using gentle heating to achieve estimated concentrations of 5–25 ppbv for each compound. A Teflon-coated fan was run for 1 min after adding the compounds to enhance mixing.

Concentrations of *n*-alkanes and/or alkyl nitrates in the chamber were monitored over time by sampling air through stainless steel tubing and then into a glass tube containing Tenax TA solid adsorbent. Prior to sampling, chamber air was drawn through the stainless steel tubing for 20 min at 250 cm^3 min^{-1} using a mass flow controller to allow the walls of the tube to equilibrate with organic compounds. Samples were then collected for 10–15 min at the same flow rate. For chamber reactions, samples were collected for analysis of *n*-alkanes 60 and 30 min before initiating the reaction, and then 30, 90, and 150 min after the reaction for analysis of *n*-alkanes and alkyl nitrates. For gas-wall partitioning experiments, samples were collected for analysis 30, 90, 170, and 240 min after adding the alkyl nitrates to the chamber.

After sampling, the Tenax cartridge was transferred to the inlet of a Hewlett Packard 1190 gas chromatograph with cryogenic oven for *n*-octane and *n*-decane experiments or an Agilent 6890 gas chromatograph for *n*-dodecane, *n*-tridecane, and *n*-

tetradecane experiments, and for gas-wall partitioning measurements. Each GC was equipped with a 30 m x 0.32 mm Agilent DB-1701 column with 1 μm film thickness and employed flame ionization detection. Analytes were thermally desorbed from the Tenax cartridge, and eluted on an 8ºC min^{-1} gradient in the 1190 GC or on an 8ºC min^{-1} to 2ºC min^{-1} gradient on the 6890 GC. The complex gradient on the 6890 GC was employed to better resolve the alkyl nitrate isomers resulting from the reactions of C_{12}-C_{14} *n*-alkanes. In spite of this approach, we note that 6- and 7-alkyl nitrate isomers formed from reactions of *n*-tridecane and *n*-tetradecane, and the 4- and 5-alkyl nitrate isomers formed from reactions of *n*-decane, were not sufficiently well resolved to determine their individual concentrations. Consequently, when calculating isomer-specific yields of alkyl nitrates, peak areas of co-eluting isomers were first summed and then the area was distributed between the isomers based on the relative yields of the two precursor RO_2• radicals calculated using the structure-reactivity method of Kwok and Atkinson (Kwok and Atkinson, 1995).

Alkyl nitrates were dissolved in CH_2Cl_2, and groups of three to five alkyl nitrates (chosen on the basis of chromatographic resolution) were pooled for simultaneous analysis. The resulting pooled solutions served both as vehicles for alkyl nitrate introduction to the chamber as well as mixed standard stock solutions for GC/FID calibration. Alkyl nitrate peak areas were compared against those of the pooled solutions syringe-injected into the GC.

Due to the impracticality of synthesizing pure alkyl nitrate analytical standards, quantitation was performed by comparing the alkyl nitrate peak area with that of the *n*-

alkane standard, corrected for effective carbon number (ECN) by the approach described by Scanlon and Willis (Scanlon and Willis, 1985). In this approach, the FID response per mole of alkane is divided by the alkane carbon number, generating the FID response per carbon number. Functional groups are accounted for by adding a group contribution factor that may increase or decrease FID response. In comparisons of GC/FID response between 25 alkanes and their corresponding alkyl nitrates (Roger Atkinson, personal communication), the nitrooxy group decreased the FID response by 1.0 ± 0.7 ECN units, causing a C_n alkyl nitrate to have the same FID response of as a C_{n-1} alkane. For wall loss experiments, synthesized alkyl nitrates were pooled into groups. The alkyl nitrates in each group were selected on the basis of chromatographic resolution so that they did not coelute with other alkyl nitrates or residual alcohols. The pooled groups were diluted in CH_2Cl_2 and the resulting solution was used as both an analytical standard and as the vehicle for introducing alkyl nitrates into the chamber. Based on the peak areas, no more than 25 ppbv of any alkyl nitrate was added to the chamber. This is well below the saturation concentrations for these compounds, which are predicted to be ≤ 350 ppbv, (Luxenhofer et al., 1996) so effects due to condensation of supersaturated vapor on the walls or particle formation were avoided.

Since alkyl nitrates present in the gas and particle phases would be lost to the chamber walls at different rates, and therefore require different corrections for wall loss, experiments were also conducted to determine the partitioning of alkyl nitrates between the gas and particle phases. In these experiments, particle-phase alkyl nitrates were quantified by analysis of filter sample extracts using high performance liquid

chromatography (HPLC) with UV detection, as we have done previously (Matsunaga and Ziemann, 2009; Matsunaga and Ziemann, 2010a). Briefly, particles were sampled onto filters (Millipore Fluoropore, 0.45 μm pore size) at a flow rate of ~14 LPM that was measured before and after filter sampling (values typically within 5%) to obtain an average flow rate that was used for sample quantification. Samples were collected for 1–3 hours depending on the aerosol mass concentration, which generally increased with increasing alkane carbon number. Filters were weighed before and after sampling to determine the mass of particles collected, and the filters were stored at -20°C until extraction. Particles were extracted twice from filters with 4 mL of ethyl acetate and the two extracts were combined. The solvent was dried in a stream of N_2 and the residue was weighed and then reconstituted in acetonitrile for injection into an Agilent 1100 LC with quaternary pump and UV/Vis detector. The column was a 4.0 x 150 mm Thermo BetaBasic C_{18} with 3 μm particles. Mobile phase A was 5% acetonitrile in water, mobile phase B was pure acetonitrile, the flow rate was 0.8 mL min^{-1}, and the gradient was 0.67 %B min^{-1}. A 6-port valve with a 100 μL sample loop was used for injection and the loop was overfilled to increase the precision of run-to-run injection volume, which was 100 μL. Water was not added to the injection solvent to avoid precipitation of sample components that might exhibit low water solubility. Alkyl nitrates were detected at 210 nm as we have done previously (Matsunaga and Ziemann, 2009; Matsunaga and Ziemann, 2010a), and for quantitation, the molar absorptivity was assumed to be equal to that of ethyl hexyl nitrate, a commercially available alkyl nitrate that was used as an analytical standard. Alkyl nitrates were not detected in particles in the *n*-octane and *n*-

decane experiments, trace amounts were detected in the *n*-dodecane and *n*-tridecane experiments, and ~10% of the mass of alkyl nitrates measured by GC/FID analysis (gas + particles) was measured in particles by HPLC analysis in the *n*-tetradecane experiments. Because the fraction of alkyl nitrates in particles was very low, it was only necessary to consider the wall losses of gaseous alkyl nitrates in the data analysis.

Results and Discussion

Initial alkyl nitrate yields with corrections for secondary reactions

Molar yields of secondary alkyl nitrates measured for the reactions of *n*-octane, *n*-decane, *n*-dodecane, *n*-tridecane, and *n*-tetradecane and corrected for secondary reactions with OH radicals according to the method of Atkinson et al. (Atkinson et al.,1982), were 0.208, 0.189, 0.165, 0.125 and 0.086, respectively. The corrections for secondary reactions, which depended on the fraction of *n*-alkane reacted and the rate constants for the reactions of the *n*-alkane and alkyl nitrate products, were approximately 2–6% of the measured yield for C_8–C_{13} alkyl nitrates and ~30% for the C_{14} alkyl nitrates. The larger correction for the C_{14} alkyl nitrates was due to the larger fraction of *n*-tetradecane that needed to be reacted in order to obtain sufficient products for analysis. The observed decrease in alkyl nitrate yield with increasing carbon number is contrary to predictions of the version of the Atkinson et al. (Atkinson et al.,1983a) model presented by Arey et al. (Arey et al., 2001), which predicts an increase to a plateau of ~0.3 at ~C_{15}. The discrepancy could not be due to sampling or analytical artifacts, since gases and particles are both efficiently collected on Tenax and experiments with standards showed that alkyl nitrates $\leq C_{14}$ were desorbed and analyzed by GC/FID without thermal decomposition. Because the amounts of alkyl nitrates measured in particles were negligible compared to the amounts in the gas phase, partitioning of alkyl nitrates to particles with subsequent loss of particles to the walls at typical rates of ~15% h^{-1} also did not provide an explanation. If predictions of the model are reasonable, then it appears that the most

likely explanation for the discrepancy between measurements and model predictions was that alkyl nitrates partitioned to the walls prior to collection of samples for analysis.

Measurements and modeling of gas-wall partitioning of alkyl nitrates

Gas-wall partitioning was investigated as a source of error in chamber experiments by synthesizing eleven C_8–C_{14} alkyl nitrates with different isomeric structures, spiking them into the chamber, and monitoring their gas-phase concentrations at 20, 90, 170, and 240 min. Plots of $[AN_g/AN_T]_t$, the ratio of the alkyl nitrate concentration measured in the gas phase, AN_g, relative to the concentration of total alkyl nitrate added to the chamber, AN_T, are shown in Figure 1.1a for the C_8, C_{10}, C_{12}, and C_{14} 2-alkyl nitrates and in Figure 1.1b for all the C_{12} 1- through 6-dodecyl nitrate isomers.

Figure 1.1: Values of $[AN_g/AN_T]_t$ measured over time in the environmental chamber following the addition of (a) C_8, C_{10}, C_{12}, and C_{14} 2-alkyl nitrates and (b) C_{12} 1- through 6-dodecyl nitrate isomers. The curves are nonlinear least-squares fits of the data to the equation $[AN_g/AN_T]_t = [AN_g/AN_T]_{eq} + (1 - [AN_g/AN_T]_{eq})e^{-t/\tau gw}$.

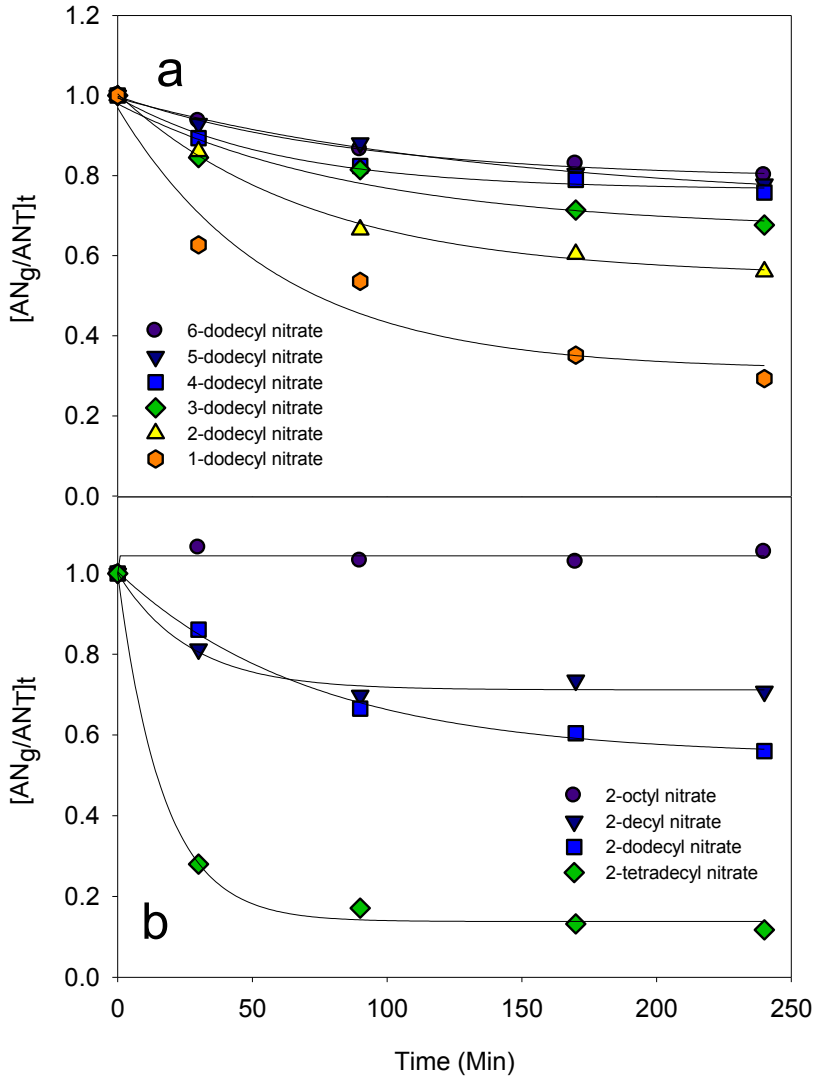

The data were fit to the exponential decay equation

$$[AN_g/AN_T]_t = [AN_g/AN_T]_{eq} + (1 - [AN_g/AN_T]_{eq})e^{-t/\tau_{gw}} \quad (1)$$

where $[AN_g/AN_T]_t$ and $[AN_g/AN_T]_{eq}$ are the fraction of the total alkyl nitrate that is in the gas phase at time t (min) and at equilibrium, respectively, and τ_{gw} (min) is the gas-wall equilibration time constant. All the data and the values of $[AN_g/AN_T]_{eq}$ and τ_{gw} determined from the fits are given in Table 1.1.

Table 1.1: Measured $[AN_g/AN_T]_t$ values and values of $[AN_g/AN_T]_{eq}$ and τ_{gw} determined by nonlinear least-squares fits of the data to the equation $[AN_g/AN_T]_t = [AN_g/AN_T]_{eq} + (1 - [AN_g/AN_T]_{eq})e^{-t/\tau gw}$.

.

	Time (min)						
	0	30	90	170	240	$[AN_g/AN_T]_{eq}$	τ_{gw}
2-octyl nitrate	1.00	1.06	1.03	1.03	1.05	1.04	0.0
5-decyl nitrate	1.00	0.96	0.96	0.95	0.92	0.92	112
2-decyl nitrate	1.00	0.81	0.70	0.74	0.71	0.71	26.6
6-dodecyl nitrate	1.00	0.94	0.86	0.83	0.80	0.79	87.7
5-dodecyl nitrate	1.00	0.93	0.88	0.80	0.78	0.73	142
4-dodecyl nitrate	1.00	0.89	0.82	0.79	0.76	0.77	60.2
3-dodecyl nitrate	1.00	0.84	0.81	0.71	0.68	0.67	90.1
2-dodecyl nitrate	1.00	0.86	0.67	0.60	0.56	0.55	72.5
1-dodecyl nitrate	1.00	0.63	0.54	0.35	0.29	0.32	58.5
7-tetradecyl nitrate	1.00	0.67	0.58	0.49	0.43	0.47	39.2
2-tetradecyl nitrate	1.00	0.28	0.17	0.13	0.12	0.14	16.8

$[AN]_T$ ranged from 10-25 ppbv, well below the saturation concentrations of all these alkyl nitrates (the minimum estimated saturation concentration was ~350 ppbv, the value for the C_{14} 1-tetradecyl nitrate (Luxenhofer et al., 1996), so supersaturation with respect to the liquid phase played no role in the observed partitioning. The results show that gas-to-wall partitioning increases with carbon number, as we observed previously for a series of other compounds (Matsunaga and Ziemann, 2010b), and also with proximity of the nitrooxy group ($-ONO_2$) to the end of the carbon chain.

The quantity needed to correct for gas-wall partitioning of an alkyl nitrate is F_{eq}, since the value of interest for yield measurements, AN_T, can be calculated from the measured value of AN_g by dividing by $[AN_g/AN_T]_{eq}$. Using the $[AN_g/AN_T]_{eq}$ values determined for the alkyl nitrate isomer standards tested, a structure-activity model was developed to estimate the gas-wall partitioning of all alkyl nitrate isomers formed in the chamber reactions. This approach was based on the carbon number effect observed for the 2-alkyl nitrates and the isomer effect observed for the 1- through 6-dodecyl nitrate isomers.

To create a mathematical relationship for the effect of carbon number on alkyl nitrate gas-wall partitioning, equilibrium values of $[AN_w/AN_g]_{eq}$ were calculated using the equation

$$[AN_w/AN_g]_{eq} = (1/[AN_g/AN_T]_{eq}) - 1 \qquad (2)$$

where AN_w is the moles of alkyl nitrate on/in the chamber walls divided by the chamber volume. Equation (2) was obtained by combining $[AN_g/AN_T]_{eq}$ with the mass balance equation $AN_T = AN_g + AN_w$. Values of $[AN_w/AN_g]_{eq}$ were then plotted versus RT/P^o, where

R is the gas constant (8.314 J K^{-1} mol^{-1}), T is temperature (K), and P^o is the vapor pressure (Pa) of the 2-alkyl nitrates determined by Luxenhofer et al. (Luxenhofer et al.,1996). As shown previously (Matsunaga and Ziemann, 2010b), such plots result in a linear relationship

$$[AN_w/AN_g]_{eq} = CRT/P^o \quad (3)$$

that can be explained by considering gas-wall partitioning to be an absorptive process analogous to gas-particle partitioning into a liquid organic aerosol. The least-squares regression line through these points was used to predict the decrease in vapor pressure due to increasing carbon number. The line was forced through zero at the y-intercept because as RT/P^o approaches zero ($P^o >> RT$), the alkyl nitrate will exist essentially entirely in the gas phase and therefore $[AN_w/AN_g]_{eq}$ will be zero. A plot of the data and the regression line ($r^2 = 0.996$), which from the slope gives a value of $C = 1.79 \times 10^{-4}$ mol m^{-3}, are shown in Figure 1.2.

Figure 1.2: Relationship between $[AN_g/AN_T]_{eq}$ and RT/P^o for C_8, C_{10}, C_{12}, and C_{14} 2-alkyl nitrates. The curve is a linear least-squares fit of the data to the equation $[AN_w]/[AN_g]_{eq} = CRT/P^o$, forced through zero at the y-intercept.

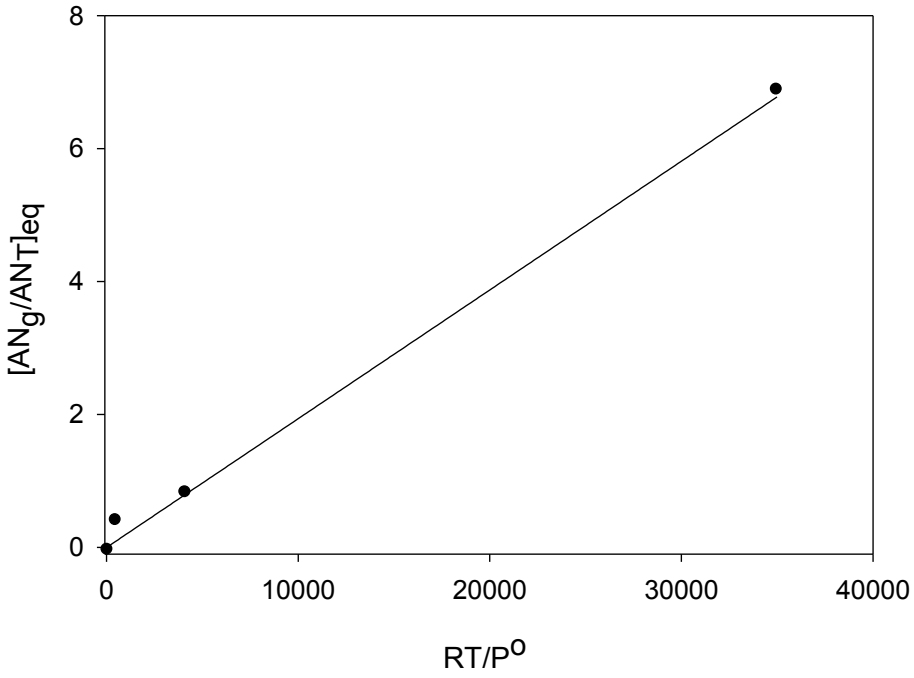

Gas-wall partitioning of alkyl nitrates was observed here to depend not only on carbon number, but also on isomer structure. In particular, the closer the nitrooxy group was to the end of the carbon chain the greater was the extent of gas-to-wall partitioning. A relationship that quantifies the effect of isomer structure on gas-wall partitioning was obtained by first defining a functional group position coefficient, λ, according to the equation

$$\lambda = 1 - z/n \tag{4}$$

where z is the position of the functional group and n is the carbon number. Values of $[AN_g/AN_T]_{eq}$ for the 1- though 6-dodecyl nitrate isomers were then plotted versus λ and fit to the expression

$$[AN_g/AN_T]_{eq} = A + B\lambda^x \tag{5}$$

with $A = 0.782$, $B = -0.877$, and $x = 7.25$, as shown in Figure 1.3.

Figure 1.3: Relationship between $[AN_g/AN_T]_{eq}$ and the position coefficient, $\lambda = 1 - z/n$, for the C_{12} 1- through 6-dodecyl nitrate isomers. The curve is a nonlinear least-squares fit of the data to the equation $[AN_g/AN_T]_{eq} = A + B\lambda^x$.

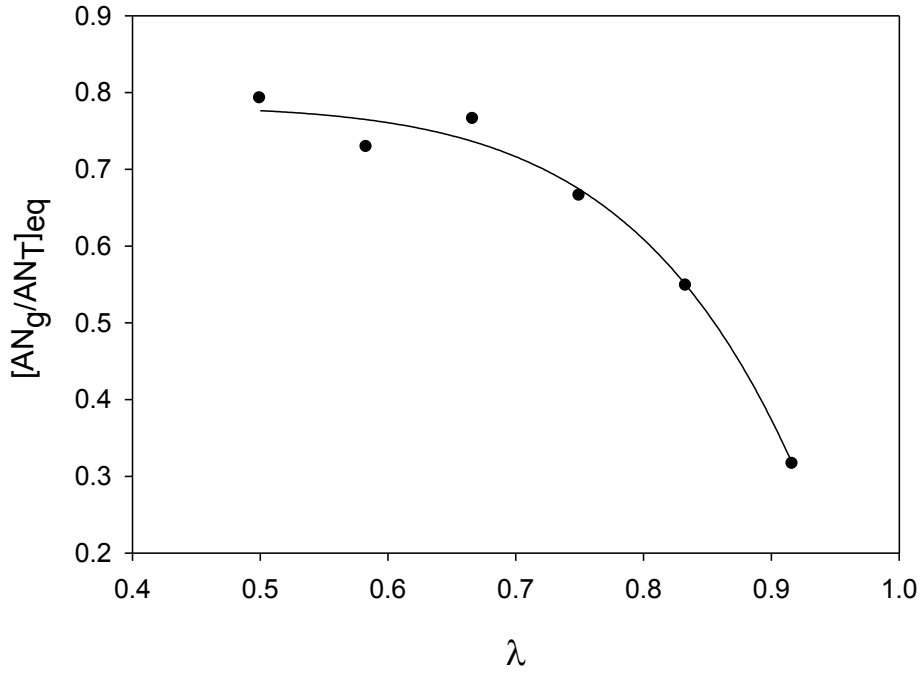

There are a variety of ways to combine the empirical relationships determined above for the effects of carbon number and isomer structure on gas-wall partitioning to correct the measured alkyl nitrate yields for partitioning to the walls. Our goal here, however, was to go somewhat beyond that immediate need and develop a more general framework for describing gas-wall partitioning in terms of fundamental physical quantities. It is hoped that such an approach will ameliorate future attempts to make similar corrections. Because of the central role of vapor pressure in determining the extent of both gas-particle partitioning and gas-wall partitioning, and the simplicity and intuitive appeal of Equation (3), our approach was to begin by combining this equation with Equation (2) to obtain

$$[AN_g/AN_T]_{eq} = (1 + CRT/P_o)^{-1} \quad (6)$$

We then assumed that the vapor pressures of monofunctional compounds such as alkyl nitrates can be described by the group contribution equation

$$logP^o = D_{fg} + D_n n + D_i \lambda^y \quad (7)$$

where the first term accounts for the effect of the specific functional group, the second term accounts for the effect of carbon number, and the third term accounts for the isomer structure. Once the values of the parameters in Equation (7) are determined it can be used with Equation (6) to calculate values of $[AN_g/AN_T]_{eq}$ for all alkyl nitrate products.

The values of D_n and $D_o = D_{fg} + D_i\lambda^y$, with D_o treated as a constant, were determined to be –0.465 and 5.36 from a linear least-squares fit of Equation (7) to a plot $logP^o$ versus n created using the vapor pressures of a series of 2-alkyl nitrates measured by Luxenhofer et al. (1996). The values of D_i, y, and $D_1 = D_{fg} + D_n n$, with D_1 treated as

constant, were determined to be –1.57, 6.53, and 0.203 from a non-linear least squares fit of Equation (7) to a plot of $logP^o$ versus λ created using vapor pressures calculated for the C_{12} 1- through 6-dodecyl nitrate isomers using the equation

$$logP^o = \log(CRT/((A + B\lambda^x)^{-1} - 1)) \qquad (8)$$

obtained by combining Equations (5) and (6). The plots are shown in Figures 1.4a and b.

Figure 1.4: Relationship between $logP^o$ and (a) carbon number, n, for C_8, C_{10}, C_{12}, and C_{14} 2-alkyl nitrates, and (b) the position coefficient, $\lambda = (1 - z/n)$, for the C_{12} 1- through 6-dodecyl nitrate isomers.

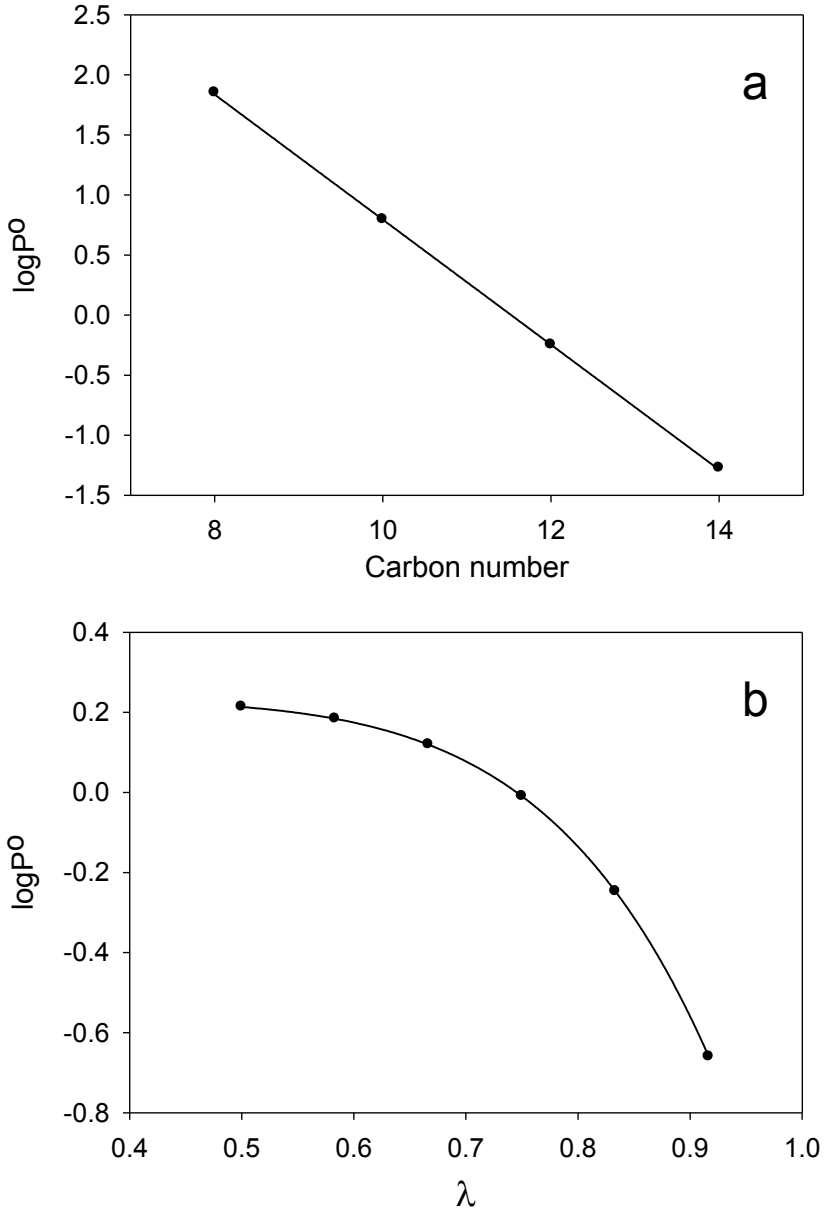

The values of D_{fg} calculated from D_o and D_1 using D_n = -0.465 D_i = -1.57, y = 6.53, n = 12, and λ = 0.833, were 5.84 and 5.78, respectively. These values are in good agreement, and an average value of 5.81 was used in future calculations. Values of $[AN_g/AN_T]_{eq}$ were then calculated for all the C_8–C_{14} alkyl nitrate isomer products by substituting values of P^o calculated using the equation

$$logP^o = 5.81 - 0.465n - 1.57\lambda^{6.53} \quad (9)$$

into Equation (6) with C = 1.79 x 10^{-4}. The values of $[AN_g/AN_T]_{eq}$ predicted by this equation are plotted against the measured values in Figure 1.5.

Figure 1.5: Values of $[AN_g/AN_T]_{eq}$ predicted by the gas-wall partitioning structure-activity model versus measured values.

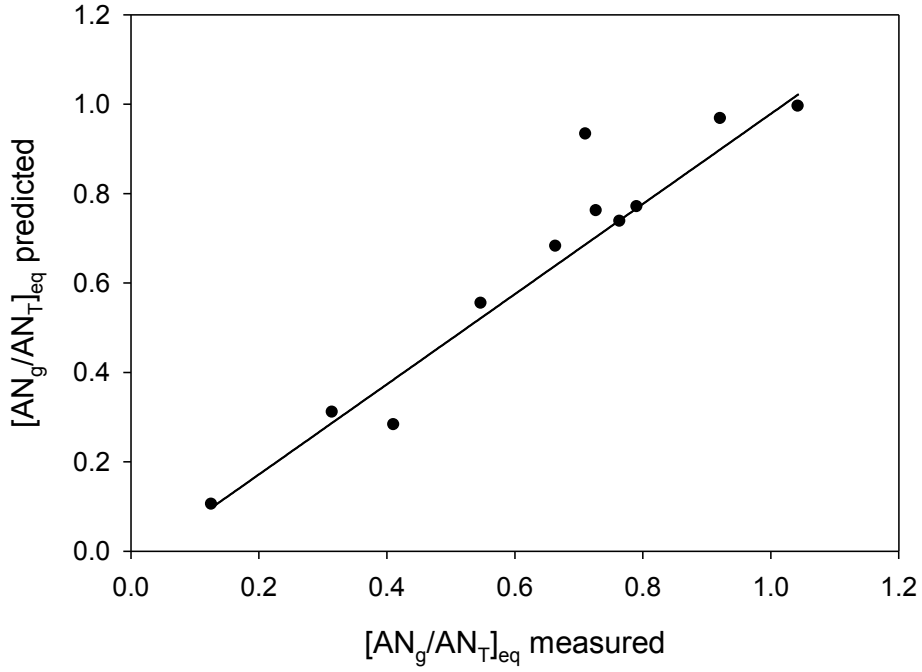

The agreement between predicted and measured values is very good: $r^2 = 0.939$, the slope of 1.01 is close to one, and the intercept of -0.036 is close to zero. This indicates that the approach employed here provides a good framework for modeling the effects of carbon number and isomer structure on gas-wall partitioning of alkyl nitrates.

Measured yields of secondary alkyl nitrates corrected for gas-wall partitioning

Molar yields of secondary alkyl nitrate isomers corrected for secondary reactions with OH radicals and for gas-wall partitioning are shown in Table 1.2, and the total yields of secondary alkyl nitrates obtained by summing the corrected isomer yields are plotted versus carbon number in Figure 1.6.

Table 1.2: Average molar yields of secondary alkyl nitrate isomers from the reactions on *n*-alkanes with OH radicals, corrected for secondary OH reaction, and for gas-wall partitioning. The previous results are from Arey et al., 2001 and Aschmann et al., 2001 for C_8 and C_{10}, respectively. The values are from the yield estimation model parameters reported by Arey et al., 2001.

n-alkane	Uncorrected Yield	Secondary Reaction Corrected Yield	Wall Loss Corrected Yield	Previous Results	Predicted
octane	0.200±0.037	0.208±0.024	0.209±0.024	0.226±0.032	0.233
decane	0.178±0.041	0.189±0.033	0.198±0.035	0.226±0.038	0.265
dodecane	0.162±0.045	0.165±0.036	0.247±0.051	—	0.278
tridecane	0.122±0.035	0.125±0.026	0.284±0.067	—	0.282
tetradecane	0.065±0.026	0.086±0.024	0.309±0.090	—	0.285

Figure 1.6: Branching ratios for alkyl nitrate formation corrected for secondary reactions (filled circles), and secondary reactions and gas-wall partitioning (empty circles), plotted as a function of carbon number. Error bars are the sum of two standard deviations and GC error of ± 5%. Also shown are measured values from Arey et al., 2001 (filled triangles), Aschmann et al., 2001 (empty triangle), and predictions of the model presented in Arey et al., 2001.

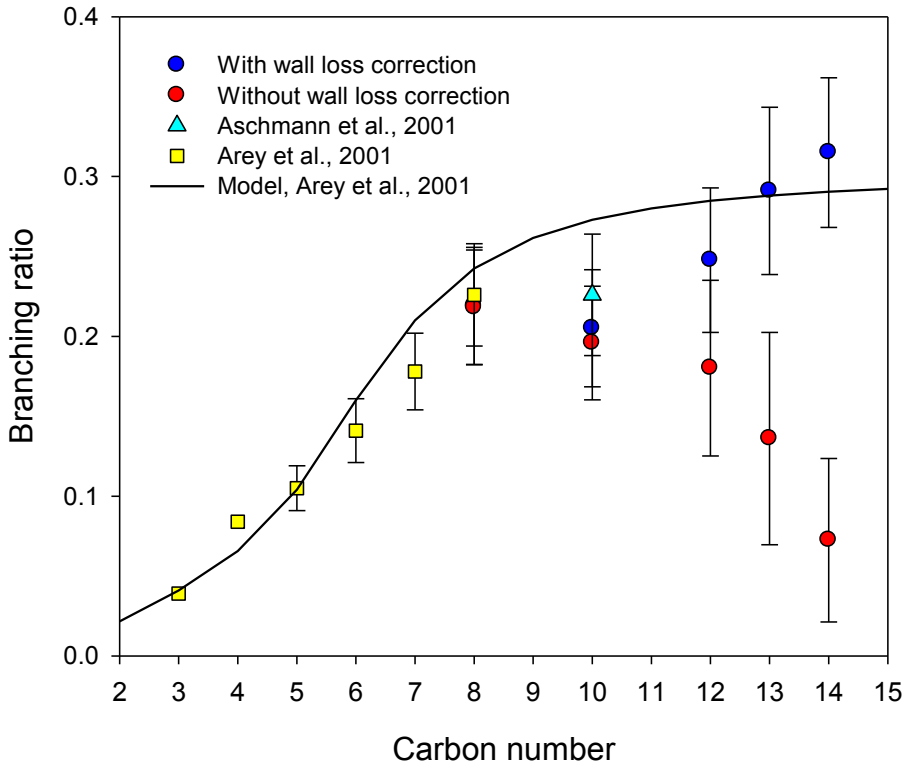

Also shown in the figure are previously-reported secondary alkyl nitrate yields measured from environmental chamber reactions of C_5–C_8 (Arey et al., 2001) and C_{10} (Aschmann et al., 2001) *n*-alkanes, and yields calculated up to C_{16} using the version of the Atkinson et al. (Atkinson et al., 1983) model presented by Arey et al. (Arey et al., 2001).

With the inclusion of corrections for gas-wall partitioning, alkyl nitrate yields were within 20% of the model-predicted yields. The largest deviation was observed for the reactions of *n*-decane, where the measured average yield of 0.198 was almost 30% lower than the predicted yield of 0.265. Those reactions were conducted at room temperatures of 300 and 301 K, which are on average 2.5 K higher than the temperature of 298 K used in the model calculations. Since according to the model the alkyl nitrate yields decrease with increasing temperature by 0.005 K^{-1}, the estimated temperature-corrected yield at 298 K is 0.21, which is still ~25% less than the predicted value. This should not necessarily be surprising, however, since the model predicts yields that are slightly higher than the values measured by Arey et al. (Arey et al., 2001) for the C_6–C_8 *n*-alkanes, even though these measurements do not have errors due to gas-wall partitioning and were used to determine the model parameters. The yields of alkyl nitrates with smaller carbon numbers and with branched and cyclic structures, which were also used to determine the model parameters, apparently shifted the model predictions to values that are slightly higher than those of (at least) the C_6–C_8 *n*-alkanes. The reactions of the C_{12}–C_{14} n-alkanes were conducted at temperatures ranging from 297–300 K with an average of 299 ± 1K.

Branching ratios for the formation of secondary alkyl nitrates from reactions of secondary RO_2• radicals with NO were also determined for individual alkyl nitrate isomers by dividing the amount of each alkyl nitrate isomer formed by the amount of the corresponding RO_2• radical isomer formed. Alkyl nitrate isomers were quantified by GC/FID measurements, and the amounts of the corresponding RO_2• radical isomers formed were determined using the measured amount of *n*-alkane reacted and the fraction of each possible RO_2• radical isomer formed, as calculated using the structure-reactivity method of Kwok and Atkinson (Kwok and Atkinson, 1995) for abstraction of H atoms by OH radicals (noting that the corresponding RO_2• radical is then formed by addition of O_2). It was also assumed that branching ratios for alkyl nitrate formation are the same for all secondary RO_2• radical isomers, regardless of the location of the peroxy group on the alkyl chain. The branching ratios corrected for secondary reactions are compared with those corrected for secondary reactions and gas-wall partitioning in Table 1.3.

Table 1.3: The branching ratios corrected for secondary reactions are compared with those corrected for secondary reactions and gas-wall partitioning. The predicted branching ratios are calculated by dividing the predicted isomer yields (Arey et al., 2001) by the predicted yields of alkyl peroxy isomers formed by the reaction of OH with n-alkane. Error is two least squares standard deviations plus ±5% GC/FID error.

Secondary reaction-corrected branching ratios

n-alkane	2-nitrate	3-nitrate	4-nitrate	5-nitrate	6-nitrate	7-nitrate	Average	Predicted
C_8	0.231±0.028	0.216±0.041	0.207±0.024	—	—	—	0.218±0.036	0.243
C_{10}	0.215±0.025	0.186±0.025	0.191±0.019	0.191±0.019	—	—	0.196±0.036	0.273
C_{12}	0.153±0.023	0.164±0.018	0.177±0.022	0.204±0.033	0.203±0.019	—	0.180±0.055	0.285
C_{13}	0.090±0.033	0.119±0.010	0.128±0.011	0.149±0.018	0.166±0.015	0.165±0.015	0.136±0.066	0.288
C_{14}	0.031±0.002	0.059±0.010	0.073±0.018	0.088±0.017	0.091±0.016	0.091±0.016	0.072±0.051	0.290

Secondary reaction- and wall loss-corrected branching ratios

n-alkane	2-nitrate	3-nitrate	4-nitrate	5-nitrate	6-nitrate	7-nitrate	Average	Predicted
C_8	0.233±0.028	0.217±0.041	0.207±0.024	—	—	—	0.219±0.037	0.243
C_{10}	0.230±0.027	0.194±0.026	0.198±0.020	0.197±0.020	—	—	0.205±0.044	0.273
C_{12}	0.273±0.042	0.238±0.026	0.236±0.030	0.263±0.042	0.259±0.025	—	0.254±0.045	0.285
C_{13}	0.319±0.119	0.292±0.025	0.262±0.023	0.281±0.034	0.297±0.027	0.297±0.027	0.291±0.052	0.288
C_{14}	0.293±0.022	0.338±0.054	0.314±0.080	0.326±0.063	0.308±0.055	0.308±0.055	0.315±0.047	0.290

The most obvious differences are at high carbon numbers, where effects of gas-wall partitioning are most pronounced. At carbon numbers C_{13} and C_{14}, branching ratios corrected only for secondary reactions deviated significantly among isomers. For example, branching ratios for the formation of 2-alkyl nitrates were ~60% of those for 7-alkyl nitrates, even though they are expected to be the same. Once the branching ratios were corrected for gas-wall partitioning, however, the values were similar and within experimental uncertainties. These results, which for C_{14} involve extremely large isomer-specific corrections of branching ratios that range from factors of 3–9, further demonstrate the power of the structure-activity model developed here for modeling gas-wall partitioning of organic compounds in Teflon film chambers.

Conclusions

In this study it was demonstrated that the branching ratios for the formation of alkyl nitrates from the reactions of *n*-alkanes with OH radicals in the presence of NO increase with increasing carbon number to a plateau of ~0.30 at about C_{13}–C_{14}. The values at the plateau are in good agreement with those predicted by the model of Arey et al. 2001, confirming the validity of this model for calculating the dependence of alkyl nitrate branching ratios on carbon number. The experiments conducted to accurately measure alkyl nitrate yields were extremely challenging due to loss of alkyl nitrates to the walls of the Teflon chamber by gas-wall partitioning. Accurate corrections for these losses were possible, however, through the use of an isomer- and carbon number-specific structure-activity model that was developed here using results of gas-wall partitioning studies conducted with synthesized alkyl nitrate standards. Corrections were necessary for carbon numbers $\geq C_{10}$, and when applied changed the trend from one in which the branching ratio decreased with increasing carbon number to one in which it increased to a plateau. These results, which for C_{14} involve extremely large isomer-specific corrections of branching ratios that range from factors of 3–9, demonstrate the power of the structure-activity model developed here for modeling gas-wall partitioning of organic compounds in Teflon film chambers. Branching ratios for the formation of β-hydroxynitrates from similar reactions of internal alkenes, 1-alkenes, and 2-methyl-1-alkenes, which could be more easily measured for large carbon numbers because they were present entirely in SOA and so suffered only minor and easily predicted wall losses, also increased with increasing carbon number to a plateau at C_{14}-C_{15} (Matsunaga 2009,

Matsunaga 2010a). Combining these results, it appears that the "cooling" effect of increased chain length on the excited alkyl peroxy-NO intermediate formed in these reactions reaches a point of diminishing returns at about C_{13}–C_{15}, as has also been predicted by computational studies (Zhang et al., 2004).

An ability to predict the branching ratios for the formation of alkyl nitrates from the reactions of alkyl peroxy radicals with NO is important, because the formation of these compounds terminates the propagation of a radical chain that would otherwise lead to the formation of lower volatility products that are more likely to form SOA. Under typical atmospheric conditions, alkyl nitrates smaller than ~C_{15} do not partition significantly into particles and so would require a second oxidation event to form SOA (Lim and Ziemann, 2009). Conversely, if an alkoxy radical is formed, then those with linear structures (and many with branched structures as well) will isomerize and react further to form a 1,4-hydroxynitrate or 1,4-hydroxycarbonyl. These multifunctional compounds are more likely to form SOA than monofunctional alkyl nitrates, which require a secondary reaction with OH to add another functional group. In this case, lower alkyl nitrate yields will probably lead to higher SOA yields. This will not necessarily be the case for branched alkanes, however, since the tendency for alkoxy radicals to decompose increases with chain branching. The effects on alkyl nitrate yields on SOA formation will therefore depend on the alkane structure.

References

1. Alfaro-Moreno, E., Nawrot, T. S., Nemmar, A., & Nemery, B. (**2007**). Particulate matter in the environment: pulmonary and cardiovascular effects. *Current Opinion in Pulmonary Medicine*, 13(2), 98-106..

2. Andreae, M. O., & Rosenfeld, D. (**2008**). Aerosol–cloud–precipitation interactions. Part 1. The nature and sources of cloud-active aerosols. *Earth-Science Reviews*, 89(1), 13-41.

3. Arey, J., Aschmann, S. M., Kwok, E. S., & Atkinson, R. (**2001**). Alkyl nitrate, hydroxyalkyl nitrate, and hydroxycarbonyl formation from the NO_x-air photooxidations of C_5-C_8 *n*-alkanes. *The Journal of Physical Chemistry A*, 105(6), 1020-1027.

4. Aschmann, S. M., Arey, J., & Atkinson, R. (**2001**). Atmospheric chemistry of three C_{10} alkanes. *The Journal of Physical Chemistry A*, 105(32), 7598-7606.

5. Aschmann, S. M., Long, W. D., & Atkinson, R. (**2006**). Pressure dependence of pentyl nitrate formation from the OH radical-initiated reaction of *n*-pentane in the presence of NO. *The Journal of Physical Chemistry A*, 110(21), 6617-6622.

6. Atkinson, R., Carter, W. P., Winer, A. M., & Pitts Jr, J. N. (**1981**). An experimental protocol for the determination of OH radical rate constants with organics using methyl nitrite photolysis as an OH radical source. *Journal of the Air Pollution Control Association*, 31(10), 1090-1092.

7. Atkinson, R., Aschmann, S. M., Carter, W. P., Winer, A. M., & Pitts Jr, J. N. (**1982**). Alkyl nitrate formation from the nitrogen oxide (NO_x)-air photooxidations of C_2-C_8 *n*-alkanes. *The Journal of Physical Chemistry*, 86(23), 4563-4569.

8. Atkinson, R., Carter, W. P., & Winer, A. M. (**1983a**). Effects of temperature and pressure on alkyl nitrate yields in the nitrogen oxide (NO_x) photooxidations of n-pentane and n-heptane. *The Journal of Physical Chemistry*, 87(11), 2012-2018.

9. Atkinson, R., Carter, W. P., & Winer, A. M. (**1983b**). Effects of pressure on product yields in the nitrogen oxide (NO_x) photooxidations of selected aromatic hydrocarbons. *The Journal of Physical Chemistry*, 87(9), 1605-1610.

10. Atkinson, R., Plum, C. N., Carter, W. P., Winer, A. M., & Pitts Jr, J. N. (**1984**). Rate constants for the gas-phase reactions of nitrate radicals with a series of organics in air at 298 ±1 K. *The Journal of Physical Chemistry*, 88(6), 1210-1215.

11. Atkinson, R., Aschmann, S. M., & Winer, A. M. (**1987**). Alkyl nitrate formation from the reaction of a series of branched RO_2 radicals with NO as a function of temperature and pressure. *Journal of Atmospheric Chemistry*, 5(1), 91-102.

12. Atkinson, R. "*Atmospheric oxidation*" pp.335-354 in *Handbook of Property Estimation Methods for Chemicals: Environmental and Health Services*; Boethling, R.S.; Mackay, D., Eds. CRC Press: Boca Raton, FL, 2000.

13. Atkinson, R., & Arey, J. (**2003**). Atmospheric degradation of volatile organic compounds. *Chemical Reviews*, 103(12), 4605-4638.

14. Atkinson, R. (**2007**). Gas-phase tropospheric chemistry of organic compounds: a review. *Atmospheric Environment*, 41, 200-240.

15. Atkinson, R., Arey, J., & Aschmann, S. M. (**2008**). Atmospheric chemistry of alkanes: Review and recent developments. *Atmospheric Environment*, 42(23), 5859-5871.

16. Ballschmiter, K. (**2002**). A marine source for alkyl nitrates. *Science*, 297(5584), 1127-1128.

17. Calvert, J.G.; Atkinson, R.; Becker, K.H.; Kamens, R.M.; Seinfeld, J.H.; Wallington, T.J.; Yarwood, G. *The Mechanisms of Atmospheric Oxidation of Aromatic Hydrocarbons*; Oxford University Press: New York, NY, 2002.

18. Carter, W. P., & Atkinson, R. (**1985**). Atmospheric chemistry of alkanes. *Journal of Atmospheric Chemistry*, 3(3), 377-405.

19. Carter, W. P., & Atkinson, R. (**1989**). Alkyl nitrate formation from the atmospheric photooxidation of alkanes; a revised estimation method. *Journal of atmospheric chemistry*, 8(2), 165-173.

20. Cassanelli, P., Johnson, D., & Cox, R. A. (**2005**). A temperature-dependent relative-rate study of the OH initiated oxidation of *n*-butane: The kinetics of the reactions of the 1-and 2-butoxy radicals. *Physical Chemistry Chemical Physics*, 7(21), 3702-3710.

21. Cassanelli, P., Fox, D. J., & Cox, R. A. (**2007**). Temperature dependence of pentyl nitrate formation from the reaction of pentyl peroxy radicals with NO. *Physical Chemistry Chemical Physics*, 9(31), 4332-4337.

22. Chow, J. M., Miller, A. M., & Elrod, M. J. (**2003**). Kinetics of the $C_3H_7O_2$+ NO reaction: Temperature dependence of the overall rate constant and the i-$C_3H_7ONO_2$ branching channel. *The Journal of Physical Chemistry A*, 107(17), 3040-3047.

23. Cleary, P.A.; Murphy, J.G.; Wooldridge, P.J.; Day, D.A.; Millet, D.B.; McKay, M.; Goldstein, A.H.; Cohen R.C. (**2005**). Observations of total alkyl nitrates within the Sacramento Urban Plume. *Atmospheric Chemistry and Physics Discussions*, 5(4), 4801-4843.

24. Day, D. A., Dillon, M. B., Wooldridge, P. J., Thornton, J. A., Rosen, R. S., Wood, E. C., & Cohen, R. C. (**2003**). On alkyl nitrates, O_3, and the "missing NO_y". *Journal of Geophysical Research*, 108(D16), 4501.

25. Day, D. A., Farmer, D. K., Goldstein, A. H., Wooldridge, P. J., Minejima, C., & Cohen, R. C. (**2009**). Observations of NO_x, ΣPNs, ΣANs, and HNO_3 at a rural site in the California Sierra Nevada Mountains: summertime diurnal cycles. *Atmospheric Chemistry and Physics*, 9(14), 4879-4896.

26. Dickerson, R. R., Kondragunta, S., Stenchikov, G., Civerolo, K. L., Doddridge, B. G., & Holben, B. N. (**1997**). The impact of aerosols on solar ultraviolet radiation and photochemical smog. *Science*, 278(5339), 827-830.

27. Espada, C., Grossenbacher, J., Ford, K., Couch, T., & Shepson, P. B. (**2005**). The production of organic nitrates from various anthropogenic volatile organic compounds. *International Journal of Chemical Kinetics*, 37(11), 675-685.

28. Etzel, R. A. (**2003**). How environmental exposures influence the development and exacerbation of asthma. *Pediatrics*, 112(Supplement 1), 233-239.

29. Finlayson-Pitts, B. J., & Pitts, J. N. (**1997**). Tropospheric air pollution: ozone, airborne toxics, polycyclic aromatic hydrocarbons, and particles. *Science*, 276(5315), 1045-1051.

30. Flocke, F., Volz-Thomas, A., Buers, H. J., Pätz, W., Garthe, H. J., & Kley, D. (**1998**). Long-term measurements of alkyl nitrates in southern Germany 1. General behavior and seasonal and diurnal variation. *Journal of Geophysical Research*, 103(D5), 5729-5746.

31. Forster, P.; Ramaswamy, V.; Artaxo, P.; Berntsen, T.; Betts, R.; Fahey, D.W.; Haywood, J.; Lean, J.; Lowe, D.C.; Myhre, G.; Nganga, J.; Prinn, R.; Raga, G.; Schulz, M.; Van Dorland, R. *"Changes in Atmospheric Constituents and in Radiative Forcing"* in *Climate Change 2007: The Physical Science Basis. Contribution of Working Group I to the Fourth Assessment Report of the Intergovernmental Panel on Climate Change*; Solomon, S.; Qin, D.; Manning, M.; Chen, Z.; Marquis, M.; Averyt, K. B.; Tignor, M.; Miller, H. L., Eds. Cambridge University Press, New York, NY, 2007.

32. Gentner, D.R.; Isaacman G.; Worton, D.R.; Chan, A.W.; Dallmann, T.R.; Davis, L.; Liu, S; Day, D.A.; Russell, L.M.; Wilson, K.R.; Weber, R.; Guha, A.; Harley, R.A.; Goldstein, A.H. (**2012**). Elucidating secondary organic aerosol from diesel and gasoline vehicles through detailed characterization of organic carbon emissions. *Proceedings of the National Academy of Sciences*, 109(45), 18318-18323.

33. Harris, S. J., & Kerr, J. A. (**1989**). A kinetic and mechanistic study of the formation of alkyl nitrates in the photo-oxidation of *n*-heptane studied under atmospheric conditions. *International Journal of Chemical Kinetics*, 21(3), 207-218.

34. Kames, J., Schurath, U., Flocke, F., & Volz-Thomas, A. (**1993**). Preparation of organic nitrates from alcohols and N_2O_5 for species identification in atmospheric samples. *Journal of Atmospheric Chemistry*, 16(4), 349-359.

35. Kvenvolden, K. A., Rapp, J. B., Golan-Bac, M., & Hostettler, F. D. (**1987**). Multiple sources of alkanes in Quaternary oceanic sediment of Antarctica. *Organic Geochemistry*, 11(4), 291-302.

36. Kwok, E. S., & Atkinson, R. (**1995**). Estimation of hydroxyl radical reaction rate constants for gas-phase organic compounds using a structure-reactivity relationship: An update. *Atmospheric Environment*, 29(14), 1685-1695.

37. Lesar, A., Hodošcek, M., Drougas, E., & Kosmas, A. M. (**2006**). Quantum mechanical investigation of the atmospheric reaction CH_3O_2+ NO. *The Journal of Physical Chemistry A*, 110(25), 7898-7903.

38. Lim, Y. B., & Ziemann, P. J. (**2005**). Products and mechanism of secondary organic aerosol formation from reactions of *n*-alkanes with OH radicals in the presence of NO_x. *Environmental Science & Technology*, 39(23), 9229-9236.

39. Lim, Y. B., & Ziemann, P. J. (**2009**). Chemistry of secondary organic aerosol formation from OH radical-initiated reactions of linear, branched, and cyclic alkanes in the presence of NO_x. *Aerosol Science and Technology*, 43(6), 604-619.

40. Lockwood, A. L., Shepson, P. B., Fiddler, M. N., & Alaghmand, M. (**2010**). Isoprene nitrates: preparation, separation, identification, yields, and atmospheric chemistry. *Atmospheric Chemistry and Physics*, 10(13), 6169-6178.

41. Lohmann, U., & Feichter, J. (**2005**). Global indirect aerosol effects: a review. *Atmospheric Chemistry and Physics*, 5(3), 715-737.

42. Lurmann, F.W.; Main, H.H. *Analysis of the Ambient VOC Data Collected in the Southern California Air Quality Study*; Final Report to California Air Resources Board Contract No. A832-130, Sacramento, CA, February 1992.

43. Luxenhofer, O., Schneider, M., Dambach, M., & Ballschmiter, K. (**1996**). Semivolatile long chain C_6–C_{17} alkyl nitrates as trace compounds in air. *Chemosphere*, 33(3), 393-404.

44. Ma, S. X., Rindelaub, J. D., McAvey, K. M., Gagare, P. D., Nault, B. A., Ramachandran, P. V., & Shepson, P. B. (**2011**). α-Pinene nitrates: synthesis,

yields and atmospheric chemistry. *Atmospheric Chemistry and Physics*, 11(13), 6337-6347.

45. Matsunaga, A., & Ziemann, P. J. (**2009**). Yields of β-hydroxynitrates and dihydroxynitrates in aerosol formed from OH radical-initiated reactions of linear alkenes in the presence of NO_x. *The Journal of Physical Chemistry A*, 113(3), 599-606.

46. Matsunaga, A., & Ziemann, P. J. (**2010a**). Yields of β-hydroxynitrates, dihydroxynitrates, and trihydroxynitrates formed from OH radical-initiated reactions of 2-methyl-1-alkenes. *Proceedings of the National Academy of Sciences*, 107(15), 6664-6669.

47. Matsunaga, A., & Ziemann, P. J. (**2010b**). Gas-wall partitioning of organic compounds in a Teflon film chamber and potential effects on reaction product and aerosol yield measurements. *Aerosol Science and Technology*, 44(10), 881-892.

48. McMurry, P. H., & Grosjean, D. (**1985**). Gas and aerosol wall losses in Teflon film smog chambers. *Environmental Science & Technology*, 19(12), 1176-1182.

49. O'Brien, J. M., Czuba, E., Hastie, D. R., Francisco, J. S., & Shepson, P. B. (**1998**). Determination of the hydroxy nitrate yields from the reaction of C_2-C_6 alkenes with OH in the presence of NO. *The Journal of Physical Chemistry A*, 102(45), 8903-8908.

50. Orlando, J. J., Iraci, L. T., & Tyndall, G. S. (**2000**). Chemistry of the cyclopentoxy and cyclohexoxy radicals at subambient temperatures. *The Journal of Physical Chemistry A*, 104(21), 5072-5079.

51. Pope, C. A., Ezzati, M., & Dockery, D. W. (**2009**). Fine-particulate air pollution and life expectancy in the United States. *New England Journal of Medicine*, 360(4), 376-386.

52. Robinson, P.J.; Holbrook, K.A. *Unimolecular Reactions* Wiley, New York, NY, 1972.

53. Rollins, A.W.; Kiendler-Scharr, A.; Fry, J.L.; Brauers, T.; Brown, S.S.; Dorn, H.-P.; Dubé, W.P.; Fuchs, H.; Mensah, A.; Mentel, T.F.; Rohrer, F.; Tillmann, R.; Wegener, R.; Wooldridge, P.J.; Cohen, R.C. (**2009**). Isoprene oxidation by nitrate radical: alkyl nitrate and secondary organic aerosol yields. *Atmospheric Chemistry and Physics*, 9(18), 6685-6703

54. Rosen, R.S., Wood E.C.; Wooldridge, P.J.; Thornton, J.A.; Day, D.A.; Kuster, W.; Williams, E.J.; Jobson, B.T.; Cohen, R.C. (**2003**). On alkyl nitrates, O_3, and the "missing NO_y". *Journal of Geophysical Research*, 108(D16), 4501.

55. Russo, R.S.; Zhou, Y.; Haase, K.B.; Wingenter, O.W.; Frinak, E.K.; Mao, H.; Talbot, R.W.; Sive, B.C. (**2010**). Temporal variability, sources, and sinks of C_1-C_5 alkyl nitrates in coastal New England. *Atmospheric Chemistry and Physics*, 10(4), 1865-1883.

56. Saito, T., Kawamura, K., Nakatsuka, T., & Huebert, B. J. (**2004**). In situ measurements of butane and pentane isomers over the subtropical North Pacific. *Geochemical Journal*, 38(5), 397-404.

57. Scanlon, J. T., & Willis, D. E. (**1985**). Calculation of flame ionization detector relative response factors using the effective carbon number concept. *Journal of Chromatographic Science*, 23(8), 333-340.

58. Schneider, M., & Ballschmiter, K. (**1999**). C_3-C_{14} alkyl nitrates in remote south Atlantic air. *Chemosphere*, 38(1), 233-244.

59. Taylor, W. D., Allston, T. D., Moscato, M. J., Fazekas, G. B., Kozlowski, R., & Takacs, G. A. (**1980**). Atmospheric photodissociation lifetimes for nitromethane, methyl nitrite, and methyl nitrate. *International Journal of Chemical Kinetics*, 12(4), 231-240..

60. Williams, J.; Koppmann, R. "*Volatile organic compounds in the atmosphere: an overview"* pp. 1-19 in *Volatile organic compounds in the atmosphere*; Koppmann, R., Ed. Blackwell Publishing Ltd.: Oxford, UK, 2007.

61. Zhang, J., Dransfield, T., & Donahue, N. M. (**2004**). On the mechanism for nitrate formation via the peroxy radical + NO reaction. *The Journal of Physical Chemistry A*, 108(42), 9082-9095.

62. Zhang, Q.; Jimenez, J.L.; Canagaratna, M.R.; Allan, J.D.; Cole, H.; Ulbrich, I.; Alfarra, M.R.; Takami, A.; Middlebrook, A.M.; Sun, Y.L.; Dzepina, K.; Dunlea, E.; Docherty, K.; DeCarlo, P.F.; Salcedo, D.; Onasch, T.; Jayne, J.T.; Miyoshi, T.; Shimono, A.; Hatakeyama, S.; Takegawa, N.; Kondo, Y.; Schneider, J.; Zrewnick, F.; Borrmann, S.; Weimer, S.; Demerjian, K.; Williams, P.; Bower, K.; Zahreini, R.; Cottrell, L.; Griffin, R.J.; Rautiainen, J.; Sun, J.Y.; Zhang, Y.M.; Worsnop, D.R. (**2007**). Ubiquity and dominance of oxygenated species in organic aerosols in anthropogenically-influenced Northern Hemisphere midlatitudes. *Geophysical Research Letters*, 34(13), L13801.

63. Zhao, Y., Houk, K. N., & Olson, L. P. (**2004**). Mechanisms of peroxynitrous acid and methyl peroxynitrite, ROONO (R = H, Me), rearrangements: A conformation-dependent homolytic dissociation. *The Journal of Physical Chemistry A*, 108(27), 5864-5871.

64. Ziemann, P. J. (**2011**). Effects of molecular structure on the chemistry of aerosol formation from the OH-radical-initiated oxidation of alkanes and alkenes. *International Reviews in Physical Chemistry*, 30(2), 161-195.

Chapter 2: Identification and product yields of 1,4-hydroxynitrates in particles formed from the reactions of C_8–C_{16} *n*-alkanes with OH radicals in the presence of NO_x

Abstract

In this study, a series of C_8–C_{16} *n*-alkanes were reacted with OH radicals in the presence of NO_x in an environmental chamber. The particles were sampled by filtration, extracted, and the 1,4-hydroxynitrate reaction products were analyzed by high-performance liquid chromatography with quantitation by UV absorption and identification by electron ionization mass spectrometry (HPLC/UV/MS). Observed mass spectral patterns can be explained using proposed mechanisms for ion fragmentation, permitting the identification of each 1,4-hydoxynitrate isomer. It is shown that the retention of these compounds in reversed-phase chromatography is determined by the length of the longer of two alkyl chains that are attached to opposite ends of the 1,4-hydroxynitrate subunit. 1,4-Hydroxynitrates were quantified in particles using authentic synthesized analytical standards for calibration, and the results were combined with gas chromatography/flame ionization detection measurements of the amounts of *n*-alkane reacted to determine the molar yields. Yields increased with increasing carbon number from 0.00 for C_8 to an average plateau value of 0.130 ± 0.008 for C_{14}–C_{16}, due primarily to enhanced gas-to-particle partitioning of less volatile 1,4-hydroxynitrates. The value at the plateau, where essentially all 1,4-hydroxynitrates were in particles, was equal to the average total yield of C_{14}–C_{16} 1,4-hydroxynitrates. The average branching ratio for the formation of C_{14}–C_{16} 1,4-hydroxynitrates from the reaction of NO with the corresponding

1,4-hydroxyperoxy radicals was calculated to be 0.184 ± 0.011 from the ratio of the measured yields of 1,4-hydroxynitrates and the yields of 1,4-hydroxyperoxy radicals calculated using the model of Arey et al. (2001). This value is similar to the plateau value of 0.15 reported for reactions of secondary 1,2-hydroxyperoxy radicals and approximately 60% the value of 0.29 reported for reactions of secondary alkyl peroxy radicals, with the lower values for secondary 1,2- and 1,4-hydroxyperoxy radicals being due to the effects of hydrogen bonding between the hydroxyl and peroxy groups in the intermediate complex that is formed with NO during formation of 1,2- and 1,4-hydroxynitrates.

Introduction

Alkanes occur in the atmosphere primarily as a result of human activity and they constitute 40-50% of anthropogenic non-methane organic compound (NMOC) emissions (Lurmann and Main, 1992; Calvert et al., 2002; Williams and Koppmann, 2007). In the atmosphere, daytime reactions with OH radicals limit alkane lifetime to days (Atkinson et al., 2008). These daytime reactions produce a variety of oxygenated compounds including organic nitrates, such as alkyl nitrates and 1,4-hydroxynitrates, as well as carbonyls, 1,4-hydroxycarbonyls, and a host of multifunctional second-generation products (Lim and Ziemann, 2009; Ziemann and Atkinson, 2012). Organic nitrate formation in an atmosphere with high concentrations of NO_x, a condition typical of polluted atmospheres, is of great importance to accurate atmospheric modeling because NO_x is sequestered by the reaction. NO_x cycling catalytically generates ozone, one of the major atmospheric oxidants, and, depending on the degree of NO_x saturation in the atmosphere, sequestration of NO_x via organic nitrate formation can increase or decrease ozone levels (Day et al., 2003). The relationship between organic nitrate formation and ozone production illustrates that both accurate inventories of alkane emissions and accurate determination of organic nitrate yields are essential to modeling ozone concentrations and the atmospheric reactions mediated by ozone.

Alkane oxidation is increasingly recognized as an important source of secondary organic aerosol (SOA), as studies have shown that emissions of large, semi-volatile alkanes are higher than previously believed (Robinson et al., 2007; Gentner et al. 2012), and their oxidation products have sufficiently low vapor pressures to partition into

existing particles (Ziemann, 2011). SOA is a major component of airborne fine particulate matter (Zhang et al., 2007), which affects global climate by influencing cloud formation and reflectivity (Forster et al., 2007; Andreae and Rosenfeld, 2008) and by absorbing and scattering radiation (Dickersen et al., 1997; Lohmann and Feichter, 2005). Human health is also affected by fine particulate matter, as heart and lung disease, asthma, and mortality have been linked to particle exposure (Etzel, 2003; Alfaro-Moreno et al., 2007; Pope, 2007). More accurate models of the formation of SOA, ozone, and NO_x, and their environmental effects, will require more comprehensive and quantitative studies of the products of alkane-OH reactions (Atkinson and Arey, 2003; Ziemann and Atkinson, 2012).

The mechanism of the reaction of *n*-alkanes with OH radicals in air in the presence of NO is shown in Scheme 2.1.

Scheme 2.1: First generation reaction mechanism of n-alkane oxidation by OH radical in the presence of NO_x.

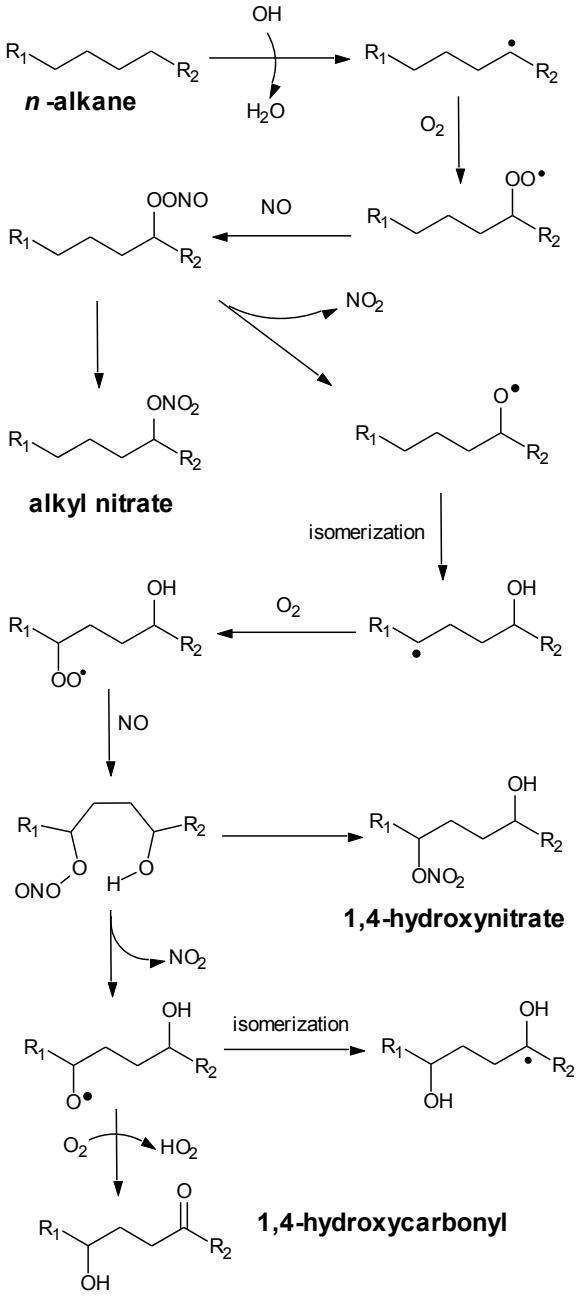

The reaction is initiated by abstraction of an H atom to form an alkyl radical and H_2O. The alkyl radical reacts solely with O_2 to form an alkyl peroxy radical, which reacts with NO to form either an alkyl nitrate or an alkoxy radical and NO_2. The alkoxy radical then isomerizes via a 1,5 H-atom shift to a 1,4-hydroxyalkyl radical, which reacts with O_2 to form a 1,4-hydroxyperoxy radical. Although alkoxy radicals can also react with O_2 or decompose, for *n*-alkanes larger than C_6 those reactions are too slow to compete with isomerization (Atkinson and Arey, 2003; Atkinson, 2007). The 1,4-hydroxyperoxy radical reacts with NO to form either a 1,4-hydroxynitrate or NO_2 and a 1,4-hydroxyalkoxy radical, which reverse isomerizes and reacts with O_2 to form a 1,4-hydroxycarbonyl and HO_2.

The molar yields of alkyl nitrates formed from reactions of *n*-alkanes have been investigated over the range of carbon numbers from C_2–C_{14} and observed to increase with increasing carbon number to a plateau value of ~0.3 at ~C_{12}–C_{14} (Arey et al., 2001; Chapter 1), consistent with model predictions (Atkinson et al., 1987; Arey et al., 2001), the yields of 1,4-hydroxynitrates are less well known. Arey et al. (Arey et al., 2001) measured yields of ~0.05 for C_5–C_8 1,4-hydroxynitrates using atmospheric pressure ionization mass spectrometry with NO_2^- as the reagent ion, whereas Lim and Ziemann (Lim and Ziemann, 2005) reported yields of ~0.15 for carbon numbers ≥ C_{14} measured using temperature-programmed thermal desorption particle beam mass spectrometry (TDPBMS). The lower yields of 1,4-hydroxynitrates compared to those of alkyl nitrates with similar carbon numbers are consistent with studies of OH radical-initiated reactions of 1-alkenes (Atkinson et al. 1995; O'Brien et al. 1998; Matsunaga and Ziemann 2009),

which indicate that branching ratios for the formation of 1,2-hydroxynitrates from reactions of 1,2-hydroxyperoxy radicals with NO are approximately one-half those of alkyl peroxy radicals due to the presence of a vicinal hydroxyl group. Nonetheless, the difference between the reported yields of 1,4-hydroxynitrates is much larger than can be explained by the difference in carbon numbers, as is likely due to the considerable uncertainties associated with both methods. More accurate yield measurements are thus necessary to better understand the effects of hydroxyl groups and molecular structure on the formation of organic nitrates.

The Aerodyne Aerosol Mass Spectrometer (AMS) (Aerodyne, Billerica, MA) is the most widely used instrument to study the composition of organic aerosols (Canagaratna et al., 2007). The AMS is typically operated to vaporize incoming particles at high temperature (600ºC), which partially fragments thermally labile compounds before they enter the electron impact ionization source. This approach is highly effective for the determination of elemental composition, but the AMS may be operated at lower temperatures as well. Vaporization at lower temperatures is useful for the determination of chemical structure of aerosol components (Robinson et al., 2011), making the AMS a potentially powerful tool for the identification of individual compounds present in aerosol. Because analytical standards of aerosol components such as the organic nitrates are unavailable, the electron impact fragmentation patterns of these compounds need to be better characterized so that they may be identified from AMS analysis of environmental chamber or ambient aerosol studies.

In the present study, C_8-C_{16} *n*-alkanes were reacted with OH radicals in the presence of NO_x in an environmental chamber and particulate 1,4-hydroxynitrates were collected on filters and analyzed by high-performance liquid chromatography with UV detection (HPLC/UV). This sampling method is well suited to determining yields at the plateau, since the vapor pressures of 1,4-hydroxynitrates larger than ~C_{12} are sufficiently low that these compounds exist essentially entirely in SOA particles formed in the reactions. The amounts of 1,4-hydroxynitrates measured in particles can therefore be used to quantify the total yields of 1,4-hydroxynitrates. These values must be corrected for losses of particles to the walls, but this correction is much simpler and more accurate than the corrections required for gas-wall partitioning of more volatile compounds such as alkyl nitrates (Chapter 1). The accuracy of quantitation was also improved by the use of authentic analytical standards of 1,4-hydroxynitrates that were purified from filter extracts and used for the preparation of standard curves. Structural confirmation of 1,4-hydroxynitrate products was obtained using the TDPBMS coupled to HPLC/UV, and an electron ionization fragmentation mechanism was developed that can be used to explain the observed mass spectra and identify each of the 1,4-hydroxynitrate isomers. Because standards of these compounds are not commercially available, this information can be useful for interpreting mass spectra obtained in laboratory and field studies using other instruments that employ electron ionization, such as the AMS (Canagaratna et al., 2007) and gas chromatography-mass spectrometers (GC-MS).

Experimental Methods

Chemicals

Acetonitrile, ethyl acetate, and water were HPLC grade and were purchased from Fisher Scientific. *n*-Octane (99+%), *n*-decane (99+%), *n*-dodecane (99+%), *n*-tridecane (99+%), *n*-pentadecane (99+%), *n*-hexadecane (99+%) and dioctyl sebacate (97%) were purchased from Sigma Aldrich. *n*-Tetradecane (99+%) was purchased from Alfa Aesar. Methyl nitrite was synthesized according to the procedure of Taylor et al. (Taylor et al., 1980) and kept on a glass vacuum rack in liquid nitrogen until used.

Environmental chamber experiments

Experiments were conducted in an 8.2 m^3 Teflon FEP environmental chamber filled with clean, dry air (<5 ppbv hydrocarbons, <0.1% RH) at room temperature (20–29°C) and pressure (740 torr). Two opposite sides of the chamber frame are covered by blacklights that are used to initiate photolysis reactions. Dioctyl sebacate (DOS) seed particles with ~100 nm diameter were generated in a flow of N_2 using an evaporation-condensation source and added to the chamber to achieve a mass concentration of ~100 μg m^{-3} as measured using a TSI 3081 scanning mobility particle sizer (SMPS) with a Model 3772 condensation particle counter, and then 1 ppmv of *n*-alkane and 10 ppmv each of methyl nitrite and NO were added from a glass bulb using a flow of N_2. The added NO prevents the formation of O_3 and NO_3 radicals. A Teflon-coated fan was run for 1 min after adding chemicals to enhance mixing, and then reactions were initiated by turning on the blacklights (irradiation equivalent to $J_{NO2} \sim 0.37$ min^{-1}) to generate OH radicals via methyl nitrite photolysis (Atkinson et al., 1981) for 3 min.

Concentrations of *n*-alkanes in the chamber were monitored over time by sampling air through stainless steel tubing and then into a glass tube containing Tenax TA solid adsorbent. Prior to sampling, chamber air was drawn through the stainless steel tubing for 20 min at 250 cm^3 min^{-1} using a mass flow controller to allow the walls of the tube to equilibrate with organic compounds. Samples were then collected for 10–15 min at the same flow rate. Samples were collected 60 and 30 min before initiating the reaction, and then 30, 90, and 150 min after the reaction. The samples were then transferred to the inlet of an Agilent 6890 gas chromatograph equipped with a 30 m x 0.32 mm Agilent DB-1701 column with 1 μm film thickness and flame ionization detection (FID). Analytes were thermally desorbed from the Tenax cartridge, and eluted on an 8ºC min^{-1} gradient.

Particle concentrations were continuously measured using the (SMPS), while reactions were monitored in real-time using a thermal desorption particle beam mass spectrometer (TDPBMS) that has been described previously (Tobias et al., 2000). Briefly, particles formed in chamber reactions are drawn through a series of aerodynamic lenses that focus the particles into a narrow beam, which then impacts in a notch on the tip of a copper rod that is resistively heated to 160ºC and located inside a high-vacuum detection chamber. The particles immediately evaporate, vapor molecules are ionized by 70 eV electrons, and the resulting ions are analyzed with a quadrupole mass spectrometer. The same instrument was used to analyze 1,4-hydroxynitrate isomers after they were fractionated by HPLC as described below, formed into an aerosol using a

Collison atomizer located downstream of the UV/Vis detector, dried of HPLC solvent by passing through diffusion driers, and then sampled into the TDPBMS for analysis.

Measurement of particulate 1,4-hydroxynitrates by HPLC/UV/MS

After turning off the lights, particles were sampled onto filters (Millipore Fluoropore, 0.45 μm pore size) at a flow rate of ~14 LPM that was measured before and after filter sampling (values typically within 5%) to obtain an average flow rate that was used for sample quantification. Samples were collected for 1–3 h depending on the aerosol mass concentration, which generally increased with increasing alkane carbon number. Filters were weighed before and after sampling to determine the mass of aerosol collected and then stored at –20°C until extraction. Particles were extracted twice from filters with 4 mL of ethyl acetate and the two extracts were combined. The solvent was dried in a stream of N_2 and the residue was weighed and then reconstituted in acetonitrile for injection into an Agilent 1100 HPLC with quaternary pump and UV/Vis detector. The column was a 4.0 x 150 mm Thermo BetaBasic C_{18} with 3 μm particles. Mobile phase A was 5% acetonitrile in water, mobile phase B was pure acetonitrile, the flow rate was 0.8 mL min^{-1}, and analytes eluted on a 0.67 %B min^{-1} gradient. A 6-port valve with a 100 μL sample loop was used for injection and the loop was overfilled to increase the precision of run-to-run injection volume, which was 100 μL. Water was not added to the injection solvent to avoid precipitation of sample components that might exhibit low water solubility. 1,4-Hydroxynitrates were detected at 210 nm as we have done previously (Matsunaga and Ziemann, 2009; Matsunaga and Ziemann, 2010a). Because UV absorbance by multifunctional compounds can be influenced by non-target functional

groups (in this case the hydroxyl group affecting the absorbance by the nitrooxy group), in order to ensure accurate quantitation an authentic analytical standard of the C_{15} 1,4-hydroxynitrates was prepared from the HPLC eluant by fraction collection. Fractions from several HPLC runs were pooled, dried under a stream of N_2, weighed, and reconstituted in acetonitrile to prepare the analytical standard. The peak area per μmol of 1,4-hydroxynitrate was determined from this standard and the resulting value was used for quantitation of all 1,4-hydroxynitrates.

Determination of molar yields of 1,4-hydroxynitrates with corrections for wall losses

Molar yields of 1,4-hydroxynitrates were calculated as the moles of product formed divided by the moles of *n*-alkane consumed. These values were corrected for the loss of particles to the chamber walls using the decay in the *m/z* 185 mass spectral peak, which is due essentially solely to nonvolatile DOS seed particles that are only removed from the chamber by deposition to the walls. *n*-Alkanes larger than ~C_{13} are partially lost to the walls by gas-wall partitioning (Matsunaga and Ziemann, 2010b), which was accounted for here by measuring the concentrations of *n*-alkanes multiple times before and after each reaction to verify that they had equilibrated with the walls. In this case the concentration of *n*-alkane reacted is $[Alk]_{reacted} = [Alk]_{T,i}(1 - FID_f/FID_i)$, where $[Alk]_{T,i}$ is the amount of *n*-alkane added to the chamber divided by the chamber volume, and FID_i and FID_f are the GC/FID signals per volume of air sampled measured before and after reaction. The following is the derivation of this expression:

The loss of *n*-alkanes to the chamber walls can be accounted for using Equation (1) in the text, which can be derived as follows. The concentration of *n*-alkane reacted, $[Alk]_{reacted}$, is given by the equation

$$[Alk]_{reacted} = [Alk]_{T,i} - [Alk]_{T,f} \quad (1)$$

where $[Alk]_{T,i}$ and $[Alk]_{T,f}$ are the total (gas + walls) initial and final concentrations of *n*-alkane in the chamber (i.e., before and after reaction). It is assumed that the *n*-alkane has equilibrated with the walls through gas-wall partitioning (Matsunaga and Ziemann, 2010b), and that the fraction of *n*-alkane in the gas phase is given by the equation

$$[Alk]_g = K[Alk]_T \quad (2)$$

where K is the partitioning coefficient. Using this equation to substitute for $[Alk]_{T,i}$ and $[Alk]_{T,f}$ in Equation (1) then gives

$$[Alk]_{reacted} = ([Alk]_{g,i} - [Alk]_{g,f})/K \quad (3)$$

If the gas-phase concentration of *n*-alkane in the chamber is proportional to the GC/FID signal measured per volume of air sampled, FID, then

$$[Alk]_g = C \times FID \quad (4)$$

where C is a calibration factor that can be determined at the beginning of the experiment by combining Equations (2) and (4) to give

$$C = [Alk]_{g,i}/FID_i = K[Alk]_{T,i}/FID_i \quad (5)$$

Substituting Equation (5) for C into Equation (4) gives

$$[Alk]_g = FID \times K[Alk]_{T,i}/FID_i \quad (6)$$

which when substituted for $[Alk]_{g,i}$ and $[Alk]_{g,f}$ in Equation (3) and rearranged gives

$$[Alk]_{reacted} = [Alk]_{T,i}(1 - FID_f/FID_i) \quad (7)$$

This equation means that as long as the *n*-alkane is in gas-wall equilibrium when $[Alk]_{g,i}$ and $[Alk]_{g,f}$ are measured, and K does not change during the experiment, then one can simply ignore gas-wall partitioning and calibrate the GC/FID signal by assuming that all the *n*-alkane added remained in the gas phase.

Results and Discussion

Identification of 1,4-hydroxynitrate isomers by HPLC/UV/MS

The 1,4-hydroxynitrate isomers of interest here have the general structure $R_1CH(OH)CH_2CH_2CH(ONO_2)R_2$ (Scheme 2.1), where R_1 and R_2 are the alkyl chains $CH_3(CH_2)_x$ and $CH_3(CH_2)_y$ with carbon numbers x + 1 and y +1. The structure of an isomer is reflected in its chromatographic and electron ionization fragmentation properties, which in this case allowed the isomer(s) associated with each of the HPLC chromatographic peaks to be identified and characterized on the basis of retention times and mass spectra. Because retention in reversed-phase chromatography is driven by hydrophobic/solvophobic interactions, the major structural feature of these compounds that determined their retention on the hydrophobic C_{18} stationary phase was the length of the longest alkyl chain. As a result, 1,4-hydroxynitrate isomers for which the –$CH(OH)CH_2CH_2CH(ONO_2)$– subunit is located near the end of the molecule would have longer retention times than those for which it was closer to the middle. A similar effect has been observed with the retention of butanediols, where 1,2-butanediol was retained longer on a C_{18} column than was 2,3-butanediol (Noël and Vangheluwe, 1987). In that study, the authors found a positive correlation between retention and the Wiener index (Wiener, 1947) for the diols in their sample set. For the 1,4-hydroxynitrate isomers the Wiener index increases as the proximity of the functional groups to the end of the molecule increases, and therefore as the length of the longest alkyl chain increases. If the trend in retention for 1,4-hydroxynitrates is similar to that reported for diols, then isomers with the longest alkyl chains will have the longest retention times.

To examine the effect of isomer structure on reversed-phase retention, the mass spectrum of each HPLC peak was scrutinized for series of ions that provide isomer-specific structural information. Two simple fragmentation pathways were identified that explain the major mass spectral peaks and patterns and are consistent with well-established mechanisms determined from electron ionization studies (McLafferty and Tureček, 1993). The proposed pathways are shown in Scheme 2.2.

Scheme 2.2: Proposed electron impact fragmentation mechanism of 1,4-hydroxynitrate isomers.

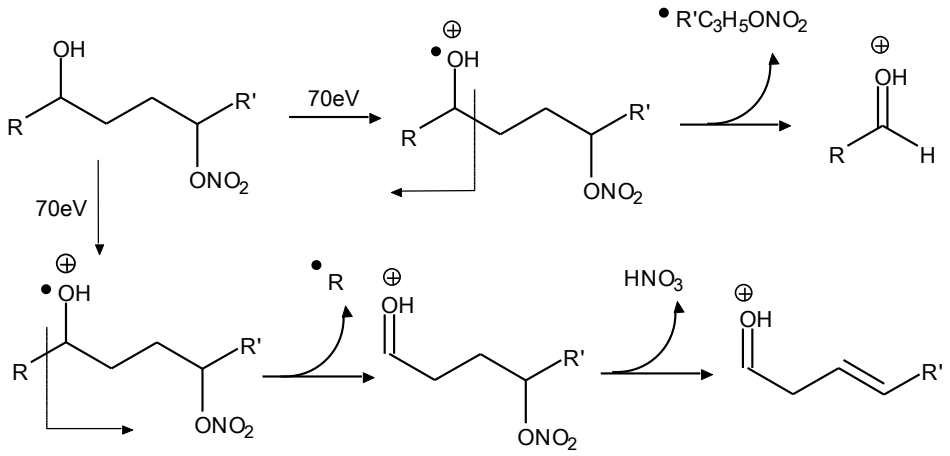

Beginning with the 1,4-hydroxynitrate structure written as $CH_3(CH_2)_xCH(OH)CH_2CH_2CH(ONO_2)(CH_2)_yCH_3$, ionization occurs at the hydroxyl group to form a molecular ion. In one case this ion undergoes α-cleavage on the right side (as drawn) of the –CH(OH)– group to form $CH_3(CH_2)_xCHOH^+$ + $\bullet CH_2CH_2CH(ONO_2)(CH_2)_yCH_3$, and in the other case the ion undergoes α-cleavage on left side of the –CH(OH)– group and loses $HONO_2$ (formed through a 1,5-H-atom shift) to form $^+HOCHCH_2CH_2CH{=}CH(CH_2)_{y-1}CH_3$+ $CH_3(CH_2)_x\bullet$ + $HONO_2$. These ions can then rearrange via two H-atom shifts and lose H_2O to form $CH_3(CH_2)_{x-2}CH{=}CHCH_2^+$ and $^+CH_2CH{=}CHCH{=}CH(CH_2)_{y-1}\ CH_3$ ions, respectively. The proposed fragmentation mechanism can be used to locate the positions of the hydroxyl and nitrooxy groups on a molecule and therefore identify the isomers responsible for each HPLC peak. This information can then be used determine if retention time increases with the length of the longest alkyl chain, C_{max}. For this discussion it is useful to designate the structures of 1,4-hydroxynitrates using the following notation: (1) hydroxy and nitrooxy groups are designated H and N, (2) the location of a group on the alkyl chain is designated by numbers and placed before the H and N, respectively, and (3) the lengths of the two alkyl chains are designated by C_n and C_m in order from smallest to largest, where n = x + 1 and m = y + 1 for a 1,4-hydroxynitrate with structure $CH_3(CH_2)_xCH(OH)CH_2CH_2CH(ONO_2)(CH_2)_yCH_3$. For example, 5-hydroxy-8-nitrooxypentadecane, $CH_3(CH_2)_3CH(OH)CH_2CH_2CH(ONO_2)(CH_2)_6CH_3$, is designated C_4-5H8N-C_7. The four characteristic ions expected for this isomer are $CH_3(CH_2)_3CHOH^+$ (*m/z* 87),

$^{+}HOCHCH_2CH_2CH=CH(CH_2)_5CH_3$ (*m/z* 169), $CH_3(CH_2)_1CH=CHCH_2^{+}$ (*m/z* 69), and $^{+}CH_2CH=CHCH=CH(CH_2)_5CH_3$ (*m/z* 151). The four HPLC/UV chromatographic peaks produced by the C_{15} 1,4-hydroxynitrooxypentadecanes are shown in Figure 2.1a, and the mass spectra of Peaks 1 and 3 are shown in Figures 2.1b and 2.1c.

Figure 2.1: (a) HPLC/UV chromatogram of filter extract of particles formed from the reaction of *n*-pentadecane with OH radicals in the presence of NO. The peaks contain the following isomers: (1) C_4-5H8N-C_7, C_5-6H9N-C_6, C_6-7H10N-C_5, and C_7-8H5N-C_4; (2) C_3-4H7N-C_8, C_8-7H4N-C_3; (3) C_2-3H6N-C_9, C_9-6H3N-C_2; (4) C_1-2H5N-C_{10}, C_{10}-5H2N-C_1. (b) Mass spectrum of peak 1. (c) Mass spectrum of peak 3.

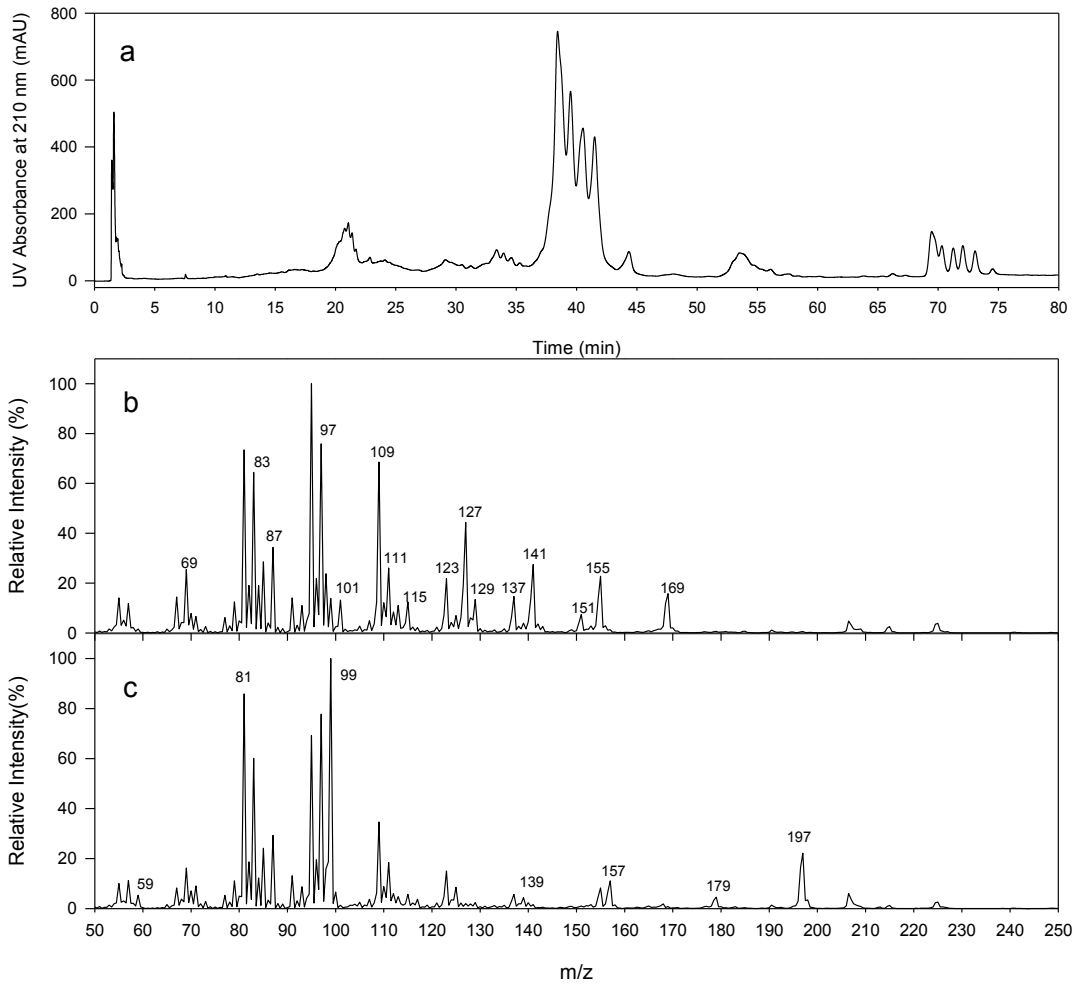

The retention times of the four peaks, the isomers associated with each peak, the ions used to identify each isomer, and the isomer C_{max} values are given in Table 2.1. The isomers associated with Peak 1 were C_4-5H8N-C_7, C_5-6H9N-C_6, C_6-7H10N-C_5, and C_7-8H5N-C_4, which correspond to values of C_{max} = 7, 6, 7, and 6, respectively. Although the peaks are not resolved in the HPLC/UV chromatogram, extracted ion chromatograms of each of the $^{+}HOCHCH_2CH_2CH{=}CH(CH_2)_{y-1}CH_3$ ions (*m/z* 169, 155, 141, and 127) that are characteristic of each isomer showed those with C_{max} = 6 (*m/z* 155 and 141) eluted ~20 s earlier than those with C_{max} = 7 (*m/z* 169 and 127). This indicates that C_{max} is the dominant factor determining the reversed-phase retention of these compounds. This hypothesis is further supported by the other values of C_{max} given in Table 2.1, which all increase with peak retention time.

Table 2.1: Retention times of the four peaks, the isomers associated with each peak, the isomer C_{max} values, and the ions used to identify each isomer.

Peak	t_r (min)	Isomers	C_{max}	Ions
1	38.7	C_4-5H8N-C_7	7	87, 169, 69, 151
		C_5-6H9N-C_6	6	101, 155, 83, 137
		C_6-7H10N-C_5	6	115, 141, 97, 123
		C_7-8H5N-C_4	7	129, 127, 111, 109
2	39.9	C_3-4H7N-C_8	8	73, 183, 55, 165
		C_8-7H4N-C_3	8	143, 113, 125, 95
3	41.0	C_2-3H6N-C_9	9	59, 197, 21, 179
		C_9-6H3N-C_2	9	157, 99, 139, 81
4	42.2	C_1-2H5N-C_{10}	10	45, 211, 27, 193
		C_{10}-5H2N-C_1	10	171, 85, 153, 67

It is worth noting that the 1,4-hydroxynitrates formed via H-atom abstraction by an OH radical at the 1-position of the carbon chain (1-hydroxy-4-nitrooxyalkanes) and those formed via isomerization of 4-alkoxy radicals (4-hydroxy-1-nitrooxyalkanes) were below the limit of detection of the TDPBMS, and thus were not identified in the chromatograms. It is not known whether they eluted in Peaks 1–4, but based on the observed retention trends, they would either elute in Peak 4 or in the small peak that eluted ~2 min later. Abstraction of H-atoms by OH radicals or by alkoxy radicals during isomerization is much slower from the $–CH_3$ group in the 1-position than from the $–CH_2–$ groups (Kwok and Atkinson, 1995; Méreau et al., 2003), so the measured total yield of 1,4-hydroxynitrates would not be significantly reduced by the omission of 1-hydroxy-4-nitrooxyalkanes or 4-hydroxy-1-nitrooxyalkanes. The molar yields reported here probably reflect the sum of particulate 1,4-hydroxynitrates formed via H-atom abstraction by OH radicals at $–CH_2–$ groups, minus the small fraction of 4-hydroxy-1-nitrooxyalkanes formed by alkoxy radical isomerization.

Measured yields of 1,4-hydroxynitrates in particles

The molar yields of 1,4-hydroxynitrates measured in particles formed from reactions of C_8–C_{16} *n*-alkanes, with corrections for loss of particles to the chamber walls, are shown in Figure 2.2a.

Figure 2.2: (a) Molar yields of 1,4-hydroxynitrates measured in particles formed from reactions of C_8–C_{16} *n*-alkanes with OH radicals in the presence of NO. (b) Branching ratios for the formation of 1,4-hydroxynitrates formed from the reactions of 1,4-hydroxyperoxy radicals with NO. Data points were calculated as the ratio of the average plateau yield measured for C_{14}-C_{16} 1,4-hydroxynitrates relative to yields of 1,4-hydroxyperoxy radicals calculated using the model of Arey et al. (2001) as described in the text. The curve was created by scaling all the values calculated using this model by a constant factor of 0.630, which is equal to the ratio the average plateau branching ratios for 1,4-hydroxyperoxy radicals and alkyl peroxy radicals. Error bars in (a) and (b) are two standard deviations plus 5%.

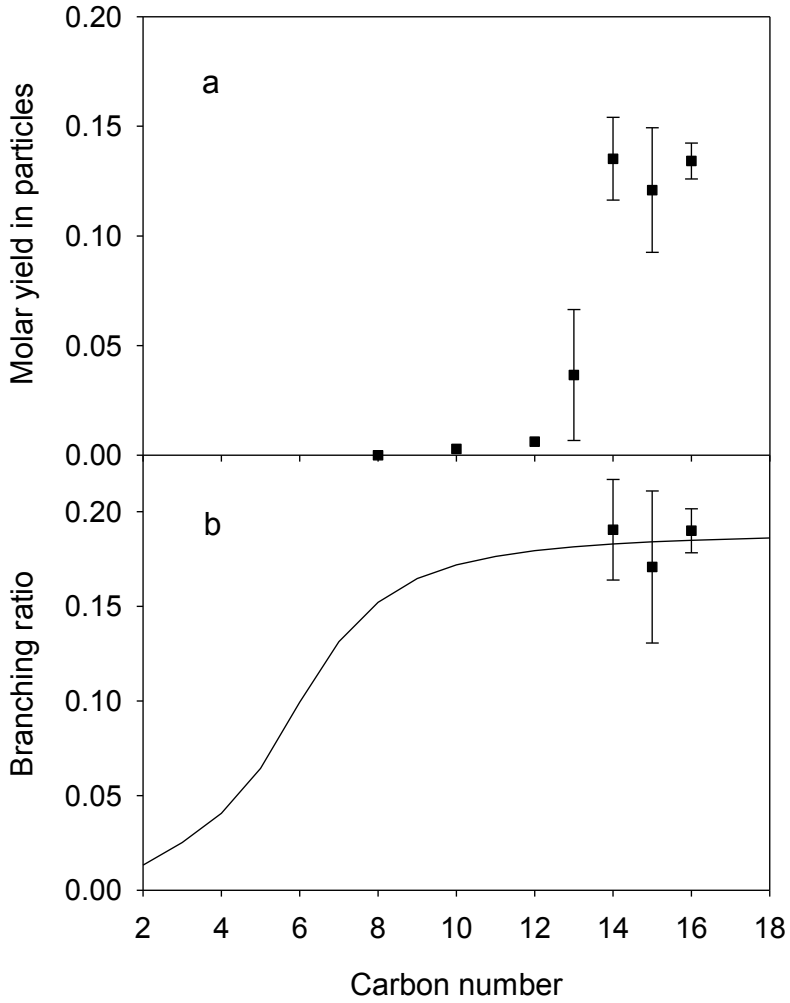

The yields were 0.00, 0.003, 0.006, 0.037, 0.135, 0.121, and 0.134 for the reactions of *n*-octane, *n*-decane, *n*-dodecane, *n*-tridecane, *n*-tetradecane, *n*-pentadecane, and *n*-hexadecane respectively. 1,4-Hydroxynitrates were detected in filter extracts from the reactions of all but the C_8 *n*-alkane, and yields increased with increasing carbon number up to an average plateau value of 0.131 ± 0.008 at C_{14}–C_{16}. The large increase in yield with increasing carbon number from 0.00 to 0.119 is due primarily to the effects of gas-particle partitioning, since only the 1,4-hydroxynitrates present in particles were measured. The results indicate that C_8 1,4-hydroxynitrates were entirely in the gas phase, C_{10}–C_{13} 1,4-hydroxynitrates were in both the gas and particle phases, and C_{14}–C_{16} 1,4-hydroxynitrates were entirely in the particles. Because the C_{14}–C_{16} 1,4-hydroxynitrates were entirely in the particles, the yield measured for these compounds is equal to the total yield (gas + particle).

The branching ratios for the formation of 1,4-hydroxynitrates from the reactions of C_{14}–C_{16} 1,4-hydroxyperoxy radicals with NO were calculated by dividing the measured yields by the yields of 1,4-hydroxyperoxy radicals calculated as (1 - alkyl nitrate yield) (Scheme 2.1), where the alkyl nitrate yield was calculated using the model of Arey et al. (Arey et al., 2001). The validity of this model for calculating alkyl nitrate yields over the entire range of carbon numbers has recently been confirmed though experimental studies that measured the yields into the plateau region (Chapter 1). Calculated yields of C_{14}–C_{16} 1,4-hydroxyperoxy radicals were 0.710, 0.708, and 0.706, giving branching ratios for the formation of 1,4-hydroxynitrates from the reactions of NO with C_{14}–C_{16} 1,4-hydroxyperoxy radicals of 0.191, 0.171, and 0.190, and thus an average

value at the plateau of 0.184 ± 0.011. The model of Arey et al. (Arey et al., 2001) can then be used to obtain branching ratios over the entire range of carbon numbers by scaling all the values calculated using this model by a constant factor of 0.630, which is equal to the ratio the average plateau branching ratios for C_{14}–C_{16} 1,4-hydroxyperoxy radicals and alkyl peroxy radicals of 0.184/0.292. The results are shown in Figure 2.2b.

This approach for measuring yields at the plateau has been used previously to determine the branching ratios for the formation of 1,2-hydroxynitrates from reactions of 1,2-hydroxyperoxy radicals with NO, where the 1,2-hydroxyperoxy radicals were formed from the reactions of linear alkenes, internal alkenes, and 2-methyl-1-alkenes with OH radicals in the presence of NO_x (Matsunaga and Ziemann, 2009; Matsunaga and Ziemann, 2010a). The yields again reached plateaus at carbon numbers ≥ C_{14}, and branching ratios for the formation of 1,2-hydroxynitrates from reactions of primary, secondary, and tertiary 1,2-hydroxyperoxy radicals with NO were calculated to be 0.12, 0.15, and 0.24, respectively, using measured isomer-specific yields of 1,2-hydroxynitrates and the yields of 1,2-hydroxyperoxy radicals calculated using the equations developed by Nishino et al. (Nishino et al., 2009) from results of kinetics studies. It was also shown that the branching ratios for the formation of 1,2-hydroxynitrates from reactions of 1-alkenes were fit well over the range of carbon numbers from C_2–C_{17} by scaling the values calculated using the model of Arey et al. (Arey et al., 2001) by a value of 0.455, within 30% of the value of 0.630 used above.

The branching ratios for the secondary 1,4-hydroxyperoxy radicals investigated here are similar to those of secondary 1,2-hydroxyperoxy radicals, indicating that the

branching ratios are not very sensitive to the position of the hydroxyl group relative to the peroxy group. These branching ratios are, however, approximately one-half those measured for alkyl peroxy radicals of the same carbon number, as has been observed in a number of studies of the reactions alkenes with a wide range of carbon numbers (Atkinson et al., 1995; O'Brien et al., 1998; Matsunaga and Ziemann, 2009; Matsunaga and Ziemann, 2010a). O'Brien et al. (O'Brien et al., 1998) have shown through quantum chemical calculations that the branching ratios are lower for 1,2-hydroxyperoxy radicals because intramolecular hydrogen bonding between the hydroxyl and peroxy groups weakens the O-O bond in the intermediate complex formed with NO (illustrated in Scheme 2.1), thus increasing the rate of dissociation to the 1,2-hydroxyalkoxy radical and NO_2 relative to the rate of formation of the 1,2-hydroxynitrate. Hydrogen bonding in the 1,2- and 1,4-hydroxyperoxy radicals occurs through five-member and seven-member rings, respectively, both of which are energetically favorable configurations in intramolecular reactions.

Conclusions

In this study, a homologous series of C_8–C_{16} *n*-alkanes were reacted with OH radicals in the presence of NO_x in an environmental chamber and the 1,4-hydroxynitrate products present in particles were sampled on filters, extracted, and analyzed by HPLC/UV/MS. The mass spectra were consistent with predictions based on simple electron ionization fragmentation mechanisms that are expected to apply to compounds with these structures, and could be used to identify individual isomers. Retention times correlated well with the length of the longest alkyl chain attached to the 1,4-hydroxynitrate subunit and therefore increasing Wiener index. A correlation of retention time and Wiener index has been observed previously for diols, and verified the assignment of isomer structures. Yields of 1,4-hydroxynitrates increased with increasing carbon number to a plateau at about C_{14}–C_{16} due to enhanced partitioning into particles, with the average value at the plateau of 0.130 ± 0.008 being equal to the total yield (gas + particle) since at these high carbon numbers essentially all 1,4-hydroxynitrates are in the particles. Combining this yield of ~0.13 with the plateau yield of ~0.29 determined in Chapter 2 for alkyl nitrates gives by mass balance a plateau yield of ~0.58 for the formation of 1,4-hydroxycarbonyls (Scheme 2.1). This value agrees well with the yield of 0.61 measured recently by Aschmann et al. (Aschmann et al., 2012) for the reaction of *n*-octane. The average branching ratio for the formation of C_{14}–C_{16} 1,4-hydroxynitrates from the reaction of NO with the corresponding 1,4-hydroxyperoxy radicals was calculated to be 0.184 ± 0.011 from the ratio of the measured yields of 1,4-hydroxynitrates and the yields of 1,4-hydroxyperoxy radicals calculated using the model

of Arey et al. (Arey et al., 2001). This value is similar to the value of 0.15 measured for secondary 1,2-hydroxyperoxy radicals formed from similar reactions of internal alkenes, 1-alkenes, and 2-methyl-1-alkenes (Matsunaga and Ziemann 2009; Matsunaga and Ziemann 2010a), and suggests a similar effect of hydrogen bonding between the hydroxyl and peroxy groups on the branching ratios.

The experimental approach employed here of analyzing organic nitrate products in SOA formed from reactions of a homologous series of parent compounds provides a relatively straightforward way for measuring plateau yields. Although corrections must be made for the loss of 1,4-hydroxynitrates to the walls via particle deposition, they are relatively small and easily made by monitoring the loss of nonvolatile seed particles using real-time particle mass spectrometry. This approach has significant advantages over methods that rely on measurements of gas-phase products, which decrease in volatility with increasing carbon number and can thus undergo gas-wall partitioning (in addition to gas-particle partitioning) that is much more difficult to quantify (see Chapter 1). The branching ratios determined from these plateau yields can be extrapolated to smaller carbon numbers by using a scaled version of the model of Arey et al. (Arey et al., 2001) to account for the dependence of the branching ratio for organic nitrate formation on carbon number.

References

1. Alfaro-Moreno, E., Nawrot, T. S., Nemmar, A., & Nemery, B. (**2007**). Particulate matter in the environment: pulmonary and cardiovascular effects. *Current Opinion in Pulmonary Medicine*, 13(2), 98-106.

2. Andreae, M. O., & Rosenfeld, D. (**2008**). Aerosol–cloud–precipitation interactions. Part 1. The nature and sources of cloud-active aerosols. *Earth-Science Reviews*, 89(1), 13-41.

3. Arey, J., Aschmann, S. M., Kwok, E. S., & Atkinson, R. (**2001**). Alkyl nitrate, hydroxyalkyl nitrate, and hydroxycarbonyl formation from the NO_x-air photooxidations of C_5-C_8 *n*-alkanes. *The Journal of Physical Chemistry A*, 105(6), 1020-1027.

4. Aschmann, S. M., Arey, J., & Atkinson, R. (**2001**). Atmospheric chemistry of three C_{10} alkanes. *The Journal of Physical Chemistry A*, 105(32), 7598-7606.

5. Aschmann, S. M., Arey, J., & Atkinson, R. (**2012**). Formation Yields of C_8 1,4-Hydroxycarbonyls from OH+ *n*-Octane in the Presence of NO. *Environmental Science & Technology*, 46(24), 13278-13283.

6. Atkinson, R., Carter, W. P., Winer, A. M., & Pitts Jr, J. N. (**1981**). An experimental protocol for the determination of OH radical rate constants with organics using methyl nitrite photolysis as an OH radical source. *Journal of the Air Pollution Control Association*, 31(10), 1090-1092.

7. Atkinson, R., Tuazon, E. C., & Aschmann, S. M. (**1995**). Products of the gas-phase reactions of a series of 1-alkenes and 1-methylcyclohexene with the OH radical in the presence of NO. *Environmental Science & Technology*, 29(6), 1674-1680.

8. Atkinson, R. (**1997**). Gas-phase tropospheric chemistry of volatile organic compounds: 1. Alkanes and alkenes. *Journal of Physical and Chemical Reference Data*, 26(2), 215-290..

9. Atkinson, R., & Arey, J. (**2003**). Atmospheric degradation of volatile organic compounds. *Chemical Reviews*, 103(12), 4605-4638.

10. Atkinson, R. (**2007**). Gas-phase tropospheric chemistry of organic compounds: a review. *Atmospheric Environment*, 41, 200-240.

11. Atkinson, R., Arey, J., & Aschmann, S. M. (**2008**). Atmospheric chemistry of alkanes: Review and recent developments. *Atmospheric Environment*, 42(23), 5859-5871.

12. Baker, J., Arey, J., & Atkinson, R. (**2005**). Rate constants for the reactions of OH radicals with a series of 1, 4-hydroxyketones. *Journal of Photochemistry and Photobiology A: Chemistry*, 176(1), 143-148.

13. Calvert, J.G.; Atkinson R.; Becker, K.H.; Kamens, R.M.; Seinfeld, J.H.; Wallington, T.J.; Yarwood, G. *The Mechanisms of Atmospheric Oxidation of Aromatic Hydrocarbons*; Oxford University Press: New York, NY, 2002

14. Canagaratna, M.R.; Jayne, J.T.; Jimenez, J.L.; Allan, J.D.; Alfarra, M.R.; Zhang, Q.; Onasch, T.B.; Drewnick, F.; Coe, H.; Middlebrook, A.; Delia, A.; Williams, L.R.; Trimborn, A.M.; Northway, M.J.; DeCarlo, P.F.; Kolb, C.E.; Davidovits, P.; Worsnop, D.R. (**2007**). Chemical and microphysical characterization of ambient aerosols with the aerodyne aerosol mass spectrometer. *Mass Spectrometry Reviews*, 26(2), 185-222.

15. Day, D. A., Dillon, M. B., Wooldridge, P. J., Thornton, J. A., Rosen, R. S., Wood, E. C., & Cohen, R. C. (**2003**). On alkyl nitrates, O_3, and the "missing NO_y". *Journal of Geophysical Research*, 108(D16), 4501.

16. Dickerson, R. R., Kondragunta, S., Stenchikov, G., Civerolo, K. L., Doddridge, B. G., & Holben, B. N. (**1997**). The impact of aerosols on solar ultraviolet radiation and photochemical smog. *Science*, 278(5339), 827-830

17. Etzel, R. A. (**2003**). How environmental exposures influence the development and exacerbation of asthma. *Pediatrics*, 112(Supplement 1), 233-239.

18. Forster, P.; Ramaswamy, V.; Artaxo, P.; Berntsen, T.; Betts, R.; Fahey, D.W.; Haywood, J.; Lean, J.; Lowe, D.C.; Myhre, G.; Nganga, J.; Prinn, R.; Raga, G.; Schulz, M.; Van Dorland, R. *Changes in Atmospheric Constituents and in Radiative Forcing"* in *Climate Change 2007: The Physical Science Basis. Contribution of Working Group I to the Fourth Assessment Report of the Intergovernmental Panel on Climate Change*; Solomon, S.; Qin, D.; Manning, M.; Chen, Z.; Marquis, M.; Averyt, K. B.; Tignor, M.; Miller, H. L., Eds. Cambridge University Press, New York, NY, 2007.

19. Gentner, D.R.; Isaacman G.; Worton, D.R.; Chan, A.W.; Dallmann, T.R.; Davis, L.; Liu, S; Day, D.A.; Russell, L.M.; Wilson, K.R.; Weber, R.; Guha, A.; Harley, R.A.; Goldstein, A.H. (**2012**). Elucidating secondary organic aerosol from diesel and gasoline vehicles through detailed characterization of organic carbon emissions. *Proceedings of the National Academy of Sciences*, 109(45), 18318-18323.

20. Kwok, E. S., & Atkinson, R. (**1995**). Estimation of hydroxyl radical reaction rate constants for gas-phase organic compounds using a structure-reactivity relationship: An update. *Atmospheric Environment*, 29(14), 1685-1695.

21. Lim, Y. B., & Ziemann, P. J. (**2005**). Products and mechanism of secondary organic aerosol formation from reactions of *n*-alkanes with OH radicals in the presence of NO_x. *Environmental Science & Technology*, 39(23), 9229-9236.

22. Lim, Y. B., & Ziemann, P. J. (**2009**). Effects of molecular structure on aerosol yields from OH radical-initiated reactions of linear, branched, and cyclic alkanes in the presence of NO_x. *Environmental Science & Technology*, 43(7), 2328-2334.

23. Lohmann, U., & Feichter, J. (**2005**). Global indirect aerosol effects: a review. *Atmospheric Chemistry and Physics*, 5(3), 715-737

24. Lurmann, F.W.; Main, H.H. *Analysis of the Ambient VOC Data Collected in the Southern California Air Quality Study*; Final Report to California Air Resources Board Contract No. A832-130, Sacramento, CA, February 1992.

25. Matsunaga, A., & Ziemann, P. J. (**2009**). Yields of β-hydroxynitrates and dihydroxynitrates in aerosol formed from OH radical-initiated reactions of linear alkenes in the presence of NO_x. *The Journal of Physical Chemistry A*, 113(3), 599-606.

26. Matsunaga, A., & Ziemann, P. J. (**2010a**). Yields of β-hydroxynitrates, dihydroxynitrates, and trihydroxynitrates formed from OH radical-initiated reactions of 2-methyl-1-alkenes. *Proceedings of the National Academy of Sciences*, 107(15), 6664-6669.

27. Matsunaga, A., & Ziemann, P. J. (**2010b**). Gas-wall partitioning of organic compounds in a Teflon film chamber and potential effects on reaction product and aerosol yield measurements. *Aerosol Science and Technology*, 44(10), 881-892.

28. McLafferty, F.W.; Tureček, F. *Interpretation of mass spectra*. University Science Books, Sausalito, CA, 1993.

29. Méreau, R., Rayez, M. T., Caralp, F., & Rayez, J. C. (**2003**). Isomerisation reactions of alkoxy radicals: theoretical study and structure–activity relationships. *Physical Chemistry Chemical Physics*, 5(21), 4828-4833.

30. Nishino, N., Arey, J., & Atkinson, R. (**2009**). Rate Constants for the Gas-Phase Reactions of OH Radicals with a Series of C_6− C_{14} Alkenes at 299 ± 2 K. *The Journal of Physical Chemistry A*, 113(5), 852-857.

31. Noël, D., & Vangheluwe, P. (**1987**). Retention behaviour and molecular structure of diols in reversed-phase liquid chromatography. *Journal of Chromatography A*, 388, 75-80.

32. O'Brien, J. M., Czuba, E., Hastie, D. R., Francisco, J. S., & Shepson, P. B. (**1998**). Determination of the hydroxy nitrate yields from the reaction of C_2-C_6

alkenes with OH in the presence of NO. *The Journal of Physical Chemistry A*, 102(45), 8903-8908.

33. Pope III, C. A. (**2007**). Mortality effects of longer term exposures to fine particulate air pollution: review of recent epidemiological evidence. *Inhalation Toxicology*, 19(S1), 33-38.

34. Reisen, F., Aschmann, S. M., Atkinson, R., & Arey, J. (**2005**). 1,4-Hydroxycarbonyl products of the OH radical initiated reactions of C_5-C_8 *n*-alkanes in the presence of NO. *Environmental science & technology*, 39(12), 4447-4453.

35. Robinson, A.L.; Donohue, N.M.; Shrivastava, M.K.; Weitkamp, E.A.; Sage, A.M.; Griesho, A.P.; Lane, T.E.; Pierce, J.R.; Pandis, S.N. (**2007**). Rethinking organic aerosols: Semivolatile emissions and photochemical aging. *Science*, 315(5816), 1259-1262.

36. Robinson, C. B., Kimmel, J. R., David, D. E., Jayne, J. T., Trimborn, A., Worsnop, D. R., & Jimenez, J. L. (**2011**). Thermal desorption metastable atom bombardment ionization aerosol mass spectrometer. *International Journal of Mass Spectrometry*, 303(2), 164-172.

37. Taylor, W. D., Allston, T. D., Moscato, M. J., Fazekas, G. B., Kozlowski, R., & Takacs, G. A. (**1980**). Atmospheric photodissociation lifetimes for nitromethane, methyl nitrite, and methyl nitrate. *International Journal of Chemical Kinetics*, 12(4), 231-240

38. Tobias, H. J., Kooiman, P. M., Docherty, K. S., & Ziemann, P. J. (**2000**). Real-time chemical analysis of organic aerosols using a thermal desorption particle beam mass spectrometer. *Aerosol Science & Technology*, 33(1-2), 170-190.

39. Wiener, H. (**1947**). Structural determination of paraffin boiling points. *Journal of the American Chemical Society*, 69(1), 17-20.

40. Williams, J.; Koppmann, R. "*Volatile organic compounds in the atmosphere: an overview"* pp. 1-19 in *Volatile organic compounds in the atmosphere*; Koppmann, R., Ed. Blackwell Publishing Ltd.: Oxford, UK, 2007

41. Ziemann, P. J. (**2011**). Effects of molecular structure on the chemistry of aerosol formation from the OH-radical-initiated oxidation of alkanes and alkenes. *International Reviews in Physical Chemistry*, 30(2), 161-195.

42. Ziemann, P. J., & Atkinson, R. (**2012**). Kinetics, products, and mechanisms of secondary organic aerosol formation. *Chemical Society Reviews*, *41*(19), 6582-6605.

43. Zhang, Q.; Jimenez, J.L.; Canagaratna, M.R.; Allan, J.D.; Cole, H.; Ulbrich, I.; Alfarra, M.R.; Takami, A.; Middlebrook, A.M.; Sun, Y.L.; Dzepina, K.; Dunlea, E.; Docherty, K.; DeCarlo, P.F.; Salcedo, D.; Onasch, T.; Jayne, J.T.; Miyoshi, T.; Shimono, A.; Hatakeyama, S.; Takegawa, N.; Kondo, Y.; Schneider, J.; Zrewnick, F.; Borrmann, S.; Weimer, S.; Demerjian, K.; Williams, P.; Bower, K.; Zahreini, R.; Cottrell, L.; Griffin, R.J.; Rautiainen, J.; Sun, J.Y.; Zhang, Y.M.; Worsnop, D.R. (**2007**). Ubiquity and dominance of oxygenated species in organic aerosols in anthropogenically-influenced Northern Hemisphere midlatitudes. *Geophysical Research Letters*, 34(13), L13801.

Chapter 3: Revised parameters for the estimation of alkyl nitrate formation yields from the reaction of organic peroxy radicals with NO

Abstract

The growing database of alkyl nitrate formation yields for the reactions of alkyl peroxy radicals with NO were used to optimize parameters of a previously developed model for calculating the branching ratios for alkyl nitrate formation as a function of carbon number, temperature, and pressure (expressed as air number concentration). The updated parameters provide an improved fit of model-calculated values to measured values of branching ratios for the formation of secondary alkyl nitrates, with the largest error at 31%, and with half of the model-calculated yields falling within 9% of the measured values. Newly available of measured yields were used to determine scaling factors that allow for calculation of branching ratios for the formation of primary and tertiary alkyl nitrates substituted organic nitrates, including various hydroxynitrates and haloalkylnitrates, using the same set of optimized parameters. The newly parameterized model can be incorporated into tropospheric models that describe the chemical transformations of organic molecules via photooxidation in NO_x-enriched atmospheres.

Introduction

Organic nitrates are ubiquitous gas- and particle-phase components of tropospheric air, and are routinely detected in polluted, rural, and marine atmospheres (Schneider and Ballschmiter, 1999; Ballschmiter, 2002; Cleary et al., 2005; 2011Russo et al., 2010). They arise primarily from the photooxidation of organic molecules by hydroxyl (OH) radical in the presence of NO_x ($NO_x \equiv NO + NO_2$), and they can also form via nighttime reactions of nitrate (NO_3) radical with unsaturated hydrocarbons. Organic nitrates routinely comprise 10-20% of total NO_y ($NO_y \equiv NO_x$ + all other oxidized nitrogen species), making them a major sink of nitrogen oxides, (Day et al., 2003) and, through the sequestration of NO_x that occurs as a result of their formation, they can affect ozone cycling. (Day et al., 2003; Atkinson, 2000) Monofunctional and multifunctional organic nitrates and unsubstituted organic nitrates (alkyl nitrates) of sufficiently low volatility can partition into particles to form secondary organic aerosol (SOA) (Ziemann, 2011). Due to their participation in NO_x and ozone cycling, and their potential to contribute to aerosol formation, accurate modeling of the formation of organic nitrates is of critical importance to atmospheric modeling of NO_x, ozone, and particulate matter.

The mechanism of the formation of alkyl nitrates, the dominant organic nitrate formed from the OH radical-initiated reaction of alkanes in air in the presence of NO_x, is shown in Scheme 3.1, where k_x (x = 1, 2, 3a, 3b) is the rate constant for the corresponding reaction.

Scheme 3.1: Mechanism of formation of alkyl nitrates from the oxidation of an alkane by OH radical in the presence of NO_x.

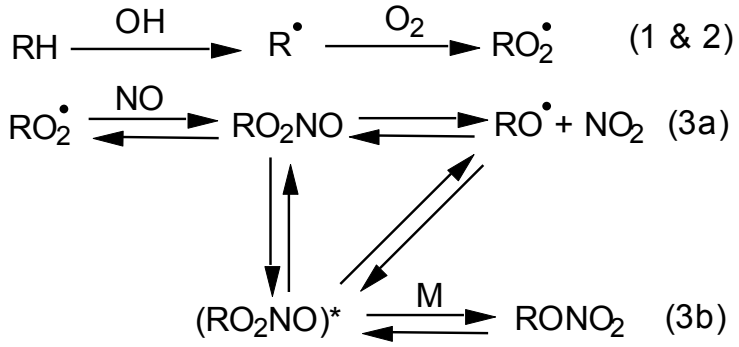

In Reaction 1, the OH radical abstracts an H atom from the alkane (RH) to yield H_2O and an alkyl radical (R•) which reacts exclusively with O_2 (Reaction 2) to form an alkyl peroxy radical (RO_2•) (Atkinson and Arey, 2003). The RO_2• radical then reacts with NO via the formation of a vibrationally excited intermediate (RO_2NO*) to produce either an alkoxy radical (RO•) and NO_2 (Reaction 3a), or an alkyl nitrate ($RONO_2$) (Reaction 3b) (Atkinson et al., 1983). The RO_2• radical can also react with NO_2 to form an alkyl peroxynitrate (RO_2NO_2), but because this compound undergoes rapid decomposition and therefore does not alter the overall reaction mechanism or products it is not shown. The mechanism of the reaction of RO_2• radicals with NO is not fully understood, but it is proposed that the excited RO_2NO* intermediate can exist as either of two non-interconverting conformers, of which only one has the potential to form alkyl nitrates (Zhao et al., 2004, Cassanelli et al., 2005, Lesar et al., 2006). Factors affecting the branching ratio for the formation of an alkyl nitrate from the reaction of an RO_2• radical with NO, $k_{3b}/(k_{3a} + k_{3b})$, and thus the alkyl nitrate yield, include temperature (Atkinson et al.,1983; Atkinson et al., 1987; Harris and Kerr; 1989, Orlando et al., 2000; Chow et al., 2003; Cassanelli et al., 2007), pressure (Atkinson et al., 1983; Atkinson et al., 1987; Aschmann et al., 2006), and structural features of the RO2• radical such as carbon number (Atkinson et al., 1982; Atkinson et al., 1987; Arey et al., 2001; Aschmann et al., 2001), alkyl chain branching (Atkinson et al., 1987; Atkinson and Arey, 2003; Espada et al., 2005; Cassanelli et al., 2007), and the presence of functional groups (O'Brien et al., 1999; Matsunaga and Ziemann, 2009; Matsunaga and Ziemann, 2010). Conditions that enhance cooling of the excited intermediate, including higher carbon number, higher

pressure, and lower temperature, increase organic nitrate yields. The presence of polar functional groups on the carbon backbone usually decreases yields, since they can weaken the O–O bond in the excited RO_2NO^* intermediate through hydrogen bonding (O'Brien et al., 1998) or electronic effects and thus enhance the rate of decomposition to RO and NO_2 relative to the rate of rearrangement to form organic nitrate. Since so many factors affect the yields of organic nitrates, modeling organic nitrate formation and its consequences becomes exceedingly complicated.

Results of studies quantifying the dependence of alkyl nitrate formation on temperature, pressure, and carbon number on nitrate formation were compiled by Atkinson et al. (Atkinson et al., 1983) to develop a model to estimate the yields of alkyl nitrates formed from the reactions of secondary alkyl peroxy radicals. The model is based on the generalized falloff equation for simple addition reactions (Troe, 1974; Luther and Troe, 1979). The falloff expression describes the dependence of the rate constant on the concentration of a third body, [M], which acts as a sink for energy that is released into the excited intermediate by bond formation, and the relationship it describes is termed the "falloff curve." The resulting model for the estimation of branching ratios for alkyl nitrate formation is composed of the following three equations:

$$\frac{k_{3b}}{k_{3a}} = \left[\frac{Y_0^{298}[M](T/298)^{-m_0}}{1 + \frac{Y_0^{298}[M](T/298)^{-m_0}}{Y_\infty^{298}(T/298)^{-m_\infty}}}\right] F^Z \quad (1)$$

$$Z = \left\{1 + \left[log\left\{\frac{Y_0^{298}[M](T/298)^{-m_0}}{Y_\infty^{298}(T/298)^{-m_\infty}}\right\}\right]^2\right\}^{-1} \quad (2)$$

$$Y_0^{298} = \alpha e^{\beta n} \quad (3)$$

Where T is temperature (K), M is number concentration of the background gas (molecule cm^{-3}), which is proportional to temperature for fixed T, n is the number of carbon atoms in the alkyl peroxy radical, and α, β, Y_∞^{298}, m_0, m_∞, and F are empirically derived parameters, some of which have physical significance. $Y_0^{298}[M]$ is the slope of the 298 K alkyl nitrate yield versus pressure plot at the low-pressure limit. Y_∞^{298} is the theoretical 298 K alkyl nitrate yield at the high-pressure limit. m_0 and m_∞ describe the temperature dependence of Y_0^{298} and Y_∞^{298}, respectively. F is the broadening coefficient that describes the degree to which changes in third body concentration affect branching. A major difference between this expression and the generalized falloff equation is that, instead of calculating branching ratio for alkyl nitrate formation directly as $k_{3b}/(k_{3a} + k_{3b})$, the ratio k_{3b}/k_{3a} is calculated first and then from this $k_{3b}/(k_{3a} + k_{3b}) = (1 + (k_{3a}/k_{3b}))^{-1}$. Because the ratio k_{3b}/k_{3a} ranges from 0 to ∞, the branching ratio for alkyl nitrate formation ranges from 0 to 1. This modification was introduced by Carter and Atkinson in 1989, to address the absence of experimental data extending to 210 K and below, and the lack of a detailed characterization of the physical dynamics of the alkyl nitrate formation mechanism (Carter and Atkinson, 1989). Since branching is expressed as k_{3b}/k_{3a}, formation yields greater than unity cannot be predicted by the expression. Since the original model was

introduced, the fitting parameters have been periodically updated to incorporate more recent measurements of alkyl nitrate yields:

1983: $\alpha = 1.29 \times 10^{-22}$, $\beta = 1.079$, $Y_\infty^{300} = 0.384$, $m_0 = 5.05$, $m_\infty = 4.16$, $F = 0.467$
(Atkinson et al., 1983)

1985: $\alpha = 1.95 \times 10^{-22}$, $\beta = 0.947$, $Y_\infty^{300} = 0.435$, $m_0 = 2.99$, $m_\infty = 4.69$, $F = 0.556$
(Carter and Atkinson, 1985)

1989: $\alpha = 1.94 \times 10^{-22}$, $\beta = 0.97$, $Y_\infty^{300} = 0.826$, $m_0 = 0$, $m_\infty = 8.1$, $F = 0.411$
(Carter and Atkinson, 1989)

2001: $\alpha = 2 \times 10^{-22}$, $\beta = 1.0$, $Y_\infty^{298} = 0.43$, $m_0 = 0$, $m_\infty = 8.0$, $F = 0.41$
(Arey et al., 2001)

In addition to the updated parameterizations, in 2001, the reference temperature was changed from 300 K to 298 K (Arey et al., 2001). A further change made here was to convert α to 1.29×10^{-22} cm^3 $molecules^{-1}$ at 300 K from the value of 4.15×10^{-6} $torr^{-1}$ reported in the original model (Atkinson et al., 1983).

All versions of this model predict a near-linear increase in the yield of secondary alkyl nitrates with increasing carbon number up to ~C_8, consistent with values measured for OH/NO_x reactions of *n*-alkanes, followed by a rapid approach to a plateau such that the yield only increases from ~0.24 at C_8 to ~0.29 between C_{13}–C_{17}. The increase in alkyl nitrate yield with increasing carbon number is due to a corresponding increase in the number of vibrational degrees of freedom, which, as sinks for vibrational energy,

decrease the rate of unimolecular decomposition of the excited RO_2NO^* intermediate, and allow more time for collisional stabilization and the rearrangement to form $RONO_2$ (Robinson, 1972; Atkinson et al., 1983). The yields are predicted to reach a plateau at a value less than unity at high carbon numbers because the reaction proceeds through the formation of two non-interconverting RO_2NO intermediate conformers, both of which can be formed by the reaction of the alkyl peroxy radical with NO (Zhang et al., 2004). Only one of the two excited RO_2NO^* intermediate conformers decomposes sufficiently slowly for this process to compete with collisional cooling, while the other conformer undergoes much faster decomposition as its only reaction pathway (Zhao et al., 2004; Cassanelli et al., 2005; Lesar et al., 2006). Although the near-linear dependence of alkyl nitrate yields on carbon number has been demonstrated experimentally for unsubstituted secondary alkyl peroxy radicals up to C_8 (Atkinson et al., 1982; Atkinson et al., 1987; Arey et al., 2001), alkyl nitrate yields have not been reported in the literature for carbon numbers large enough to observe the occurrence of a plateau. This was done, however, as part of the thesis research described in Chapter 1, where a plateau was observed in the region above ~C_{12}–C_{14}. Similar behavior has also been observed for the reactions of NO with primary, secondary, and tertiary β-hydroxyperoxy radicals formed from the reactions of OH radicals with 1-alkenes and 2-methyl-1-alkenes (Matsunaga and Ziemann, 2009, Matsunaga and Ziemann, 2010).

Recent studies of the dependence of organic nitrate formation on carbon number, temperature, pressure, and added functional groups have supplemented the database of organic nitrate yield data, but have not been used to update the parameters in the alkyl

nitrate yield model. In the present study, organic nitrate yield data from 18 studies was compiled and used to update these parameters, and to determine scaling factors extending the model to organic nitrate formation from primary, secondary , and tertiary organic peroxy radicals containing β-hydroxyl, δ-hydroxyl, and bromo groups.

Experimental Methods

Model parameters were determined by fitting the measured branching ratios to the model equations using IGOR Pro software (WaveMetrics, Portland, OR). The values reported by Arey et al., 2001.Arey et al., 2001 were used as initial guesses for each parameter. The effects of functional groups on reactions of each class of radical were determined by fitting branching ratios measured for substituted alkyl peroxy radicals to Equation (4):

$$\frac{3b}{3a} = \gamma \left[\frac{Y_0^{298}[M](T/298)^{-m_0}}{1 + \frac{Y_0^{298}[M](T/298)^{-m_0}}{Y_\infty^{298}(T/298)^{-m_\infty}}} \right] F^Z \qquad (4)$$

which is Equation (1) multiplied by a scaling factor, γ. Since the parameters were determined by fitting to the equation the branching ratios measured for unsubstituted secondary alkyl peroxy radicals, the scaling factor for unsubstituted secondary alkyl peroxy radicals is one.

Data from Atkinson et al., 1984, and Atkinson et al., 1987 were not used because calibration errors resulted in alkyl nitrate yields that were too high. This problem was also encountered in Atkinson et al., 1983, but branching ratios measured for the formation of secondary pentyl and heptyl nitrates in later experiments (Arey et al., 2001; Aschmann et al., 2006) were used to normalize the results for calibration errors. These data points were important to include because the only other rigorous investigation of temperature dependence was that by Cassanelli et al. on pentyl nitrates (Cassanelli et al, 2005). Branching ratios measured by Aschmann et al, 2006 for the formation of 3-pentyl

nitrates at pressures ≤499 torr were not used because of the formation of 3-pentyl nitrates from the reaction of NO_2 with the 3-pentoxy radical. The additional pathway for 3-pentyl nitrate formation caused the measurements to be too high (Aschmann et al., 2006). Studies of 2-pentyl nitrates did not suffer this problem since isomerization was sufficiently fast that nitrate formation from the 2-pentoxy radical reaction with NO_2 was not significant. Branching ratios reported in Aschmann et al., 2001 for the formation of decyl nitrates were not used because the authors cited loss to the walls as a possible source of error in decyl nitrate measurements (Aschmann et al., 2001). Branching ratios reported by Yeh and Ziemann (Chapter 1) for decyl nitrates were used instead, and although measured yields were lower than those reported in Aschmann et al., 2001, they were corrected for losses of decyl nitrates to the chamber walls. These experiments were performed at a higher temperature than those of Aschmann et al., however, which is a possible explanation for the lower decyl nitrate yields.

Yields reported by O'Brien et al, 1998 for β-hydroxynitrates formed from the reactions of 1-alkenes and internal alkenes were converted to yields per OH addition to the C=C bond by using the equations of Nishino et al. (Nishino et al., 2009) to calculate the fraction of reaction that occurs by addition and H-atom abstraction. For ethene and 2-butene, yields per OH addition are equal to the branching ratio because of the symmetry around the C=C double bond, whereas for the asymmetrical alkenes propene, 1-butene, and 1-hexene, yields per OH addition were converted to branching ratios by applying a 65:35 preference for OH addition to the 1- and 2-carbons in the C=C double bond (Cvetanovic 1976, Matsunaga and Ziemann, 2010). It is important to note that most of

the branching ratios used here were extracted from yield measurements with the aid of calculations similar to the ones described above for the yield measurements of O'Brien et al., 1998. Such calculations included the determination of the probability of attack of the OH radical to certain carbons, either by addition or H-atom abstraction, as well as corrections for secondary reactions. These calculations were necessary because, in almost all cases, the yield of organic peroxy radicals is not known, and can only be estimated from the amount of organic precursor that reacted. These corrections add to the uncertainty in reported branching ratios.

Results and Discussion

The optimized parameters and scaling factors for various types of organic peroxy radicals are as follows:

Parameters (± one standard deviation):

$\alpha = 2.37 \times 10^{-22} \pm 1.55 \times 10^{-23}$
$\beta = 0.792 \pm 0.018$
$Y_{\infty}^{298} = 0.372 \pm 0.013$
$m_0 = 1.19 \pm 0.75$
$m_{\infty} = 7.00 \pm 0.52$
$F = 0.688 \pm 0.033$

Scaling factors (γ):

0.71 - primary peroxy radicals
1.00 - secondary
1.13 - tertiary
0.39 - primary β-hydroxy
0.43 - secondary β-hydroxy
0.92 - tertiary β-hydroxy
0.58 - secondary δ-hydroxy
0.71 - primary γ- bromo*
0.54 - secondary β-bromo*
*only one data point was available for the determination of γ

The fit to each data point is given in Table 3.1. The expression predicts secondary alkyl nitrate branching ratios within 31% of each experimental data point, and half of the model-calculated branching ratios are within 9% of the measured ones.

Table 3.1: Measured and calculated organic nitrate branching ratios. Reference codes for experimental data are: a = Atkinson et al., 1982*, b = Atkinson et al., 1983[†], c = Shepson et al., 1985[‡], d = Muthuramu et al., 1993[‡], e = Atkinson et al., 1995, f = O'Brien et al., 1998[‡], g = Platz et al., 1999, h = Orlando et al., 2000, i = Arey et al., 2001, j = Espada et al., 2005[†], k = Aschmann et al., 2006, l = Cassanelli et al., 2007, m = Matsunaga and Ziemann, 2009[§], n = Matsunaga and Ziemann, 2010[§], o = Butkovskaya et al. 2010, p = Aschmann et al., 2011, q = Chapter 1, r = Chapter 2 b[§]

* Data for n>5 not used to determine model parameters, adjusted branching ratios given in Arey et al., 2001

[†] Branching ratios for pentyl and heptyl nitrates recalculated using Aschmann et al., 2006 and Arey et al., 2001, respectively, to determine correction factors

[‡] T, P not specified; 1 atm and 298 K assumed

[§] Data for n<14 not used to determine model parameters; yields measured in particle phase, and gas-particle partitioning affects measurements for n<14

		Temp	Air Number Concentration	Branching Ratio		Difference
Radical	Ref.	(K)	(molecule cm^{-3})	Measured	Calc.	(%)
Primary Alkyl:						
1-Propyl	a	299	2.370E+19	0.020 ± 0.009	0.028	39%
1-Butyl	j	298	2.461E+19	0.077 ± 0.030	0.048	-37%
Neopentyl	l	298	2.429E+19	0.080 ± 0.020	0.073	-9%
	l	290	2.496E+19	0.070 ± 0.010	0.081	16%
	l	283	2.558E+19	0.090 ± 0.010	0.089	-1%
	l	273	2.652E+19	0.110 ± 0.020	0.102	-7%
	l	268	2.701E+19	0.100 ± 0.030	0.109	9%
	l	263	2.752E+19	0.130 ± 0.020	0.116	-10%
	l***	298	2.429E+19	0.070 ± 0.020	0.073	4%
	l***	273	2.652E+19	0.120 ± 0.030	0.102	-15%
	l***	267	2.711E+19	0.130 ± 0.030	0.110	-15%
	l***	262	2.763E+19	0.140 ± 0.030	0.118	-16%
Secondary Alkyl:						
2-Propyl	a*	299	2.389E+19	0.039	0.040	2%
	o	299	1.776E+18	0.006 ± 0.001	0.004	-31%
	o	299	2.259E+18	0.005 ± 0.001	0.005	13%
	o	299	2.743E+18	0.008 ± 0.001	0.006	-24%
	o	299	3.228E+18	0.010 ± 0.002	0.007	-30%
	o	299	4.843E+18	0.009 ± 0.002	0.010	22%
	o	299	6.467E+18	0.012 ± 0.002	0.014	15%
	o	299	8.068E+18	0.014 ± 0.003	0.017	16%

	o	299	9.683E+18	0.016 ± 0.004	0.019	20%
	o	299	1.130E+19	0.020 ± 0.004	0.022	10%
	o	299	1.291E+19	0.022 ± 0.004	0.025	11%
	o	299	1.614E+19	0.027 ± 0.005	0.029	8%
2-Butyl	a*	298	2.397E+19	0.084	0.068	-19%
	j	298	2.461E+19	0.070 ± 0.020	0.069	-2%
2-Pentyl	a	299	2.370E+19	0.129 ± 0.016	0.101	-22%
	b	284	2.520E+19	0.124 ± 0.014	0.124	0%
	b	284	1.210E+19	0.083 ± 0.012	0.083	0%
	b	284	5.270E+18	0.053 ± 0.009	0.047	-11%
	b	300	2.380E+19	0.105 ± 0.002	0.100	-5%
	b	300	1.630E+19	0.078 ± 0.009	0.083	7%
	b	300	1.130E+19	0.075 ± 0.013	0.068	-9%
	b	300	4.960E+18	0.047 ± 0.005	0.040	-16%
	b	300	1.820E+18	0.024 ± 0.005	0.018	-27%
	b	328	2.180E+19	0.064 ± 0.004	0.069	7%
	b	326	1.190E+19	0.050 ± 0.008	0.053	5%
	b	327	4.460E+18	0.031 ± 0.003	0.029	-5%
	b	337	2.120E+19	0.062 ± 0.005	0.061	-2%
	e**	296	2.413E+19	0.106 ± 0.000	0.105	0%
	l	298	2.429E+19	0.110 ± 0.020	0.103	-6%
	l	286	2.531E+19	0.140 ± 0.040	0.121	-13%
	l	273	2.652E+19	0.140 ± 0.030	0.145	3%
	l	263	2.752E+19	0.180 ± 0.040	0.165	-8%
	k	297	2.395E+19	0.096 ± 0.009	0.104	8%
	k	297	1.622E+19	0.078 ± 0.011	0.086	10%
	k	297	9.748E+18	0.052 ± 0.006	0.064	23%
	k	297	6.532E+18	0.039 ± 0.005	0.049	27%
	k	297	3.250E+18	0.029 ± 0.006	0.029	1%
	k	297	1.657E+18	0.019 ± 0.002	0.017	-12%
3-Pentyl	a	299	2.370E+19	0.131 ± 0.016	0.101	-23%
	b	284	2.520E+19	0.136 ± 0.015	0.124	-9%
	b	284	1.210E+19	0.094 ± 0.014	0.083	-11%
	b	284	5.270E+18	0.059 ± 0.010	0.047	-20%
	b	300	2.380E+19	0.115 ± 0.007	0.100	-13%
	b	300	1.630E+19	0.084 ± 0.010	0.083	-1%
	b	300	1.130E+19	0.081 ± 0.009	0.068	-16%
	b	300	4.960E+18	0.046 ± 0.004	0.040	-14%
	b	300	1.820E+18	0.024 ± 0.005	0.018	-27%
	b	328	2.180E+19	0.066 ± 0.005	0.069	4%

	b	326	1.190E+19	0.052 ± 0.005	0.053	1%
	b	327	4.460E+18	0.035 ± 0.005	0.029	-16%
	b	337	2.120E+19	0.064 ± 0.005	0.061	-4%
	e**	296	2.413E+19	0.126	0.105	-16%
	k	297	2.395E+19	0.116 ± 0.009	0.104	-10%
	k	297	1.622E+19	0.091 ± 0.010	0.086	-6%
2-Hexyl	i	298	2.397E+19	0.140	0.143	2%
3-Hexyl	i	298	2.397E+19	0.158	0.143	-9%
Cyclohexyl	g	296	2.364E+19	0.160 ± 0.040	0.146	-9%
	h	296	1.304E+19	0.150 ± 0.040	0.114	-24%
	j	298	2.461E+19	0.170 ± 0.040	0.145	-15%
	p	298	2.380E+19	0.160 ± 0.020	0.143	-11%
2-Heptyl	b	284	2.520E+19	0.183 ± 0.028	0.226	23%
	b	285	1.180E+19	0.153 ± 0.025	0.175	14%
	b	283	5.430E+18	0.100 ± 0.011	0.129	28%
	b	284	1.970E+18	0.071 ± 0.010	0.072	2%
	b	300	2.380E+19	0.179 ± 0.014	0.178	0%
	b	300	1.140E+19	0.142 ± 0.014	0.142	0%
	b	300	5.150E+18	0.090 ± 0.012	0.102	14%
	b	300	1.800E+18	0.062 ± 0.004	0.058	-6%
	b	323	2.210E+19	0.125 ± 0.015	0.125	-1%
	b	324	1.060E+19	0.100 ± 0.017	0.101	1%
	b	324	4.650E+18	0.064 ± 0.007	0.073	15%
	b	321	1.790E+18	0.044 ± 0.004	0.047	7%
	b	339	2.110E+19	0.098 ± 0.015	0.097	-1%
	b	342	4.520E+18	0.055 ± 0.005	0.058	6%
	i	298	2.397E+19	0.177	0.184	4%
3-Heptyl	b	284	2.520E+19	0.216 ± 0.023	0.226	5%
	b	285	1.180E+19	0.179 ± 0.024	0.175	-2%
	b	283	5.430E+18	0.120 ± 0.010	0.129	7%
	b	284	1.970E+18	0.087 ± 0.015	0.072	-17%
	b	300	2.380E+19	0.200 ± 0.009	0.178	-11%
	b	300	1.140E+19	0.180 ± 0.061	0.142	-21%
	b	300	5.150E+18	0.109 ± 0.016	0.102	-6%
	b	300	1.800E+18	0.075 ± 0.009	0.058	-22%
	b	323	2.210E+19	0.139 ± 0.015	0.125	-10%
	b	324	1.060E+19	0.110 ± 0.017	0.101	-8%
	b	324	4.650E+18	0.075 ± 0.011	0.073	-2%
	b	321	1.790E+18	0.054 ± 0.007	0.047	-13%
	b	339	2.110E+19	0.106 ± 0.006	0.097	-8%

	b	342	4.520E+18	0.059 ± 0.006	0.058	-1%
	i	298	2.397E+19	0.193	0.184	-5%
4-Heptyl	b	284	2.520E+19	0.193 ± 0.018	0.226	17%
	b	285	1.180E+19	0.163 ± 0.024	0.175	7%
	b	283	5.430E+18	0.108 ± 0.009	0.129	19%
	b	284	1.970E+18	0.074 ± 0.010	0.072	-3%
	b	300	2.380E+19	0.175 ± 0.009	0.178	2%
	b	300	1.140E+19	0.145 ± 0.015	0.142	-2%
	b	300	5.150E+18	0.094 ± 0.008	0.102	9%
	b	300	1.800E+18	0.065 ± 0.006	0.058	-10%
	b	323	2.210E+19	0.123 ± 0.015	0.125	1%
	b	324	1.060E+19	0.098 ± 0.015	0.101	2%
	b	324	4.650E+18	0.063 ± 0.008	0.073	17%
	b	321	1.790E+18	0.045 ± 0.005	0.047	4%
	b	339	2.110E+19	0.094 ± 0.004	0.097	3%
	b	342	4.520E+18	0.052 ± 0.004	0.058	13%
	i	298	2.397E+19	0.175	0.184	5%
2-Octyl	i	298	2.397E+19	0.224	0.215	-4%
	q	302	2.423E+19	0.233 ± 0.028	0.202	-13%
3-Octyl	i	298	2.397E+19	0.238	0.215	-10%
	q	302	2.423E+19	0.217 ± 0.041	0.202	-7%
4-Octyl	i	298	2.397E+19	0.243	0.215	-12%
	q	302	2.423E+19	0.208 ± 0.024	0.202	-3%
2-Decyl	q	301	2.431E+19	0.230 ± 0.027	0.235	2%
3-Decyl	q	301	2.431E+19	0.194 ± 0.026	0.235	21%
4-Decyl	q	301	2.431E+19	0.198 ± 0.020	0.235	19%
5-Decyl	q	301	2.431E+19	0.197 ± 0.020	0.235	19%
2-Dodecyl	q	298	2.455E+19	0.273 ± 0.042	0.259	-5%
3-Dodecyl	q	298	2.455E+19	0.238 ± 0.026	0.259	9%
4-Dodecyl	q	298	2.455E+19	0.236 ± 0.030	0.259	10%
5-Dodecyl	q	298	2.455E+19	0.263 ± 0.042	0.259	-1%
6-Dodecyl	q	298	2.455E+19	0.259 ± 0.025	0.259	0%
2-Tridecyl	q	299	2.447E+19	0.319 ± 0.119	0.257	-19%
3-Tridecyl	q	299	2.447E+19	0.292 ± 0.025	0.257	-12%
4-Tridecyl	q	299	2.447E+19	0.262 ± 0.023	0.257	-2%
5-Tridecyl	q	299	2.447E+19	0.281 ± 0.034	0.257	-8%
6-Tridecyl	q	299	2.447E+19	0.300 ± 0.027	0.257	-14%
7-Tridecyl	q	299	2.447E+19	0.294 ± 0.027	0.257	-12%
2-Tetradecyl	q	299	2.447E+19	0.293 ± 0.022	0.259	-11%
3-Tetradecyl	q	299	2.447E+19	0.338 ± 0.054	0.259	-23%

4-Tetradecyl	q	299	2.447E+19	0.314 ± 0.080	0.259	-18%
5-Tetradecyl	q	299	2.447E+19	0.326 ± 0.063	0.259	-21%
6-Tetradecyl	q	299	2.447E+19	0.314 ± 0.056	0.259	-17%
7-Tetradecyl	q	299	2.447E+19	0.302 ± 0.054	0.259	-14%
Tertiary Alkyl:						
2-Methyl-2-butyl	l	305	2.373E+19	0.120 ± 0.050	0.106	-11%
	l	298	2.429E+19	0.110 ± 0.040	0.117	6%
	l	273	2.652E+19	0.140 ± 0.080	0.163	17%
	l	261	2.774E+19	0.240 ± 0.110	0.191	-20%
Primary β-Hydroxy Alkyl:						
2-Hydroxy-1-ethyl	f	296	2.478E+19	0.0086 ± 0.0003	0.009	2%
2-Hydroxy-1-propyl	f	296	2.478E+19	0.018 ± 0.001	0.016	-8%
2-Hydroxy-1-propyl	c	298	2.461E+19	0.019	0.016	-16%
2-Hydroxy-1-butyl	f	296	2.478E+19	0.032 ± 0.003	0.028	-13%
2-Hydroxy-1-hexyl	f	296	2.478E+19	0.067 ± 0.015	0.058	-13%
2-Hydroxy-1-tetradecyl	m	298	2.461E+19	0.073	0.104	43%
2-Hydroxy-1-pentadecyl	m	298	2.461E+19	0.093	0.104	12%
2-Hydroxy-2-methyl-1-tetradecyl	n	298	2.461E+19	0.122	0.104	-15%
2-Hydroxy-1-hexadecyl	m	298	2.461E+19	0.125	0.105	-16%
2-Hydroxy-1-heptadecyl	m	298	2.461E+19	0.116	0.105	-10%
Secondary β-Hydroxy Alkyl:						
1-Hydroxy-2-propyl	c	298	2.461E+19	0.022	0.017	-21%
1-Hydroxy-2-propyl	f	296	2.478E+19	0.014	0.018	25%
1-Hydroxy-2-butyl	f	296	2.478E+19	0.022	0.030	38%
3-Hydroxy-2-butyl	f	296	2.478E+19	0.034	0.030	-12%
3-Hydroxy-2-butyl	d	298	2.461E+19	0.037	0.029	-21%
1-Hydroxy-2-hexyl	f	296	2.478E+19	0.050	0.063	26%
1-Hydroxy-2-tetradecyl	m	298	2.461E+19	0.168	0.112	-33%
1-Hydroxy-2-pentadecyl	m	298	2.461E+19	0.154	0.113	-27%
1-Hydroxy-2-hexadecyl	m	298	2.461E+19	0.134	0.113	-16%
1-Hydroxy-2-heptadecyl	m	298	2.461E+19	0.143	0.114	-21%
Secondary δ-Hydroxy Alkyl:						
1,4-Hydroxytetradecyl	r	299	2.447E+19	0.190 ± 0.027	0.181	-5%
1,4-Hydroxypentadecyl	r	298	2.455E+19	0.171 ± 0.040	0.185	8%
1,4-Hydroxyhexadecyl	r	299	2.447E+19	0.190 ± 0.012	0.182	-4%

Tertiary β-Hydroxy Alkyl:						
1-Hydroxy-2-methyl-2-tridecyl	n	298	2.461E+19	0.238	0.243	2%
1-Hydroxy-2-methyl-2-tetradecyl	n	298	2.461E+19	0.249	0.244	-2%
Primary Haloalkyl:						
1-Bromo-3-propyl	j	298	2.461E+19	0.029 ± 0.010	0.029	0%
Secondary Haloalkyl:						
1-Bromo-2-propyl	j	298	2.461E+19	0.022 ± 0.010	0.022	0%

*yield measured in Atkinson 1982, and updated in Arey et al., 2001
**yield measured in Atkinson et al., 1995, and branching ratio reported in Arey et al., 2001
***measured by ECD

The updated coefficients are reasonably close to those determined previously (Arey et al., 2001). The most significant changes were for the broadening coefficient (*F*), and the theoretical maximum yield at 298 K (Y_{∞}^{298}). The updated broadening coefficient of 0.688 is closer to the value of 0.6 used routinely by NASA to estimate rate coefficients for termolecular reactions (Sander et al., 2006) and is in excellent agreement with the value of 0.7 calculated by Donahue and coworkers (Zhang et al., 2004). The theoretical maximum yield at 298 K decreased from 0.43 to 0.372. This is due in part to the addition of branching ratios measured for reactions of larger alkanes, which were slightly lower than those calculated using the previous parameterization (Chapter 1). The branching ratios measured as a function of pressure by Butkovskaya et al., 2010, aided in the determination of the pressure dependence of nitrate formation (Butkovskaya et al., 2010). The corrected branching ratios for pentyl and heptyl nitrate formation as a function of temperature (Atkinson et al., 1983; Arey et al., 2001; Aschmann et al., 2006) and the measurements of Cassanelli et al. (Cassanelli et al., 2005), aided in the determination of the temperature dependence of nitrate formation. Compared to the previous parameterization, which was based on a much smaller dataset, the updated parameterization has less tendency to overpredict branching ratios. The linear regressions evaluating the correlation of model-calculated and measured branching ratios are shown in Figure 3.1.

Figure 3.1: Comparison of measured branching ratios for alkyl nitrate formation with model values calculate using the parameterizations reported in (a) Arey et al., 2001 and (b) the present study.

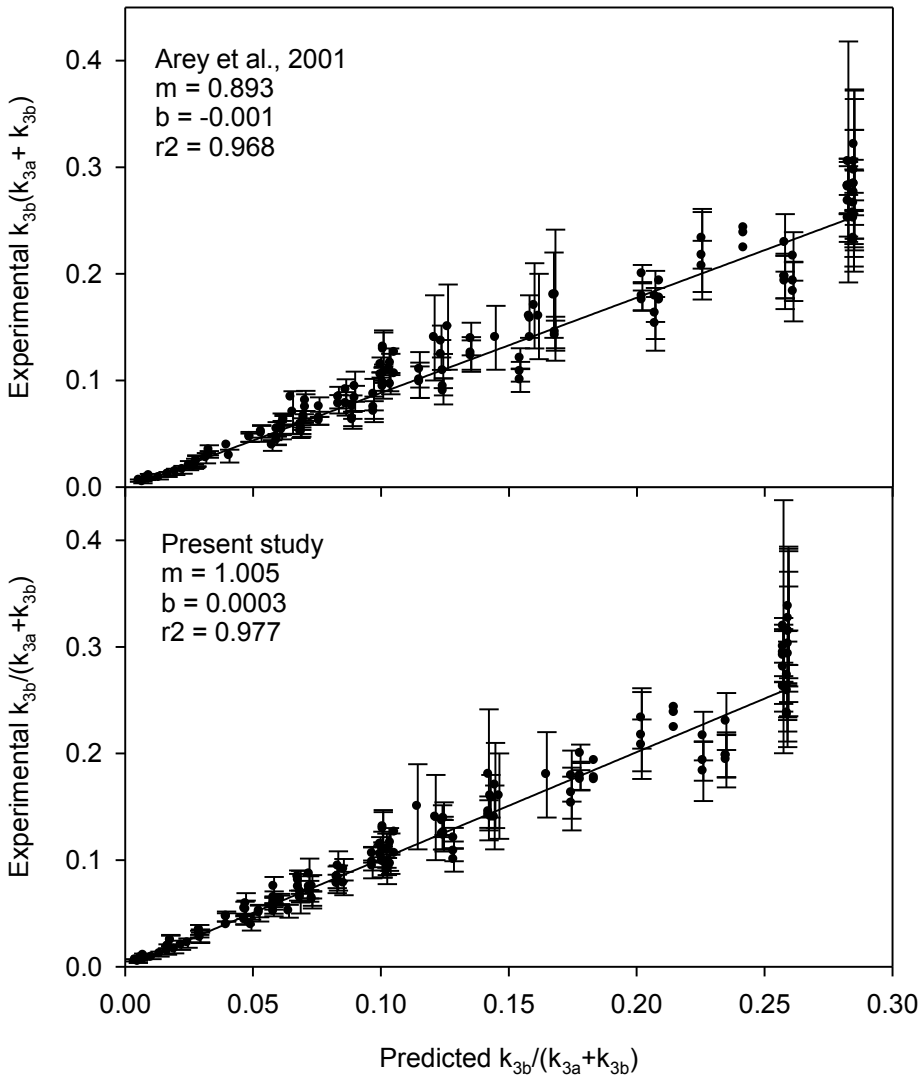

The parameterization of Arey et al., 2001 gives a slope of 0.893, and a y-intercept of −0.001, with an r^2 of 0.968, indicating that these parameterizations provide a good fit to experimental data, even though the database used to determine those fitting parameters was much more limited than the database used for this update. The updated parameterization gives a slope of 1.005, and a y-intercept of -0.0003, with an r^2 of 0.977. Although the r^2 is not substantially improved from the previous parameterization, the slope of the regression is closer to one, indicating the updated parameters have a reduced tendency to overestimate nitrate yield. The updated parameters also produce estimates that tend to be unbiased in relation to carbon number, pressure, and temperature. The scatter of the errors, quantified as the percent difference between model-calculated and measured values, is reasonably random when plotted relative to these values, as shown in Figure 3.2.

Figure 3.2: Percent difference of measured and model-calculated branching ratios for secondary alkyl nitrate formation plotted as a function of carbon number (a), air number concentration (b), and temperature (c).

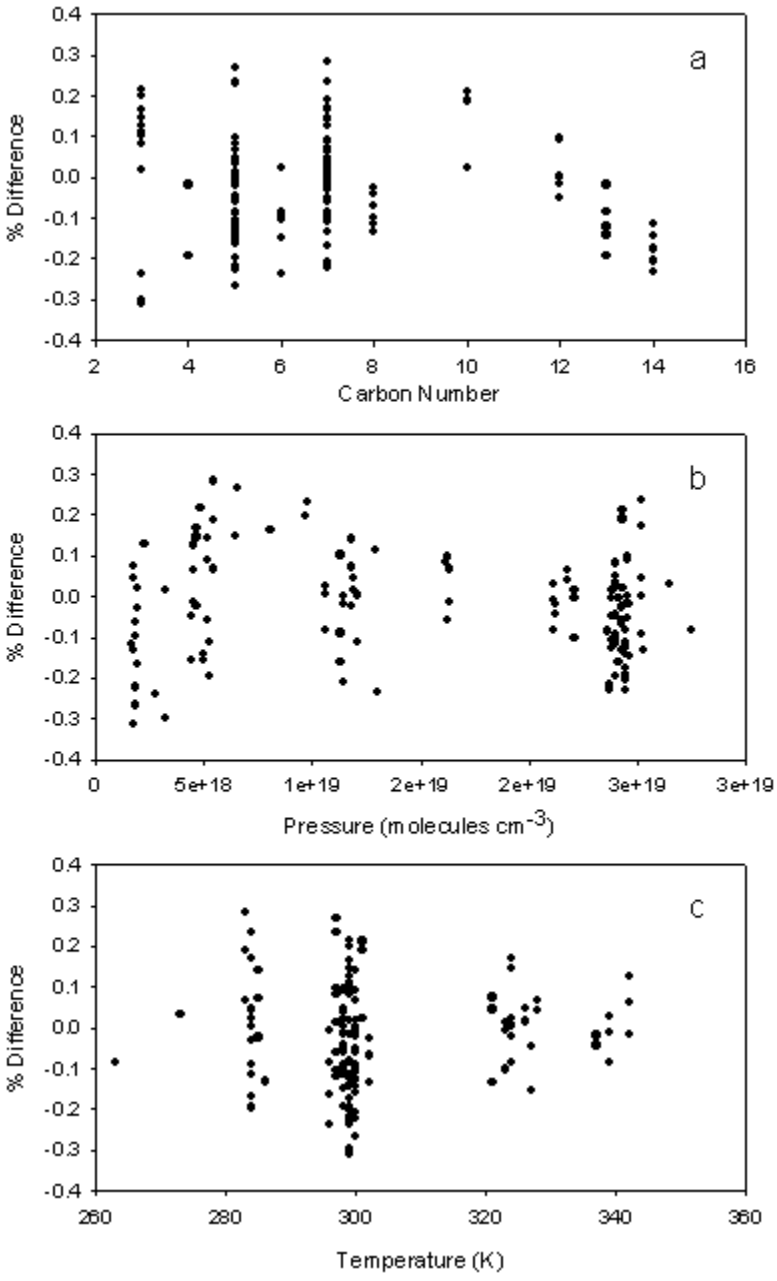

The reasonably random scatter of error versus temperature and air number concentration suggests a lack of systematic error inherent in the updated parameterization. This is also generally the case for the dependence on carbon number, although there is a slight tendency for the model to underpredict alkyl nitrate yields for carbon numbers ≥10. This could be due to experimental errors in the alkyl nitrate yields measured for the larger alkanes. In the chamber experiments conducted to measure these yields, gas-wall partitioning of alkyl nitrate products was observed, and which in some cases necessitated large correction factors to that were determined by quantifying the gas-wall partitioning of alkyl nitrate standards (Chapter 1). The larger experimental errors accompanying these measurements could be the main cause of the trend towards underprediction, which would then not necessarily indicate a problem with the model parameters. Additional measurements of alkyl nitrate yields for reactions of large alkanes would improve the accuracy of the Y_{∞}^{298} fitting parameter, which is the primary factor that determines alkyl nitrate yields at high carbon numbers and room temperature and pressure, but these measurements are inherently difficult.

The optimized scaling factors (γ) for alkyl peroxy radicals are 0.71 for primary, 1.00 for secondary, 1.13 for tertiary, 0.39 for primary β-hydroxy, 0.43 for secondary β-hydroxy, 0.92 for tertiary β-hydroxy radicals, 0.58 for secondary δ-hydroxy radicals, 0.71 for primary γ-bromo , and 0.54 for secondary β-bromo. Model-calculated alkyl nitrate yields are lower for reactions of primary than secondary alkyl peroxy radicals, but the difference is less than previously reported; in the 1989 parameterization the scaling factor was 0.4 (Carter and Atkinson, 1989), but the updated parameter of 0.71 indicates that

primary alkyl nitrates are formed more easily than previously thought. The updated scaling factor of 1.13 for tertiary alkyl nitrates indicates that tertiary alkyl nitrates form about as readily as secondary ones (scaling factor = 1.00, by definition), contrary to the previous parameterization where the scaling factor was 0.3 (Carter and Atkinson, 1989). The inhibitory effect of hydroxyl groups on organic nitrate formation is essentially the same as that reported previously (Matsunaga and Ziemann, 2009) with scaling factors for the formation of primary and secondary β-hydroxynitrates of 0.43 and 0.455, respectively. The nearly identical scaling factors in the updated parameterization of 0.39 and 0.43 for the formation of primary and secondary β-hydroxynitrates suggest that hydrogen bonding between the hydroxyl group and peroxy groups in the excited intermediate is the main determinant of branching ratio. If the hydroxyl group exerted less influence, the effect of carbon substitution would likely be more apparent, and the difference between primary and secondary β-hydroxyalkyl nitrate scaling factors would be larger. The surprisingly high scaling factor of 0.92 for tertiary β-hydroxynitrates suggests that the adjacent methyl group may constrain the conformation of the intermediate so as to limit the degree of hydrogen bonding between the hydroxyl and peroxy groups. The scaling factors also indicate that the distance between the hydroxyl and peroxy groups has a significant effect on organic nitrate yields since the scaling factor of 0.58 for the formation of secondary δ-hydroxynitrates is significantly higher than the value of 0.43 for secondary β-hydroxynitrates. It is not possible to meaningfully comment on the yields of haloalkyl radicals without a more complete dataset, but the overall effect of the halogen groups on organic nitrate yield is an inhibitory one.

Atmospheric profiles of alkyl nitrate formation

The model can be used to calculate the branching ratios for alkyl nitrate formation in the troposphere, which are sensitive to altitude because of the large temperature and pressure gradients. Branching ratios calculated as a function of altitude (expressed as standard atmospheres) are shown in Figure 3.3.

Figure 3.3: Model-calculated branching ratios for alkyl nitrate formation from the reactions of C_3–C_{12} alkyl peroxy radicals, plotted as a function of standard atmospheres from sea level to 12 km.

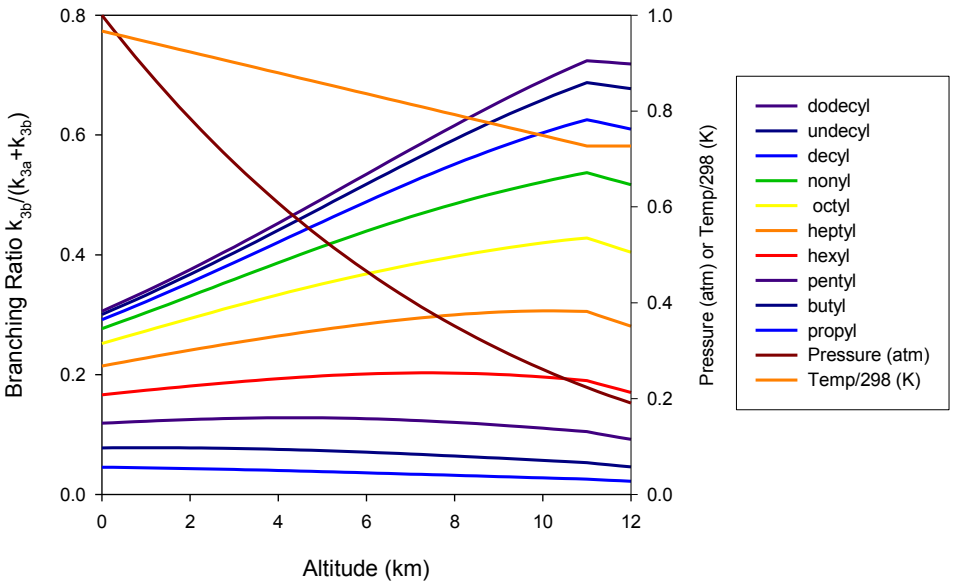

The updated model parameters do not have a large impact on the calculated branching ratios compared to Arey et al., 2001 parameters (not shown). The yields near the tropopause are slightly lower, but the magnitude of the temperature dependence is mostly unchanged. In both parameterizations, the branching ratios for alkyl nitrate formation increase with altitude due to the decrease in temperature from ~290 K at the surface to ~210K at the tropopause, with the effects of temperature on branching ratios increasing with increasing carbon number. This effect is important when modeling the formation of organic nitrates from smaller alkanes that have sufficiently long lifetimes to be mixed throughout the troposphere (~10 days), and also hydrocarbons from jettisoned fuel tanks or partially combusted jet fuel, which is composed primarily of alkanes with carbon numbers C_8–C_{16} (Hemighaus et al., 2006).

Conclusions

A set of updated model parameters was determined for calculating the branching ratios for the formation of organic nitrates from reactions alkyl peroxy radicals with NO. The updated parameters slightly improved the agreement between model-calculated and measured values compared to the previous parameterization. Improvements were possible because of an expanded data set on secondary alkyl nitrate yields as a function of carbon number, temperature, and air number concentration that has become available since the last optimization was conducted. Scaling factors that were not previously part of the model were determined for calculating the branching ratios for alkyl nitrate formation from reactions of primary and tertiary alkyl peroxy radicals, indicating a reduced tendency for the formation of primary alkyl nitrates compared to the secondary and tertiary products. The expanded dataset also permitted the determination of scaling factors for the formation of organic nitrates from reactions of substituted alkyl peroxy radicals. The model with updated parameters can be incorporated into tropospheric models to more accurately describe organic nitrate formation, NO_x concentrations, and the formation of ozone for a wide range of organic precursors, temperatures and pressures.

References

1. Arey, J., Aschmann, S. M., Kwok, E. S., & Atkinson, R. (**2001**). Alkyl nitrate, hydroxyalkyl nitrate, and hydroxycarbonyl formation from the NO_x-air photooxidations of C_5-C_8 n-alkanes. *The Journal of Physical Chemistry A*, 105(6), 1020-1027.

2. Aschmann, S. M., Arey, J., & Atkinson, R. (**2001**). Atmospheric chemistry of three C_{10} alkanes. *The Journal of Physical Chemistry A*, 105(32), 7598-7606.

3. Aschmann, S. M., Long, W. D., & Atkinson, R. (**2006**). Pressure dependence of pentyl nitrate formation from the OH radical-initiated reaction of *n*-pentane in the presence of NO. *The Journal of Physical Chemistry A*, 110(21), 6617-6622.

4. Aschmann, S. M., Arey, J., & Atkinson, R. (**2011**). Reactions of OH Radicals with C_6–C_{10} Cycloalkanes in the Presence of NO: Isomerization of C_7–C_{10} Cycloalkoxy Radicals. *The Journal of Physical Chemistry A*, 115(50), 14452-14461.

5. Atkinson, R., Aschmann, S. M., Carter, W. P., Winer, A. M., & Pitts Jr, J. N. (**1982**). Alkyl nitrate formation from the nitrogen oxide (NO_x)-air photooxidations of C_2-C_8 n-alkanes. *The Journal of Physical Chemistry*, 86(23), 4563-4569.

6. Atkinson, R., Carter, W. P., & Winer, A. M. (**1983**). Effects of temperature and pressure on alkyl nitrate yields in the nitrogen oxide (NO_x) photooxidations of n-pentane and n-heptane. *The Journal of Physical Chemistry*, 87(11), 2012-2018.

7. Atkinson, R., Plum, C. N., Carter, W. P., Winer, A. M., & Pitts Jr, J. N. (**1984**). Rate constants for the gas-phase reactions of nitrate radicals with a series of organics in air at 298 ±1 K. *The Journal of Physical Chemistry*, 88(6), 1210-1215.

8. Atkinson, R., Aschmann, S. M., & Winer, A. M. (**1987**). Alkyl nitrate formation from the reaction of a series of branched RO_2 radicals with NO as a function of temperature and pressure. *Journal of Atmospheric Chemistry*, 5(1), 91-102.

9. Atkinson, R., Kwok, E. S., Arey, J., & Aschmann, S. M. (**1995**). Reactions of alkoxyl radicals in the atmosphere. *Faraday Discussions*, 100, 23-37.

10. Atkinson, R. "*Atmospheric oxidation*" pp.335-354 in *Handbook of Property Estimation Methods for Chemicals: Environmental and Health Services*; Boethling, R.S.; Mackay, D., Eds. CRC Press: Boca Raton, FL, 2000.

11. Atkinson, R., & Arey, J. (**2003**). Atmospheric degradation of volatile organic compounds. *Chemical Reviews*, 103(12), 4605-4638

12. Ballschmiter, K. (**2002**). A marine source for alkyl nitrates. *Science*, 297(5584), 1127-1128.

13. Butkovskaya, N. I., Kukui, A., & Le Bras, G. (**2010**). Pressure Dependence of Iso-Propyl Nitrate Formation in the i-$C_3H_7O_2$ + NO Reaction. *Zeitschrift fuer Physikalische Chemie*, 224(7-8), 1025-1038.

14. Carter, W. P., & Atkinson, R. (**1985**). Atmospheric chemistry of alkanes. *Journal of Atmospheric Chemistry*, 3(3), 377-405.

15. Carter, W. P., & Atkinson, R. (**1989**). Alkyl nitrate formation from the atmospheric photooxidation of alkanes; a revised estimation method. *Journal of Atmospheric Chemistry*, 8(2), 165-173.

16. Cassanelli, P., Johnson, D., & Cox, R. A. (**2005**). A temperature-dependent relative-rate study of the OH initiated oxidation of *n*-butane: The kinetics of the reactions of the 1-and 2-butoxy radicals. *Physical Chemistry Chemical Physics*, 7(21), 3702-3710.

17. Cassanelli, P., Fox, D. J., & Cox, R. A. (**2007**). Temperature dependence of pentyl nitrate formation from the reaction of pentyl peroxy radicals with NO. *Physical Chemistry Chemical Physics*, 9(31), 4332-4337.

18. Chow, J. M., Miller, A. M., & Elrod, M. J. (**2003**). Kinetics of the $C_3H_7O_2$+ NO reaction: Temperature dependence of the overall rate constant and the i-$C_3H_7ONO_2$ branching channel. *The Journal of Physical Chemistry A*, 107(17), 3040-3047.

19. Cleary, P.A.; Murphy, J.G.; Wooldridge, P.J.; Day, D.A.; Millet, D.B.; McKay, M.; Goldstein, A.H.; Cohen R.C. (**2005**). Observations of total alkyl nitrates within the Sacramento Urban Plume. *Atmospheric Chemistry and Physics Discussions*, 5(4), 4801-4843.

20. Cvetanovic, R. J. 12th International Symposium on Free Radicals, Laguna Beach, CA, Jan 4–9, 1976. Cited in: Atkinson, R. *Journal of Physical and Chemical Reference Data* 1989

21. Day, D. A., Dillon, M. B., Wooldridge, P. J., Thornton, J. A., Rosen, R. S., Wood, E. C., & Cohen, R. C. (**2003**). On alkyl nitrates, O_3, and the "missing NO_y". *Journal of Geophysical Research*, 108(D16), 4501-4510.

22. Espada, C., Grossenbacher, J., Ford, K., Couch, T., & Shepson, P. B. (**2005**). The production of organic nitrates from various anthropogenic volatile organic compounds. *International Journal of Chemical Kinetics*, 37(11), 675-685.

23. Harris, S. J., & Kerr, J. A. (**1989**). A kinetic and mechanistic study of the formation of alkyl nitrates in the photo-oxidation of *n*-heptane studied under atmospheric conditions. *International Journal of Chemical Kinetics*, 21(3), 207-218.

24. Hemighaus, G., Boval. T., Bacha, J., Barnes, F., Franklin, M., Gibbs, L., Hogue, N., Jones, J., Lesnini, D., Lind, J., & Morris, J. (**2006**) Chevron Corporation Aviation Fuels Technical Review.

25. Kwok, E. S., & Atkinson, R. (**1995**). Estimation of hydroxyl radical reaction rate constants for gas-phase organic compounds using a structure-reactivity relationship: An update. *Atmospheric Environment*, 29(14), 1685-1695.

26. Lesar, A., Hodošcek, M., Drougas, E., & Kosmas, A. M. (**2006**). Quantum mechanical investigation of the atmospheric reaction CH_3O_2+ NO. *The Journal of Physical Chemistry A*, 110(25), 7898-7903.

27. Lockwood, A. L., Shepson, P. B., Fiddler, M. N., & Alaghmand, M. (**2010**). Isoprene nitrates: preparation, separation, identification, yields, and atmospheric chemistry. *Atmospheric Chemistry and Physics*, 10(13), 6169-6178.

28. Matsunaga, A., & Ziemann, P. J. (**2009**). Yields of β-hydroxynitrates and dihydroxynitrates in aerosol formed from OH radical-initiated reactions of linear alkenes in the presence of NO_x. *The Journal of Physical Chemistry A*, 113(3), 599-606.

29. Matsunaga, A., & Ziemann, P. J. (**2010**). Yields of β-hydroxynitrates, dihydroxynitrates, and trihydroxynitrates formed from OH radical-initiated reactions of 2-methyl-1-alkenes. *Proceedings of the National Academy of Sciences*, 107(15), 6664-6669.

30. Luther, K., & Troe, J. (1979, December). Weak collision effects in dissociation reactions at high temperatures. In Symposium (International) on Combustion (Vol. 17, No. 1, pp. 535-542). Elsevier

31. Muthuramu, K., Shepson, P. B., & O'Brien, J. M. (**1993**). Preparation, analysis, and atmospheric production of multifunctional organic nitrates. *Environmental science & technology*, 27(6), 1117-1124.

32. Sander, S. P., Golden, D. M., Kurylo, M. J., Moortgat, G. K., Wine, P. H., Ravishankara, A. R., Kolb, C. E., Molina, M. J., Finlayson-Pitts, B. J., Huie, R. E., & Orkin, V. L. (**2006**). Chemical kinetics and photochemical data for use in atmospheric studies evaluation number 15.

33. Nishino, N., Arey, J., & Atkinson, R. (**2009**). Rate Constants for the Gas-Phase Reactions of OH Radicals with a Series of C_6– C_{14} Alkenes at 299 ± 2 K. *The Journal of Physical Chemistry A*, 113(5), 852-857.

34. O'Brien, J. M., Czuba, E., Hastie, D. R., Francisco, J. S., & Shepson, P. B. (**1998**). Determination of the hydroxy nitrate yields from the reaction of C_2-C_6 alkenes

with OH in the presence of NO. *The Journal of Physical Chemistry A*, 102(45), 8903-8908.

35. Orlando, J. J., Iraci, L. T., & Tyndall, G. S. (**2000**). Chemistry of the cyclopentoxy and cyclohexoxy radicals at subambient temperatures. *The Journal of Physical Chemistry A*, 104(21), 5072-5079.

36. Peeters, J., Boullart, W., Pultau, V., Vandenberk, S., & Vereecken, L. (**2007**). Structure-activity relationship for the addition of OH to (poly) alkenes: Site-specific and total rate constants. *The Journal of Physical Chemistry A*, 111(9), 1618-1631.

37. Platz, J., Sehested, J., Nielsen, O. J., & Wallington, T. J. (**1999**). Atmospheric Chemistry of Cyclohexane: UV Spectra of c-C_6H_{11} and (c-C_6H_{11}) O_2 Radicals, Kinetics of the Reactions of (c-C_6H_{11})O_2 Radicals with NO and NO_2, and the Fate of the Alkoxy Radical (c-C_6H_{11})O. *The Journal of Physical Chemistry A*, 103(15), 2688-2695.

38. Robinson, P.J.; Holbrook, K.A. *Unimolecular Reactions* Wiley, New York, NY, 1972.

39. Russo, R.S.; Zhou, Y.; Haase, K.B.; Wingenter, O.W.; Frinak, E.K.; Mao, H.; Talbot, R.W.; Sive, B.C. (**2010**). Temporal variability, sources, and sinks of C_1-C_5 alkyl nitrates in coastal New England. *Atmospheric Chemistry and Physics*, 10(4), 1865-1883.

40. Saito, T., Kawamura, K., Nakatsuka, T., & Huebert, B. J. (**2004**). In situ measurements of butane and pentane isomers over the subtropical North Pacific. *Geochemical Journal*, 38(5), 397-404.

41. Schneider, M., & Ballschmiter, K. (**1999**). C_3-C_{14} alkyl nitrates in remote south Atlantic air. *Chemosphere*, 38(1), 233-244.

42. Shepson, P. B., Edney, E. O., Kleindienst, T. E., Pittman, J. H., & Namie, G. R. (**1985**). Production of organic nitrates from hydroxide and nitrate reaction with propylene. *Environmental Science & Technology*, 19(9), 849-854

43. Troe, J. (**1974**). Fall-off Curves of Unimolecular Reactions. *Berichte der Bunsengesellschaft für physikalische Chemie*, 78(5), 478-488.

44. Ziemann, P. J. (**2011**). Effects of molecular structure on the chemistry of aerosol formation from the OH-radical-initiated oxidation of alkanes and alkenes. *International Reviews in Physical Chemistry*, 30(2), 161-195.

45. Zhang, J., Dransfield, T., & Donahue, N. M. (**2004**). On the mechanism for nitrate formation via the peroxy radical + NO reaction. *The Journal of Physical Chemistry A*, 108(42), 9082-9095.

46. Zhao, Y., Houk, K. N., & Olson, L. P. (**2004**). Mechanisms of peroxynitrous acid and methyl peroxynitrite, ROONO (R= H, Me), rearrangements: A conformation-dependent homolytic dissociation. *The Journal of Physical Chemistry A*, 108(27), 5864-5871.

Chapter 4: Products and mechanism of the reaction of 1-pentadecene with NO_3 radicals, and the effect of the nitrooxy group on the branching ratio for alkoxy radical decomposition:isomerization

Abstract

Secondary organic aerosol (SOA) and particulate β-hydroxynitrates, β-carbonylnitrates, and organic peroxides formed from the reaction of 1-pentadecene with NO_3 radicals in a Teflon environmental chamber were quantified using a variety of methods. Results were used to estimate molar yields of β-hydroxypentadecyl nitrate, β-oxopentadecyl nitrate, β-hydroxperoxypentadecyl nitrate, tetradecanal, and products formed from the isomerization of β-nitrooxypentadecyloxy radicals of 0.10, 0.17, 0.02, 0.54, and 0.17, and branching ratios for decomposition and isomerization of β-nitrooxypentadecyloxy radicals of 0.76 and 0.24, respectively. The branching ratio for decomposition of these C_{15} β-nitrooxyalkoxy radicals was larger than the values of 0.42 and 0.65 reported for C_8 and C_{14} β-hydroxyalkoxy radicals formed from reactions of 1-octene and 7-tetradecene with OH radicals in the presence of NO. Because β-nitrooxyalkoxy radicals formed from reactions of alkenes with NO_3 radicals (where NO is low) are much less energetic than those formed in the presence of NO, the estimated branching ratio for decomposition of C_{15} β-nitrooxyalkoxy radicals is a lower limit. These results indicate that the presence of nitrooxy groups on organic compounds can increase the likelihood of fragmentation upon subsequent atmospheric oxidation, an

effect that can reduce the tendency of the reaction products to partition to particles and form SOA.

Introduction

Alkenes are the most abundant non-methane organic compounds (NMOC) in the atmosphere. They are emitted mostly from biogenic sources, which emit NMOC in amounts that are approximately an order of magnitude larger than those from anthropogenic sources (Guenther et al., 1995). Alkenes primarily react with OH radicals during the day, NO_3 radicals at night, and O_3 during the day and night (Atkinson and Arey 1997; Atkinson and Arey 2003a). The reactions with NO_3 radicals have recently been shown to dictate nighttime formation of secondary organic aerosol (SOA) (Rollins et al., 2012), which in general is formed when volatile organic compounds (VOC) react with atmospheric oxidants to form less volatile products that partition into particles. SOA comprises a significant fraction of atmospheric fine particulate matter, in many cases dominating overall particle mass (Zhang et al., 2007; DeGouw and Jimenez 2009). Atmospheric aerosol is a significant human health risk, linked to respiratory disorders and mortality (Etzel, 2003; Abel-Moreno et al., 2007; Pope, 2009), and it also affects regional and global climate by scattering and absorbing light and by acting as cloud condensation nuclei (Lohmann and Feichter, 2005; Forster et al., 2007). Because alkenes are abundant and reactive during both the day and night, accurate modeling of the role of these compounds in SOA formation requires detailed characterization and quantitation of the dominant reaction products of their atmospheric reactions with NO_3 radicals.

Although the mechanisms of gas phase atmospheric oxidation of VOC are usually complex, for the purposes of understanding SOA formation it is often useful to focus on two types of reaction pathways: (1) those that lead to the addition of functional groups to

the intact carbon backbone of the parent VOC (functionalization), and (2) those that lead to cleavage of C–C bonds and result in the formation of products with smaller carbon numbers than the parent VOC (fragmentation) (Kroll et al., 2009; Chacon-Madrid et al., 2010; Chacon-Madrid and Donahue, 2011; Lambe et al., 2012). In general, functionalization forms less volatile products and more SOA, whereas fragmentation forms more volatile products and less SOA, although heterogeneous/multiphase oligomerization reactions can incorporate fairly volatile compounds into particles. Although there are many VOC reaction pathways that lead to functionalization, fragmentation occurs primarily when alkoxy radicals, which are reaction intermediates common to the oxidation of essentially all VOCs (Atkinson and Arey, 2003a; Ziemann and Atkinson, 2012), decompose by cleavage of C–C bonds as shown in Scheme 4.1.

Scheme 4.1: Alkoxy radical decomposition.

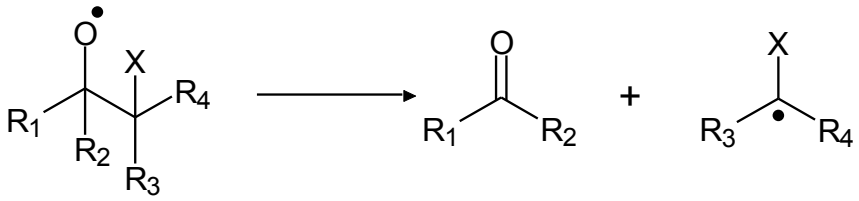

For the alkoxy radical structure shown, R_1–R_4 are alkyl groups or H atoms and X is a functional group such as –OH or –ONO_2. Decomposition occurs by cleavage of the •OCa–CbX bond between the alkoxy radical and functional group C atoms and leads to the formation of two fragments, one a carbonyl (aldehyde or ketone) and the other an alkyl radical. If the parent VOC is acyclic, then two fragmentation products are formed, whereas if it is cyclic a single ring-opened product is formed. When an acyclic VOC loses more than two carbons the vapor pressures of both fragmentation products will usually be higher than that of the parent VOC (Pankow and Asher 2008, Chacon-Madrid et al., 2010, Chacon-Madrid and Donahue, 2011).

If the structure shown in Scheme 4.1 is a simple linear secondary alkoxy radical, $R_1HC_a(O•)–C_bH_2R_2$, with R_1 and R_2 having carbon numbers $\geq C_3$ or C_2, respectively, then the alkoxy radical will react almost entirely by isomerization through a 1,5 H-atom shift. If a functional group or alkyl group is substituted for an H atom on the C_b atom adjacent to the alkoxy radical, however, the rate of decomposition is enhanced by orders of magnitude and decomposition competes with isomerization. The branching between decomposition and isomerization can be estimated for a variety of structures using the structure-reactivity method of Atkinson (Atkinson, 2007). Among the functional groups most often present in VOC reaction products, such as carbonyl, hydroxyl, carboxyl, hydroxperoxy, nitrooxy, ester, and ether (Ziemann and Atkinson 2012), only the effects of carbonyl, hydroxyl, and ether groups have been investigated and incorporated into the estimation method (Atkinson 2007).

In the study presented here, we investigated the reaction of 1-pentadecene with NO_3 radicals in an environmental chamber and measured the yields of SOA and a number of particle-phase reaction products using a variety of methods. The results were used to quantify the major reaction pathways, including the branching ratio for decomposition:isomerization of β-nitrooxyalkoxy radicals. This is a key multifunctional intermediate in the reaction of alkenes with NO_3 radicals, and can also be formed following abstraction of a vicinal H-atom from an organic nitrate by an OH radical. These gas-phase OH radical reactions are important in the atmospheric aging of saturated organic compounds and can lead to volatilization of SOA via a mechanism in which the formation of volatile fragmentation products induces particle evaporation in order to re-establish gas-particle partitioning equilibrium (Robinson et al., 2007). It is expected that the nitrooxy group, which, like the hydroxyl group, is electron withdrawing, will increase the rate of alkoxy radical decomposition. The effect could be substantial, since Aschmann et al. (Aschmann et al., 2010) have recently shown that the decomposition:isomerization branching ratios for C_8 and C_{14} β-hydroxyalkoxy radicals formed from the OH radical-initiated reactions of 1-octene and 7-tetradecene in the presence of NO_x were 0.42:0.58 and 0.65:0.35. Such information is valuable for predicting the fate of organic compounds in the atmosphere and for modeling SOA formation.

Experimental Methods

Chemicals

Acetonitrile, ethyl acetate, and water were HPLC grade and were purchased from Fisher Scientific (Hampton, NH). *n*-Pentadecene (99%), ethyl hexyl nitrate (97%), tetramethylethylene (2,3-dimethyl-2-butene or TME) (99%), and dioctyl sebacate (DOS) were purchased from Sigma Aldrich. N_2O_5 was synthesized according to the procedures of Atkinson et al. (Atkinson et al., 1984**)** and was stored in a glass vacuum bulb submerged in liquid nitrogen until used.

Environmental chamber reaction conditions

Experiments were conducted in an 8.2 m^3 Teflon FEP environmental chamber filled with clean, dry air (<5 ppbv hydrocarbons, <0.1% RH) at room temperature (23°C) and pressure (740 torr). Dioctyl sebacate (DOS) seed particles with ~100 nm diameter were generated in a flow of N_2 using an evaporation-condensation source and added to the chamber to achieve a mass concentration of ~100 μg m^{-3} as measured using a TSI 3081 scanning mobility particle sizer (SMPS) with a Model 3772 condensation particle counter. Then 1 ppmv of 1-pentadecene was added by evaporating it from a glass bulb with gentle heating into a flow of N_2, and the reaction was initiated by adding 0.33 ppmv of N_2O_5 by a similar method but without heating. A Teflon-coated fan was run for 1 min after adding chemicals to enhance mixing. The N_2O_5 thermally decomposes to NO_3 and NO_2, and the NO_3 rapidly reacts with the 1-pentadecene C=C double bond. Immediately after adding N_2O_5, 0.6 ppmv of TME was added to consume excess NO_3 radicals and thereby minimize the reaction of NO_3 radicals with β-nitrooxyperoxy radicals formed by

thermal decomposition of β-nitrooxyperoxynitrates and also secondary reactions with dihydrofurans formed by cyclization and dehydration of 1,4-hydroxycarbonylnitrates.

Concentrations of 1-pentadecene were measured before and after reaction by sampling air through stainless steel tubing and then into a glass tube containing Tenax TA solid adsorbent. Prior to sampling, chamber air was drawn through the stainless steel tubing for 20 min at 250 cm^3 min^{-1} using a mass flow controller to allow the walls of the tube to equilibrate with organic compounds. Samples were then collected for 10–15 min at the same flow rate. Samples were collected 60 and 30 min before initiating the reaction, and then 30, 90, and 150 min after the reaction. The samples were then transferred to the inlet of an Agilent 6890 gas chromatograph equipped with a 30 m x 0.32 mm Agilent DB-1701 column with 1 μm film thickness and flame ionization detection. Analytes were thermally desorbed from the Tenax cartridge, and eluted on an 8ºC min^{-1} to 2ºC min^{-1} gradient.

Particle concentrations were continuously measured using the (SMPS), while reactions were monitored in real-time using a thermal desorption particle beam mass spectrometer (TDPBMS) that has been described previously (Tobias et al., 2000). Briefly, particles formed in chamber reactions are drawn through a series of aerodynamic lenses that focus the particles into a narrow beam, which then impacts in a notch on the tip of a copper rod that is resistively heated to 160ºC and located inside a high-vacuum detection chamber. The particles immediately evaporate, vapor molecules are ionized by 70 eV electrons, and the ions are analyzed with an Extrel CMS quadrupole mass spectrometer. The same instrument was used to analyze β-hydroxynitrates and β-

carbonylnitrates after they were fractionated by HPLC as described below, formed into an aerosol using a Collison atomizer located downstream of the UV/Vis detector, dried of HPLC solvent by passing through diffusion driers, and then sampled into the TDPBMS for analysis.

Analysis of particulate β-Hydroxynitrates, β-Carbonylnitrates, and organic peroxides

Immediately after adding TME, particles were sampled for 30 min onto filters (Millipore Fluoropore, 0.45 μm pore size) at a flow rate of ~14 LPM that was measured before and after filter sampling (values typically within 5%) to obtain an average flow rate that was used for sample quantification. Filters were weighed before and after sampling to determine the mass of aerosol collected and then stored at –20°C until extraction. Particles were extracted twice from filters with 4 mL of ethyl acetate and the two extracts were combined. The solvent was dried in a stream of N_2 and the residue was weighed and then reconstituted in acetonitrile containing an ethylhexyl nitrate internal standard for injection into an Agilent 1100 HPLC with quaternary pump and UV/Vis detector. The column was a 4.0 x 150 mm Thermo BetaBasic C_{18} with 3 μm particles. Mobile phase A was 5% acetonitrile in water, mobile phase B was pure acetonitrile, the flow rate was 0.8 mL min^{-1}, and the gradient was 0-55%B in 15 minutes, followed by a shallower gradient of 55-95%B in 65 minutes. Before injection, the column was equilibrated for a minimum of 20 minutes at 0% B. A 6-port valve with a 100 μL sample loop was used for injection and the loop was overfilled to increase the precision of run-to-run injection volume, which was 100 μL. Water was not added to the injection solvent

to avoid precipitation of sample components that might exhibit low water solubility. Organic nitrates were detected at 210 nm as we have done previously (Matsunaga and Ziemann, 2009; Matsunaga and Ziemann 2010a). Because UV absorbance by multifunctional compounds can be influenced by non-target functional groups (in this case the hydroxyl and carbonyl groups affecting the absorbance by the nitrooxy group), in order to ensure accurate quantitation authentic analytical standards of the C_{15} β-hydroxynitrates and β-carbonylnitrates were prepared from the HPLC eluant by fraction collection. Fractions of each compound from several HPLC runs were pooled, dried under a stream of N_2, weighed, and reconstituted in acetonitrile to prepare the analytical standards. The peak areas per μmol of β-hydroxynitrate and β-carbonylnitrate were determined from these standards and the resulting values were used for quantitation. A portion of the dried fractions were also reconstituted in $CDCl_3$ and ^1H NMR analysis on a Varian INOVA 400 MHz NMR. Structures of both the β-hydroxynitrates and β-carbonylnitrates were confirmed and tabulated values for their chemical shifts are given in Table 4.1.

Table 4.1: Tabulated chemical shifts and peak assignments for the ^{1}H NMR spectra of the β-carbonylnitrate and β-hydroxynitrate purified in this study. Chemical shifts of four-carbon β-hydroxynitrates analyzed by Treves et al., 2000 and Muthuramu et al., 1993, and a fourteen-carbon β-hydroxynitrate (Matsunaga and Ziemann, 2009) are included for comparison. (s) is a singlet, (d) is a doublet, (t) is a triplet, (m) is a multiplet, (dd) is a doublet of a doublet, (dq) is a doublet of a quartet, and (br) is a broad peak.

	Chemical Shifts				
Compound	C_{15} (present study)	C_{14} (Matsunaga and Ziemann, 2009)	C_4 (Treves et al., 2000)	C_4 (Muthuramu et al., 1993)	Assignment
1-nitrooxy-2-alcohol	0.891 (t)	0.889 (t)	0.99 (t)	1.018 (t)	C**H**$_3$
	1.271 (m)	1.270 (m)			C**H**$_2$
	1.546 (m)	1.535 (m)	1.55	1.581 (m)	C**H**$_2$CHOH
				2.330 (br)	CHO**H**
	3.951 (m)	3.955 (m)	3.87 (m)	3.875 (m)	C**H**OH
	4.339-4.386 (dd)	4.362 (dd)		4.365 (dd)	C**H**$_2$ONO$_2$
	4.480-4.515 (dd)	4.497 (dd)	4.3-4.5 (dq)	4.502 (dd)	C**H**$_2$ONO$_2$
1-nitrooxy-2-ketone	0.890 (t)				C**H**$_3$
	1.267 (m)				C**H**$_2$
	1.647 (m)				C**H**$_2$CH$_2$CH=O
	2.466 (t)				C**H**$_2$CH=O
	4.951 (s)				C**H**$_2$ONO$_2$

Chemical shifts observed for β-hydroxynitrates were in excellent agreement with those previously determined for 1-nitrooxy-2-hydroxytetradecane (Matsunaga and Ziemann, 2009) and 1-nitrooxy-2-hydroxybutane (Treves et al., 2000; Muthuramu et al., 1993).

Total particulate organic peroxides, which in these experiments are expected to consist of β-hydroperoxynitrates and β-nitrooxyperoxynitrates, were measured by UV spectrophotometry using an iodometric-spectrophotometric method that has been previously described (Docherty et al. 2005). Immediately after sampling and extracting filters (and a blank) as described above, each extract was mixed with 3 mL of an acetic acid/chloroform/water solution (0.53:0.27:0.20 v/v) in a 5 mL microreaction vial. Solutions were purged of O_2 by bubbling with N_2, 50 mg of potassium iodide was added, and the solution was allowed to stand at room temperature for 1 h. Absorbance was then measured at 470 nm relative to the solvent in an Ocean Optics USB UV/Vis spectrophotometer. Total organic peroxide was quantitated against a standard curve prepared from a series of benzoyl peroxide solutions in ethyl acetate, and treated identically as samples in ethyl acetate.

Determination of molar yields of SOA, β-Hydroxynitrates, β-Carbonylnitrates, and organic peroxides with corrections for wall losses

The molar yield of SOA was estimated from the maximum aerosol volume concentration measured with the SMPS (with DOS seed particle concentration subtracted). This value was multiplied by an assumed density of 1.10 g cm^{-3} and divided by an assumed mean molecular weight of 288 g mol^{-1} for SOA compounds to determine the moles of SOA formed, which was then divided by the moles of 1-pentadecene reacted

to obtain the molar yield of SOA. The density of 1.10 g cm^{-3} is the average of values of 1.13 and 1.06 g cm^{-3} determined using a syringe and balance to measure the volume and mass of dried filter extracts of SOA formed from the reactions of 1-tetradecene (Matsunaga et al., 2009) and *n*-pentadecane (Lim and Ziemann, 2009) with OH radicals in the presence of NO_x, reactions that should lead to products with similar structures to those formed here. Theses values are similar to the density of 1.05 g cm^{-3} calculated using the parameterization developed by Kuwata et al. (Kuwata et al., 2012) and the CHO composition estimated from the expected molecular composition of SOA products, with the assumption that the effect of N on density is the same as O. The mean molecular weight of SOA products was assumed to be 288 g mol^{-1}, the value expected if all SOA compounds from the reaction of 1-pentadecene were first-generation, non-cyclized products.

Molar yields of β-hydroxynitrates, β-carbonylnitrates, and peroxides (β-hydroperoxynitrates + nitrooxyperoxynitrates) were calculated as the moles of product formed divided by the moles of 1-pentdecene reacted. These values were corrected for the loss of particles to the chamber walls using the decay in the *m/z* 185 mass spectral peak, which is due essentially solely to nonvolatile DOS seed particles that are only removed from the chamber by deposition to the walls. Because of the low vapor pressures of these products they should exist essentially entirely in the particles, and thus the yields determined from analysis of particles should be the same as the total yields. 1-Alkenes larger than ~C_{13} are partially lost to the walls by gas-wall partitioning (Matsunaga and Ziemann, 2010b), which was accounted for here by measuring the

concentration of 1-pentadecene multiple times before and after each reaction to verify that it had equilibrated with the walls. In this case the concentration of 1-pentadecene reacted is $[PD]_{reacted} = [PD]_{T,i}(1 - FID_f/FID_i)$, where $[PD]_{T,i}$ is the amount of 1-pentadecene added to the chamber divided by the chamber volume, and FID_i and FID_f are the GC/FID signals per volume of air sampled measured before and after reaction. A derivation of this expression is presented in Chapter 2.

Results and Discussion

Products and mechanism of the reaction of linear 1-alkenes with NO_3 radicals

Reactions of linear 1-alkenes with NO_3 radicals are expected to produce a variety of multifunctional SOA products, the identity of which are consistent with previous TDPBMS mass spectra and thermal desorption profiles measured for the reaction of 1-hexadecene (Gong et al., 2005). The mechanism of reaction of a linear 1-alkene with NO_3 radicals in air to form the major first-generation products is shown in Scheme 4.2, where values of α_i correspond to the branching ratios for particular reaction pathways.

Scheme 4.2: Mechanism of the reaction of linear 1-alkenes with NO_3 radicals in air.

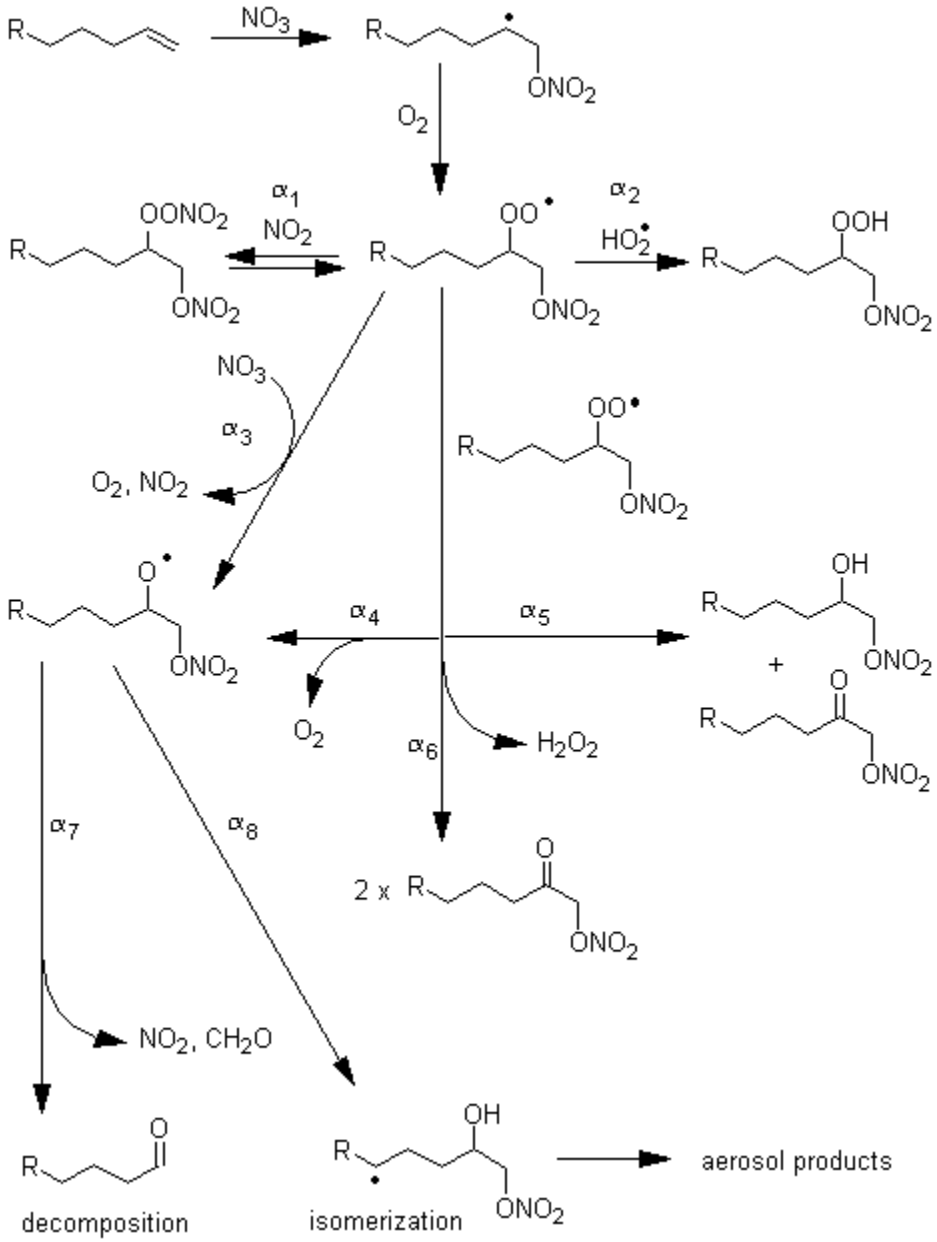

In this reaction, the NO_3 radical reacts almost solely by adding to the C=C double bond to form a β-nitrooxyalkyl radical. Although H-atom abstraction to form HNO_3 can occur, it is too slow in non-conjugated alkenes to be of importance (Mason et al., 2009). The β-nitrooxyalkyl radical reacts solely with O_2 to form a β-nitrooxyperoxy radical, an intermediate that can react by six major pathways. (Note that these reactions occur in the absence of NO, since NO_3 radicals react too fast with NO to co-exist). The β-nitrooxyperoxy radical can react to form two organic peroxides, one a relatively short-lived β-nitrooxyperoxynitrate by reaction with NO_2 and the other a β-hydroperoxynitrate by reaction with HO_2, or it can react with an NO_3 radical to form a β-nitrooxyalkoxy radical. β-Nitrooxyperoxy radicals can also undergo self-reactions to form two β-nitrooxyalkoxy radicals, a β-hydroxynitrate and β-carbonylnitrate via the Russell mechanism (Russell, 1957), or two carbonylnitrates via the Bennett and Summers mechanism (Bennett and Summers, 1974).

Formation of β-hydroperoxynitrate, β-hydroxynitrate, and β-carbonylnitrate molecular products terminates the reaction, whereas β-nitrooxyalkoxy radicals react further by either decomposition or isomerization and eventually form molecular products. Decomposition results in the formation of an aldehyde with one less carbon than the parent alkene and formaldehyde. The large aldehyde is only slightly less volatile than the parent alkene, so unless it undergoes heterogeneous/multiphase reactions to form an oligomer, products formed through the decomposition pathway are not expected to form SOA. The aldehyde products formed from reactions of NO_3 radicals with internal alkenes (those with the C=C double bond away from the ends of the molecule) are even more

volatile. In contrast to decomposition, isomerization of β-nitrooxyalkoxy radicals likely leads to SOA products via the formation of a β-hydroxynitrooxy alkyl radical. This radical adds O_2 to form a β-hydroxynitrooxyperoxy radical, which reacts by the same pathways as the β-nitrooxyperoxy radical to form analogous products but with an additional hydroxyl group. One difference is that the β-hydroxynitrooxyalkoxy radical intermediate also undergoes reverse isomerization that leads to the formation of a 1-nitrooxy-2-oxo-5-hydroxy alkane. With the exception of a dihydroxynitrate, all products formed via the isomerization pathway contain a 1,4-hydroxycarbonyl structure, and therefore can cyclize into hemiacetals on/in particles. These hemiacetals can dehydrate to form unsaturated dihydrofurans that can react rapidly with NO_3 radicals to form second-generation products, although the time scale for dehydration is probably too long for this to occur during the few minutes when NO_3 radicals are present.

All the organic reaction products discussed above are expected to undergo significant gas-to-particle partitioning, except for the large C_{14} aldehyde, tetradecanal, and formaldehyde. For example, using gas-particle partitioning theory (Pankow, 1994) and compound vapor pressures estimated using a group-contribution method (Pankow and Asher, 2008), it is estimated that for the ~900 μg m^{-3} of aerosol present in the chamber that the fraction of β-carbonylnitrate, the most volatile multifunctional product, and tetradecanal in the particles was approximately 90% and 3%, respectively. Quantification of the branching ratio for the β-nitrooxyalkoxy radical decomposition pathway that leads to the formation of the large aldehyde and formaldehyde is therefore critical to the prediction of the SOA yield. Unfortunately, accurate quantitation of large

gas-phase aldehydes such as the tetradecanal formed in these reactions is challenging because they undergo substantial partitioning to the Teflon walls of the environmental chamber. For example, in a recent study it was shown that ~50% of a C_{13} 2-ketone added to the chamber partitioned to the walls (Matsunaga and Ziemann, 2010b). Although corrections can be made by using standards to quantify the losses, the experiments are difficult and can lead to significant uncertainties (Chapter 2). Conducting experiments with smaller alkenes in order to form more volatile aldehydes that are more easily measured is not an alternative, because then the fraction of multifunctional products in the gas-phase increases and so also losses due to gas-wall partitioning. For these reasons, a mass-balance approach that combined measurements of the yields of SOA and particulate products was employed here to quantify the branching ratio for the formation of β-nitrooxyalkoxy radicals from the self-reaction β-nitrooxyperoxy radicals, and for the decomposition of β-nitrooxyalkoxy radicals. Both of these quantities are of interest for understanding fundamental reaction mechanisms.

Measured molar yields of SOA, β-hydroxynitrates, β-carbonylnitrates, and organic peroxides

The real-time TDPBMS mass spectrum of SOA formed in the reaction of 1-pentadecene with NO_3 radicals is shown in Figure 4.1.

Figure 4.1: Real-time TDPBMS mass spectrum of SOA formed in the reaction of 1-pentadecene with NO_3 radicals.

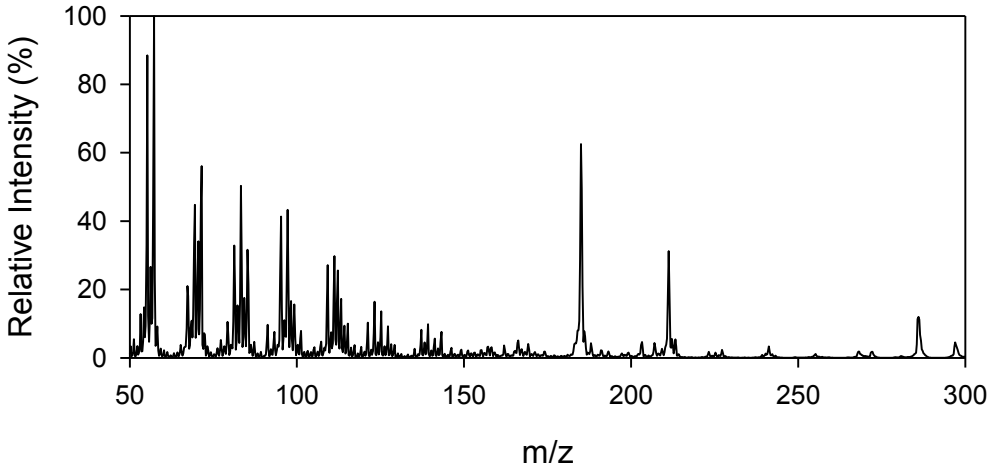

The major peaks correspond to those observed previously for the reaction of 1-hexadecene with NO_3 radicals (Gong et al., 2005), even though the experiments differed in that TME was added here to minimize the reaction of NO_3 radicals with β-nitrooxyperoxy radicals formed by thermal decomposition of β-nitrooxyperoxynitrates and also secondary reactions with dihydrofurans formed by cyclization and dehydration of 1,4-hydroxycarbonylnitrates. There was no evidence of dehydration, as the relative intensities of all product peaks remained fairly constant throughout the experiment. The mass spectrum indicated that β-hydroxynitrates and β-carbonyl nitrates were present in the particles (significant peaks at *m/z* 211 and 213) but not tetradecanal (no significant peaks at *m/z* 184 and 194), consistent with the reaction mechanism and gas-particle partitioning calculations. The estimated molar yield of SOA was 0.46, indicating that approximately one-half of the reaction products did not partition into particles. Assuming then that all the organic reaction products other than tetradecanal and formaldehyde are present entirely in the particles, the molar yields of tetradecanal and formaldehyde were each $1 - 0.46 = 0.54$.

In this study, β-hydroxynitrate and β-carbonylnitrate were quantified by HPLC/UV analysis. They were the largest peaks in the chromatogram measured at 210 nm, where nitrate groups absorb strongly. The chromatogram is shown in Figure 4.2.

Figure 4.2: HPLC/UV chromatogram of SOA formed from the reaction of 1-pentadecene with NO_3 radicals with absorbance at 210 nm.

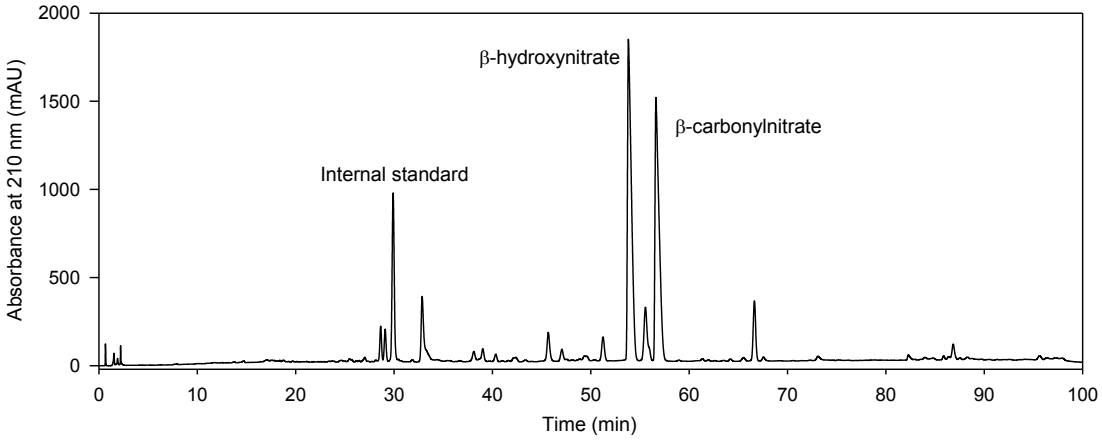

The molar yields determined from these measurements were 0.100 and 0.168 for β-hydroxypentadecyl nitrate and β-oxopentadecyl nitrate, respectively, with a sum of 0.27. Because the self-reaction of β-nitrooxyperoxy radicals via the Russell mechanism produces equal amounts of alcohols and carbonyls (Russell, 1957), we propose that the measured excess of β-oxopentadecyl nitrate was formed by one or both of two possible reactions. One is the β-nitrooxyperoxy radical self-reaction shown in Scheme 4.2 in which two β-carbonylnitrates and H_2O_2 are formed via the Bennett and Summers mechanism (Bennett and Summers, 1974). The other is the cross-reaction between β-nitrooxypentadecyl peroxy radicals and β-nitrooxyperoxy radicals formed from the reactions of TME with NO_3 radicals. Because the latter are tertiary peroxy radicals, and thus have no H atom to transfer to β-nitrooxypentadecyl peroxy radicals, the reaction can only form β-oxopentadecyl nitrate. The molar yield of organic peroxides was 0.02. Calculations conducted using a kinetic model run with Facsimile 4 software (MCPA Software Ltd) indicated that most of organic peroxide was β-nitrooxypentadecyl hydroperoxide, because of fast decomposition of β-nitrooxypentadecyl peroxynitrate to the β-nitrooxyperoxy radical and NO_2. β-Nitrooxypentadecyl peroxynitrate accumulated before TME was added, but afterwards peroxy radicals formed from the reaction of TME with NO_3 radicals began to compete for NO_2, β-nitrooxypentadecyl peroxynitrates decomposed rapidly, and by the end of the reaction very little β-nitrooxypentadecyl peroxynitrate remained.

Thus, from Scheme 4.2, since the sum of the molar yields of β-nitrooxypentadecyl hydroperoxide, β-nitrooxypentadecyl peroxynitrate, β-hydroxypentadecyl nitrate, β-

oxopentadecyl nitrate, and tetradecanal are 0.02 + 0.27 + 0.54 = 0.83, by difference the molar yield of isomerization products is 1 – 0.83 = 0.17. This means that $\alpha_1 = 0$, $\alpha_2 = 0.02$, and because $\alpha_1 + \alpha_2 + \alpha_3 + \alpha_4 + \alpha_5 + \alpha_6 = 1$, by difference $\alpha_3 + \alpha_4 + \alpha_5 + \alpha_6 = 0.98$. Furthermore, because $\alpha_5 + \alpha_6 = 0.27$, by difference $\alpha_3 + \alpha_4 = 0.71$, which is the molar yield of β-nitrooxypentadecyl peroxy radicals. The values of α_7 and α_8 are equal to the molar yields of tetradecanal and isomerization products divided by the molar yield of β-nitrooxypentadecyl peroxy radicals, and therefore 0.54/0.71 = 0.76 and 0.17/0.71 = 0.24, respectively. The values are listed in Table 4.2.

Table 4.2: Yields and branching ratios of reaction products formed by the reaction of nitrate radical with 1-pentadecene.

Product	Molar yield	Branching ratio
β-nitrooxyhydroperoxide + β-nitrooxyperoxynitrate	0.02	$\alpha_1 + \alpha_2 = 0.02$
β-nitrooxyalkoxy radical	0.71[a]	$\alpha_3 + \alpha_4 = 0.73$
β-hydroxynitrate + β-carbonylnitrate	0.27	$\alpha_5 + \alpha_6 = 0.27$
β-nitrooxyalkoxy radical decomposition products	0.54	$\alpha_7 = 0.76$
β-nitrooxyalkoxy radical 1,4-isomerization products	0.17	$\alpha_8 = 0.24$

[a] yield of a radical intermediate, and excluded from sum of molar yields of molecular products

These results can also be used to estimate the lower limit to the branching ratios for the formation of β-nitrooxypentadecyloxy radicals and molecular products from the self-reaction of β-nitrooxypentadecyl peroxy radicals, which are equal to $\alpha_4/(\alpha_4 + \alpha_5 + \alpha_6)$ and $(\alpha_5 + \alpha_6)/(\alpha_4 + \alpha_5 + \alpha_6)$, respectively. Assuming that none of the β-nitrooxypentadecyloxy radicals are formed from the reaction of β-nitrooxypentadecyl peroxy radicals with NO_3 radicals, so that $\alpha_3 = 0$ and $\alpha_4 + \alpha_5 + \alpha_6 = 0.98$, and because $\alpha_5 + \alpha_6 = 0.27$, the branching ratios for formation of β-nitrooxypentadecyloxy radicals and molecular products are 0.79 and 0.21. At the other extreme, assuming that all β-nitrooxypentadecyloxy radicals are formed from the reaction of β-nitrooxypentadecyl peroxy radicals with NO_3 radicals, so that $\alpha_4 = 0$, the branching ratios for formation of β-nitrooxypentadecyloxy radicals and molecular products are 0 and 1. The results do not place very tight constraints on the branching ratios, indicating only that they are in the range of approximately 0–0.8 and 0.2–1 for the formation of β-nitrooxypentadecyloxy radicals and molecular products.

Conclusions

The tendency for a multifunctional alkoxy radical to decompose depends on the functional groups present and their positions on the carbon backbone relative to the alkoxy radical group, with vicinal functional groups having the largest effect on the rate of decomposition (Atkinson 2007). For example, decomposition rate constants calculated by RKKM theory were roughly 10^6 times greater for β-hydroxybutoxy radicals compared to 1-butoxy radicals (Méreau et al., 2000), and decomposition:isomerization branching ratios measured for C_8 and C_{14} β-hydroxyalkoxy radicals formed from the OH radical-initiated reactions of 1-octene and 7-tetradecene in the presence of NO_x were 0.42:0.58 and 0.65:0.35, respectively (Aschmann et al., 2010), whereas they are ~0 for unsubstituted linear alkoxy radicals ≥ C_6 (Atkinson and Arey, 2003a). The results of the present study, for which the estimated decomposition:isomerization branching ratios measured for C_{14} β-nitrooxyalkoxy radicals were 0.76:0.24, indicate that nitrooxy groups may have an even larger effect than hydroxyl groups on the rate of decomposition of the alkoxy radicals.

The relatively high tendency for β-nitrooxyalkoxy radicals to decompose is not surprising, since the activation energy for alkoxy decomposition is predominantly related to the stability of the leaving group (Atkinson, 2007). For comparison, decomposition of an unsubstituted alkoxy radical produces an aldehyde and an alkyl radical, with the low stability of the alkyl radical leaving group leading to slow decomposition. Conversely, the presence of a vicinal nitrooxy group on the alkyl radical leaving group allows facile

decomposition to an aldehyde and NO_2, both stable products, as shown in Scheme 4.3. This enhances the rate of decomposition of the β-nitrooxyalkoxy radicals.

Scheme 4.3: Mechanism of decomposition of a β-nitrooxyalkoxy radical.

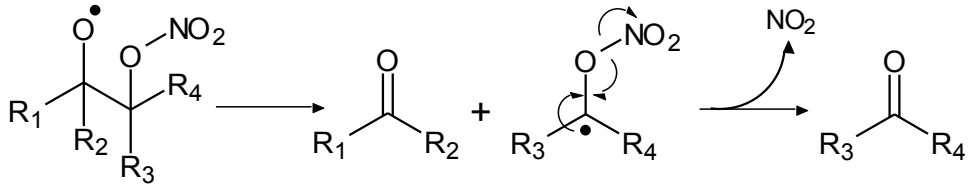

Finally, the β-nitrooxyalkoxy radicals studied here were formed by reactions of β-nitrooxyperoxy radicals with other organic peroxy radicals and probably NO_3 radicals. Alkoxy radicals can also be formed from the daytime reactions VOC with OH radicals and O_3 in the presence of NO. It is important to note that the alkoxy radicals formed from these reactions are not the same. Reactions of organic peroxy radicals with other organic peroxy radicals to form alkoxy radicals are slightly endothermic, whereas reactions involving NO are exothermic by 10–11 kcal mol^{-1}(IUPAC, 2007). In the latter case a fraction of the alkoxy radicals are chemically activated by the large release of energy and undergo "prompt" decomposition (Wallington et al., 1996; Orlando et al., 1998; Vereecken et al., 1999), whereas those formed in the absence of NO are thermalized and should decompose more slowly. Since the alkoxy radicals formed in the present study were not chemically activated, the estimated decomposition:isomerization branching ratio for β-nitrooxyalkoxy radicals should be a lower limit with those formed from reactions involving NO being even more likely to decompose.

References

1. Alfaro-Moreno, E., Nawrot, T. S., Nemmar, A., & Nemery, B. (**2007**). Particulate matter in the environment: pulmonary and cardiovascular effects. *Current Opinion in Pulmonary Medicine*, 13(2), 98-106.

2. Aschmann, S. M., Tuazon, E. C., Arey, J., & Atkinson, R. (**2010**). Products and Mechanisms of the Gas-Phase Reactions of OH Radicals with 1-Octene and 7-Tetradecene in the Presence of NO. *Environmental Science & Technology*, 44(10), 3825-3831.

3. Aschmann, S. M., & Atkinson, R. (**2011**). Effect of Structure on the Rate Constants for Reaction of NO_3 Radicals with a Series of Linear and Branched C_5–C_7 1-Alkenes at 296 ± 2 K. *The Journal of Physical Chemistry A*, 115(8), 1358-1363.

4. Atkinson, R., Plum, C. N., Carter, W. P., Winer, A. M., & Pitts Jr, J. N. (**1984**). Rate constants for the gas-phase reactions of nitrate radicals with a series of organics in air at 298 ± 1 K. *The Journal of Physical Chemistry*, 88(6), 1210-1215.

5. Atkinson, R., Tuazon, E. C., & Aschmann, S. M. (**1995**). Products of the gas-phase reactions of a series of 1-alkenes and 1-methylcyclohexene with the OH radical in the presence of NO. *Environmental Science & Technology*, 29(6), 1674-1680.

6. Atkinson, R. (**1997**). Gas-phase tropospheric chemistry of volatile organic compounds: 1. Alkanes and alkenes. *Journal of Physical and Chemical Reference Data*, 26(2), 215-290.

7. Atkinson, R., & Arey, J. (**2003a**). Atmospheric degradation of volatile organic compounds. *Chemical Reviews-Columbus*, 103(12), 4605-4638.

8. Atkinson, R., & Arey, J. (**2003b**). Gas-phase tropospheric chemistry of biogenic volatile organic compounds: a review. *Atmospheric Environment*, 37, 197-219

9. Atkinson, R. (**2007**). Rate constants for the atmospheric reactions of alkoxy radicals: An updated estimation method. *Atmospheric Environment*, 41(38), 8468-8485.

10. Bennett, J. E., & Summers, R. (**1974**). Product studies of the mutual termination reactions of sec-alkylperoxy radicals: Evidence for non-cyclic termination. *Canadian Journal of Chemistry*, 52(8), 1377-1379.

11. Chacon-Madrid, H. J., Presto, A. A., & Donahue, N. M. (**2010**). Functionalization vs. fragmentation: *n*-aldehyde oxidation mechanisms and secondary organic aerosol formation. *Physical Chemistry Chemical Physics*, 12(42), 13975-13982.

12. Chacon-Madrid, H. J., & Donahue, N. M. (**2011**). Fragmentation vs. functionalization: chemical aging and organic aerosol formation. *Atmospheric Chemistry and Physics*, 11(10), 553.

13. Crable, G. F., & Coggeshall, N. D. (**1958**). Application of total ionization principles to mass spectrometric analysis. *Analytical Chemistry*, 30(3), 310-313.

14. De Gouw, J., & Jimenez, J. L. (**2009**). Organic aerosols in the Earth's atmosphere. Environmental science & technology, 43(20), 7614-7618.Dickerson, R.R.; Kondragunta, S.; Stenchikov, G.; Civerolo, K.L.; Doddridge, B.G.; Holben, B.N. *Science*, 1997, *278*, 827-830

15. Docherty, K. S., Wu, W., Lim, Y. B., & Ziemann, P. J. (**2005**). Contributions of organic peroxides to secondary aerosol formed from reactions of monoterpenes with O3. *Environmental Science & Technology*, 39(11), 4049-4059.

16. Etzel, R. A. (**2003**). How environmental exposures influence the development and exacerbation of asthma. *Pediatrics*, 112(Supplement 1), 233-239..

17. Forster, P.; Ramaswamy, V.; Artaxo, P.; Berntsen, T.; Betts, R.; Fahey, D.W.; Haywood, J.; Lean, J.; Lowe, D.C.; Myhre, G.; Nganga, J.; Prinn, R.; Raga, G.; Schulz, M.; Van Dorland, R. *Changes in Atmospheric Constituents and in Radiative Forcing"* in *Climate Change 2007: The Physical Science Basis. Contribution of Working Group I to the Fourth Assessment Report of the Intergovernmental Panel on Climate Change*; Solomon, S.; Qin, D.; Manning, M.; Chen, Z.; Marquis, M.; Averyt, K. B.; Tignor, M.; Miller, H. L., Eds. Cambridge University Press, New York, NY, 2007.

18. Gong, H., Matsunaga, A., & Ziemann, P. J. (**2005**). Products and mechanism of secondary organic aerosol formation from reactions of linear alkenes with NO3 radicals. *The Journal of Physical Chemistry A*, 109(19), 4312-4324.

19. Guenther, A., Hewitt, C. N., Erickson, D., Fall, R., Geron, C., Graedel, T., Harley, P.; Klinger, L.; Lerdau, M.; McKay, W.A.; Pierce, T.; Scholes, B.; Steinbrecher, R.; Tallamraju, R.; Taylor, J.; Zimmerman, P. (**1995**). A global model of natural volatile organic compound emissions. *Journal of Geophysical Research*, 100(D5), 8873-8892.

20. IUPAC, 2007. Evaluated Kinetic Data for Atmospheric Chemistry. IUPAC Subcommittee for Gas Kinetic Data Evaluation, http://www.iupac-kinetic.ch.cam.ac.ukS.

21. Kiendler-Scharr, A., Wildt, J., Dal Maso, M., Hohaus, T., Kleist, E., Mentel, T. F., Tillmann, R., Uerlings, R., Schurr, U., & Wahne, A (**2009**). New particle formation in forests inhibited by isoprene emissions. *Nature*, 461(7262), 381-384.

22. Kroll, J. H., Smith, J. D., Che, D. L., Kessler, S. H., Worsnop, D. R., & Wilson, K. R. (**2009**). Measurement of fragmentation and functionalization pathways in the heterogeneous oxidation of oxidized organic aerosol. *Physical Chemistry Chemical Physics*, 11(36), 8005-801.

23. Kuwata, M., Zorn, S. R., & Martin, S. T. (**2011**). Using elemental ratios to predict the density of organic material composed of carbon, hydrogen, and oxygen. *Environmental Science & Technology*, 46(2), 787-794.

24. Lambe, Andrew T., Timothy B. Onasch, David R. Croasdale, Justin P. Wright, Alexander T. Martin, Jonathan P. Franklin, Paola Massoli, Kroll, J.H.; Canagaratna, M.R.; Brune, W.H.; Worsnop, D.R.; Davidovits, P. (**2012**). Transitions from functionalization to fragmentation reactions of laboratory secondary organic aerosol (SOA) generated from the OH oxidation of alkane precursors. *Environmental science & technology*, 46(10), 5430-5437.

25. Lohmann, U., & Feichter, J. (**2005**). Global indirect aerosol effects: a review. *Atmospheric Chemistry and Physics*, 5(3), 715-737.

26. Mason, S. A., Arey, J., & Atkinson, R. (**2009**). Rate Constants for the Gas-Phase Reactions of NO3 Radicals and O3 with C6− C14 1-Alkenes and 2-Methyl-1-alkenes at 296±2 K. *The Journal of Physical Chemistry A*, 113(19), 5649-5656.

27. Matsunaga, A., & Ziemann, P. J. (**2009**). Yields of β-hydroxynitrates and dihydroxynitrates in aerosol formed from OH radical-initiated reactions of linear alkenes in the presence of NO x. *The Journal of Physical Chemistry A*, 113(3), 599-606.

28. Matsunaga, A., & Ziemann, P. J. (**2010**). Yields of β-hydroxynitrates, dihydroxynitrates, and trihydroxynitrates formed from OH radical-initiated reactions of 2-methyl-1-alkenes. *Proceedings of the National Academy of Sciences*, 107(15), 6664-6669.

29. Méreau, R., Rayez, M. T., Caralp, F., & Rayez, J. C. (**2000**). Theoretical study on the comparative fate of the 1-butoxy and β-hydroxy-1-butoxy radicals. *Physical Chemistry Chemical Physics*, 2(9), 1919-1928.

30. Méreau, R., Rayez, M. T., Caralp, F., & Rayez, J. C. (**2003**). Isomerisation reactions of alkoxy radicals: theoretical study and structure–activity relationships. *Physical Chemistry Chemical Physics*, 5(21), 4828-4833.

31. Orlando, J.J., Tyndall, G.S., Bilde, M., Ferronato, C., Wallington, T.J., Vereecken, L., Peeters, J., (**1998**). Laboratory and theoretical study of the oxy radicals in the OH- and Cl initiated oxidation of ethene. *Journal of Physical Chemistry A* 102, 8116–8123.

32. Pankow, J. F., & Asher, W. E. (**2008**). SIMPOL. 1: a simple group contribution method for predicting vapor pressures and enthalpies of vaporization of multifunctional organic compounds. *Atmospheric Chemistry and Physics*, 8(10), 2773-2796.

33. Pope, C. A., Ezzati, M., & Dockery, D. W. (**2009**). Fine-particulate air pollution and life expectancy in the United States. *New England Journal of Medicine*, 360(4), 376-386.

34. Tobias, H. J., Kooiman, P. M., Docherty, K. S., & Ziemann, P. J. (**2000**). Real-time chemical analysis of organic aerosols using a thermal desorption particle beam mass spectrometer. *Aerosol Science & Technology*, 33(1-2), 170-190.

35. Treves, K., Shragina, L., & Rudich, Y. (**2000**). Henry's law constants of some β-, γ-, and δ-hydroxy alkyl nitrates of atmospheric interest. *Environmental Science & Technology*, 34(7), 1197-1203.

36. Tuazon, E. C., & Atkinson, R. (**1989**). A product study of the gas-phase reaction of methyl vinyl ketone with the OH radical in the presence of NOx. *International Journal of Chemical Kinetics*, 21(12), 1141-1152.

37. Russell, G. A. (**1957**). Deuterium-isotope Effects in the Autoxidation of Aralkyl Hydrocarbons. Mechanism of the Interaction of Peroxy Radicals. *Journal of the American Chemical Society*, 79(14), 3871-3877.

38. Vereecken, L., Peeters, J., Orlando, J.J., Tyndall, G.S., Ferronato, C., (**1999**) Decomposition of β-hydroxypropoxy radicals in the OH-initiated oxidation of propene. A theoretical and experimental study. *Journal of Physical Chemistry A* 103, 4693–4702.

39. Wallington, T.J., Hurley, M.D., Fracheboud, J.M., Orlando, J.J., Tyndall, G.S., Sehested, J., Møgelberg, T.E., Nielsen, O.J., (**1996**) Role of excited CF 3 CFHO radicals in the atmospheric chemistry of HFC-134a. *Journal of Physical Chemistry* 100, 18116–18122.

40. Zhang, Q.; Jimenez, J.L.; Canagaratna, M.R.; Allan, J.D.; Cole, H.; Ulbrich, I.; Alfarra, M.R.; Takami, A.; Middlebrook, A.M.; Sun, Y.L.; Dzepina, K.; Dunlea, E.; Docherty, K.; DeCarlo, P.F.; Salcedo, D.; Onasch, T.; Jayne, J.T.; Miyoshi, T.; Shimono, A.; Hatakeyama, S.; Takegawa, N.; Kondo, Y.; Schneider, J.; Zrewnick, F.; Borrmann, S.; Weimer, S.; Demerjian, K.; Williams, P.; Bower, K.; Zahreini, R.; Cottrell, L.; Griffin, R.J.; Rautiainen, J.; Sun, J.Y.; Zhang, Y.M.; Worsnop, D.R. (**2007**). Ubiquity and dominance of oxygenated species in organic aerosols in anthropogenically-influenced Northern Hemisphere midlatitudes. *Geophysical Research Letters*, 34(13), L13801.

Chapter 5: Conclusions and future research

In the study described in the first chapter of this work, C_8–C_{14} *n*-alkanes were reacted with OH radicals in the presence of NO_x in a Teflon film environmental chamber and isomer-specific yields of alkyl nitrates were determined. In order to accurately determine yields, it was necessary to characterize the degree of gas-wall partitioning for the alkyl nitrates formed from these reactions. Eleven model secondary alkyl nitrates in the size range studied were synthesized, spiked into the environmental chamber, and their concentrations were measured over time. Gas-wall partitioning increased with increasing carbon number and with proximity of the nitrooxy group to the terminal carbon, with observed losses to walls as high as 86%. The partitioning measurements were used to develop a structure-activity model to predict the effects of carbon number and isomer structure on gas-wall partitioning, which was then used to correct the measured yields of the 27 secondary alkyl nitrate isomers formed in chamber reactions. Molar yields of alkyl nitrates formed from reactions of *n*-octane, *n*-decane, *n*-dodecane, *n*-tridecane, and *n*-tetradecane after corrections for secondary reactions with OH radicals were 20.8, 18.9, 16.5, 12.5, and 8.5%, respectively, and after correction for wall partitioning, were 20.9, 19.8, 24.7, 28.4, and 30.9, respectively. Corrected yields agreed well with values predicted by the model of Arey et al.(Arey et al., 2001) for the carbon number dependence of alkyl nitrate formation, and indicate that a plateau is reached at ~C_{12}–C_{14}, also consistent with model predictions.

In the study described in the second chapter, a series of C_8–C_{16} *n*-alkanes were reacted with OH radicals in the presence of NO_x in an environmental chamber. The

resulting particles were sampled by filtration, extracted, and the 1,4-hydroxynitrate reaction products were analyzed by high-performance liquid chromatography with quantitation by UV absorption and identification by electron ionization mass spectrometry (HPLC/UV/MS). Observed mass spectral patterns were explained using proposed mechanisms for ion fragmentation that permitted the identification of each of the 1,4-hydoxynitrate isomers. The degree of retention of these compounds by reversed-phase chromatography was governed by the length of the longer of two alkyl chains attached to opposite ends of the 1,4-hydroxynitrate subunit, which can be mathematically represented as an increasing Wiener index (Wiener, 1947). Studies of the reverse-phase retention behavior of diols, bifunctional molecules structurally similar to hydroxynitrates, showed that Wiener index positively correlated with retention (Noël and Vangheluwe, 1987), and if the mechanism of diol retention is similar to that of hydroxynitrates, the peak retention times confirmed the peak assignments made in mass spectra. 1,4-Hydroxynitrates were quantified in particles using authentic purified calibration standards. Yields increased with increasing carbon number from 0.00 for C_8 to an average plateau value of 0.130 ± 0.008 for C_{14}–C_{16}, due primarily to enhanced gas-to-particle partitioning of less volatile 1,4-hydroxynitrates at carbon numbers less than C_{14}. The average branching ratio for the formation of C_{14}–C_{16} 1,4-hydroxynitrates from the reaction of NO with the corresponding 1,4-hydroxyperoxy radicals was 0.184 ± 0.011, calculated from the ratio of the measured yields of 1,4-hydroxynitrates and the yields of 1,4-hydroxyperoxy radicals calculated using the model of Arey et al. (Arey et al., 2001). This value is similar to the plateau value of 0.15 reported for reactions of secondary 1,2-

hydroxyperoxy radicals (Matsunaga and Ziemann, 2010), and approximately 60% of the value of 0.29 estimated for reactions of secondary alkyl peroxy radicals of these carbon numbers (Arey et al, 2001). Yields of secondary 1,2- and 1,4-hydroxyperoxy radicals are due to the effects of hydrogen bonding between the hydroxyl and peroxy groups in the intermediate complex that is formed with NO during formation of 1,2- and 1,4-hydroxynitrates.

The growing database of alkyl nitrate formation yields from the reactions of secondary alkyl peroxy radicals with NO, including the yields determined in Chapters 1 and 2 of this work, were used to optimize fitting parameters of the expression (Atkinson et al., 1983; Atkinson et al., 1987; Carter and Atkinson, 1989; Arey et al., 2001) for the estimation of the branching of alkyl nitrate formation as a function of carbon number, temperature, and pressure. The updated parameters provided an improved fit of predicted secondary alkyl nitrate formation yields to the experimentally-determined yields, with the largest error at 31%, and with half of the predicted yields falling within 9% of the measured ones. The updated fitting parameters are $\alpha = 2.37 \times 10^{-22} \pm 1.55 \times 10^{-23}$, $\beta = 0.792 \pm 0.018$, $Y_{\infty}^{298} = 0.372 \pm 0.013$, $m_0 = 1.19 \pm 0.75$, $m_{\infty} = 7.00 \pm 0.52$, and $F = 0.688 \pm 0.033$. The value of the last parameter, *F*, commonly referred to as the "broadening coefficient," is closer to the value of 0.6, the value recommended by NASA/JPL (Sander et al., 2006), than the broadening coefficient reported in previous parameterizations, and is extremely close to the value of 0.7 determined from computational analysis of the RO_2–NO intermediate (Zhang et al., 2004).

The availability of formation yield measurements of primary and tertiary alkyl nitrates permitted determination of updated scaling factors to adjust the estimation of nitrate formation from primary and tertiary alkyl peroxy radicals. Scaling factors were also determined for the branching of substituted organic nitrates, including various hydroxynitrates and haloalkylnitrates. The scaling factors are 0.71 for primary peroxy radicals, 1.13 for tertiary radicals, 0.39 for primary β-hydroxy radicals, 0.43 for secondary β-hydroxy radicals, 0.58 for secondary δ-hydroxy radicals, 0.92 for tertiary β-hydroxy radicals, 0.71 for primary γ-bromoalkyl radicals, and 0.54 for secondary β-bromoalkyl radicals. The newly parameterized method may be incorporated into tropospheric models that incorporate mechanistic transformations of organic molecules via photooxidation in NO_x-enriched atmospheres.

In the study described in Chapter 4 of this work, product yields of particulate hydroxynitrates, carbonylnitrates, and organic peroxides resulting from the reaction of 1-pentadecene with nitrate radical were measured. In conjunction with aerosol yield measurement, these results were used to extrapolate the branching of decomposition of the nitrooxyalkoxy radical. The degree of nitrooxyalkoxy radical decomposition measured was greater than the decomposition of unsubstituted alkoxy radicals and was also greater than the decomposition of hydroxy-substituted alkoxy radicals measured in previous studies (Aschmann et al., 2010). Because the β-nitrooxyalkoxy radicals produced by the nitrate radical-alkene reaction mechanism are thermalized, the degree of decomposition observed represents a lower limit of β-nitrooxyalkoxy decomposition, as radicals arising from other processes contain more internal energy and will more readily

fragment. These results indicate that incorporation of nitrooxy groups by VOCs in atmospheric reactions can increase the likelihood of fragmentation upon subsequent oxidation, an effect that can reduce the tendency of oxidation products to partition in the gas phase.

Future research: gas-wall partitioning

Future research should further investigate the gas-wall partitioning of branched and cyclic alkyl nitrates, as well as other semi-volatile, substituted alkanes and aromatics. The effectiveness of the approach described in this work that effectively predicted the partitioning of alkyl nitrate isomers ($logP^o = D_{fg} + D_n n + D_i \lambda^y$) should be investigated with substituted alkanes such as ketones, aldehydes, and alcohols. The effect of functional groups such as carboxylic acids, and the effect of polyfunctionalization in molecules like diols, diones, and diacids may be investigated. In future studies, an internal reference compound that is not lost to chamber walls, that is easily analyzed by gas chromatography, and that does not coelute with the test compounds should be put into solution with the test compounds, and that solution can be introduced into the chamber and used for GC calibration. This approach will greatly improve the precision of the experiment by negating any measurement errors due to variations in sampling volume, chamber volume, or ambient pressure. This research is imperative because, as shown with the alkyl nitrates (Chapter 1), accurate absolute determination of gas-phase analyte concentrations may be severely impacted by partitioning of analytes into Teflon chamber walls. To correct apparent concentrations, quantitative characterization of wall effects is critical for any compound measured in environmental chamber studies.

Future research: Use of gas chromatographic retention time to estimate gas-wall partitioning

The gas chromatograph has been successfully used to estimate vapor pressure by correlation of vapor pressure to retention time (Van den Dool and Kratz, 1963; Bidleman, 1984; Eitzer and Hites, 1988; Fischer et al., 1992; Donovan, 1996; Luxenhofer et al., 1996). Analogously, reversed-phase liquid chromatography has been successfully used to determine octanol-water partitioning coefficients (Braumann et al., 1986; Slater et al., 1994; Lombardo et al., 2000; Giaginis and Tsantili-Kakoulidou, 2008). The general chromatographic mechanism for both LC and GC, wherein retention is governed by the relative affinity of a given analyte to differing mobile and stationary phases, is ideal for the characterization of the partitioning characteristics of retained compounds. The DB-5 GC column (Agilent Technologies, Santa Clara, CA), a cross-linked/surface bonded 5% phenyl, 95% methylpolysiloxane capillary, gives a good estimation of vapor pressure (Lei et al., 1999). Since gas-wall partitioning has been shown to be correlated to vapor pressure, measurements of gas-wall partitioning may correlate well with GC retention times. If the DB-5 stationary phase proves unsuitable for partitioning correlation, DB-1 (100% dimethyl polysiloxane) or DB-210 (100% trifluoropropyl methyl polysiloxane) stationary phases may be used to more closely approximate the chemical partitioning characteristics of the FEP (fluorinated ethylene propylene) Teflon film used for environmental chamber construction. Such an approach has been employed in the pharmaceutical industry, where customization of the stationary phase has been shown to increase the correlation between retention time and octanol-water partitioning (Ong et al.,

1996). A genuine Teflon capillary may be substituted for a silica-based GC capillary column, but in that case the GC oven will most likely need to be operated at subambient temperatures for at least part of the duration of the temperature gradient in order to ensure adequate, reproducible analyte retention times. If either approach proves successful, a researcher may substitute GC analysis for the slow and painstaking process of monitoring compound concentrations over time. With good correlation, a researcher may only need to directly measure gas-wall partitioning of a few model compounds, and to use those compounds as retention standards for the GC, potentially avoiding the need for mathematical derivations of gas-wall partitioning. Another advantage of a GC retention-based approach is insensitivity to impurities present in test compounds.

Future research: Reactions of symmetrical, internal alkenes with nitrate radical for direct measurement of β-nitrooxyalkoxy radical decomposition

To more accurately determine the branching of β-nitrooxyalkoxy radical decomposition, direct GC measurement of decomposition products (aldehydes) may be performed. By reacting 6-dodecene, 7-tetradecene, and 8-hexadecene (symmetrical internal alkenes with even carbon numbers) with nitrate radical, any decomposition of the resulting of β-nitrooxyalkoxy radicals will yield hexanal, heptanal, and octanal from 6-dodecene, 7-tetradecene, and 8-hexadecene reactions, respectively. With gas-wall partitioning measurements having been made on aldehydes formed from the decomposition if internal β-nitrooxyalkoxy radicals instead of 1,2- β-nitrooxyalkoxy radicals, direct measurement of decomposition branching can be performed, and will not depend on aerosol yield measurement to extrapolate yields and branching ratios. By this

approach, a complementary dimension of yield measurement will provide additional confirmation of the accuracy of measurement of β-nitrooxyalkoxy decomposition.

References

1. Aschmann, S. M., Tuazon, E. C., Arey, J., & Atkinson, R. (2010). Products and Mechanisms of the Gas-Phase Reactions of OH Radicals with 1-Octene and 7-Tetradecene in the Presence of NO. Environmental science & technology, 44(10), 3825-3831.

2. Arey, J., Aschmann, S. M., Kwok, E. S., & Atkinson, R. (**2001**). Alkyl nitrate, hydroxyalkyl nitrate, and hydroxycarbonyl formation from the NO_x-air photooxidations of C_5-C_8 *n*-alkanes. *The Journal of Physical Chemistry A*, *105*(6), 1020-1027.

3. Atkinson, R., Carter, W. P., & Winer, A. M. (**1983**). Effects of temperature and pressure on alkyl nitrate yields in the nitrogen oxide (NO_x) photooxidations of n-pentane and n-heptane. *The Journal of Physical Chemistry*, 87(11), 2012-2018.

4. Atkinson, R., Aschmann, S. M., & Winer, A. M. (**1987**). Alkyl nitrate formation from the reaction of a series of branched RO_2 radicals with NO as a function of temperature and pressure. *Journal of atmospheric chemistry*, 5(1), 91-102.

5. Bidleman, T. F. (**1984**). Estimation of vapor pressures for nonpolar organic compounds by capillary gas chromatography. *Analytical chemistry*, 56(13), 2490-2496.

6. Braumann, T. (**1986**). Determination of hydrophobic parameters by reversed-phase liquid chromatography: theory, experimental techniques, and application in studies on quantitative structure-activity relationships. *Journal of Chromatography A*, 373, 191-225.

7. Carter, W. P., & Atkinson, R. (**1989**). Alkyl nitrate formation from the atmospheric photooxidation of alkanes; a revised estimation method. Journal of atmospheric chemistry, 8(2), 165-173.

8. Donovan, S. F. (**1996**). New method for estimating vapor pressure by the use of gas chromatography. *Journal of Chromatography A*, 749(1), 123-129.

9. Eitzer, B. D., & Hites, R. A. (**1988**). Vapor pressures of chlorinated dioxins and dibenzofurans. *Environmental science & technology*, 22(11), 1362-1364.

10. Felhofer, J. L., Blanes, L., & Garcia, C. D. (**2010**). Recent developments in instrumentation for capillary electrophoresis and microchip-capillary electrophoresis. *Electrophoresis*, *31*(15), 2469-2486.

11. Fischer, R. C., Wittlinger, R., & Ballschmiter, K. (**1992**). Retention-index based vapor pressure estimation for polychlorobiphenyl (PCB) by gas chromatography. *Fresenius' journal of analytical chemistry*, 342(4-5), 421-425.

12. Giaginis, C., & Tsantili-Kakoulidou, A. (**2008**). Current state of the art in HPLC methodology for lipophilicity assessment of basic drugs. A review. *Journal of Liquid Chromatography & Related Technologies*, 31(1), 79-96.

13. Lei, Y. D., Wania, F., & Shiu, W. Y. (**1999**). Vapor pressures of the polychlorinated naphthalenes. *Journal of Chemical & Engineering Data*, *44*(3), 577-582.

14. Luxenhofer, O., Schneider, M., Dambach, M., & Ballschmiter, K. (**1996**). Semivolatile long chain C_6–C_{17} alkyl nitrates as trace compounds in air. *Chemosphere*, 33(3), 393-404.

15. Lombardo, F., Shalaeva, M. Y., Tupper, K. A., Gao, F., & Abraham, M. H. (**2000**). ElogPoct: a tool for lipophilicity determination in drug discovery. *Journal of medicinal chemistry*, 43(15), 2922-2928.

16. Matsunaga, A., & Ziemann, P. J. (**2010**). Yields of β-hydroxynitrates, dihydroxynitrates, and trihydroxynitrates formed from OH radical-initiated reactions of 2-methyl-1-alkenes. *Proceedings of the National Academy of Sciences*, *107*(15), 6664-6669.

17. Noël, D., & Vangheluwe, P. (**1987**). Retention behaviour and molecular structure of diols in reversed-phase liquid chromatography. *Journal of Chromatography A*, *388*, 75-80.

18. Ong, S., Liu, H., & Pidgeon, C. (**1996**). Immobilized-artificial-membrane chromatography: measurements of membrane partition coefficient and predicting drug membrane permeability. *Journal of Chromatography A*, 728(1), 113-128.

19. Sander, S. P., Golden, D. M., Kurylo, M. J., Moortgat, G. K., Wine, P. H., Ravishankara, A. R., Kolb, C. E., Molina, M. J., Finlayson-Pitts, B. J., Huie, R. E., & Orkin, V. L. (**2006**). Chemical kinetics and photochemical data for use in atmospheric studies evaluation number 15.

20. Slater, B., McCormack, A., Avdeef, A., & Comer, J. E. (**1994**). Ph-metric log P. 4. Comparison of partition coefficients determined by HPLC and potentiometric methods to literature values. *Journal of pharmaceutical sciences*, 83(9), 1280-1283.

21. Van den Dool, H., & Dec Kratz, P. (**1963**). A generalization of the retention index system including linear temperature programmed gas—liquid partition chromatography. *Journal of Chromatography A*, *11*, 463-471.

22. Wiener, H. (**1947**). Structural determination of paraffin boiling points. *Journal of the American Chemical Society*, *69*(1), 17-20.

23. Zhang, J., Dransfield, T., & Donahue, N. M. (**2004**). On the mechanism for nitrate formation via the peroxy radical+ NO reaction. *The Journal of Physical Chemistry A*, 108(42), 9082-9095.